Russian Original Vol. 42, No. 5, May, 1977

November, 1977

SATEAZ 42(5) 399-502 (1977)

SOVIET ATOMIC ENERGY

АТОМНАЯ ЭНЕРГИЯ
(ATOMNAYA ÉNERGIYA)

TRANSLATED FROM RUSSIAN

CONSULTANTS BUREAU, NEW YORK

SOVIET ATOMIC ENERGY

Soviet Atomic Energy is a cover-to-cover translation of *Atomnaya Énergiya*, a publication of the Academy of Sciences of the USSR.

An agreement with the Copyright Agency of the USSR (VAAP) makes available both advance copies of the Russian journal and original glossy photographs and artwork. This serves to decrease the necessary time lag between publication of the original and publication of the translation and helps to improve the quality of the latter. The translation began with the first issue of the Russian journal.

Consultants Bureau journals appear about six months after the publication of the original Russian issue. For bibliographic accuracy, the English issue published by Consultants Bureau carries the same number and date as the original Russian from which it was translated. For example, a Russian issue published in December will appear in a Consultants Bureau English translation about the following June, but the translation issue will carry the December date. When ordering any volume or particular issue of a Consultants Bureau journal, please specify the date and, where applicable, the volume and issue numbers of the original Russian. The material you will receive will be a translation of that Russian volume or issue.

Subscription
$117.50 per volume (6 Issues)
2 volumes per year

Single Issue: $50
Single Article: $7.50

Prices somewhat higher outside the United States.

CONSULTANTS BUREAU, NEW YORK AND LONDON

227 West 17th Street
New York, New York 10011

Published monthly. Second-class postage paid at Jamaica, New York 11431.

Soviet Atomic Energy is abstracted or indexed in *Applied Mechanics Reviews, Chemical Abstracts, Engineering Index, INSPEC—Physics Abstracts and Electrical and Electronics Abstracts, Current Contents,* and *Nuclear Science Abstracts.*

SOVIET ATOMIC ENERGY

A translation of *Atomnaya Énergiya*

November, 1977

Volume 42, Number 5 May, 1977

CONTENTS

CONTENTS

(continued)

Engl./Russ.

CONTENTS

(continued)

Engl./Russ.

The Russian press date (podpisano k pechati) of this issue was 4/25/1977. Publication therefore did not occur prior to this date, but must be assumed to have taken place reasonably soon thereafter.

ARTICLES

TOTAL ^{137}Cs AND ^{90}Sr CONTAMINATION AND EXTERNAL-RADIATION DOSES IN THE TERRITORY OF THE USSR

L. I. Boltneva, Yu. A. Izraél',
V. A. Ionov, and I. M. Nazarov

UDC 614.876:632.15

Data on radiation background are basic to the establishment and application of criteria for the safe use of atomic energy for peaceful purposes. The radiation background is determined by the radioactive contamination of a locality, the natural radioactivity of the environment, and cosmic rays.

In this article we consider the components of the radiation background for the territory of the USSR. The actual data concerning the total ^{137}Cs contamination and the natural radioactivity were obtained from airborne γ-spectral surveys [1, 2]. The errors of the airborne measurements do not, for the most part, exceed 15-20%.

^{137}Cs Contamination of the Soil and Vegetation Cover. The distribution of the surface density (the concentration) of ^{137}Cs for 1974 over the territory of the USSR is shown in Fig. 1. As is shown by the estimates of [2], the concentration of ^{137}Cs varies only slightly with time and will remain practically the same for the next few years. The average concentration of ^{137}Cs in the territory of the USSR amounts to 92 μCi/km^2 (excluding the regions of high mountains where no investigations have been conducted). The observed values of the concentration amount in practice to 15-20 μCi/km^2. The frequency distribution of the concentration values can be satisfactorily approximated by the normal law. The mean-square deviation is 33 μCi/km^2.

The distribution of ^{137}Cs is characterized by marked differences between latitude zones. Against the background of this overall rule, there is considerable spottiness in the distribution of contamination levels, due to the local peculiarities of individual regions. The maximum contamination levels are concentrated chiefly in the latitude belt from 50 to 60° north. Here the ^{137}Cs concentrations amount to 100-175 μCi/km^2. North and south of this belt the contamination levels decrease. The minimum value (25-50 μCi/km^2) is found north of 70° and south of 45° north latitude.

In addition to varying with latitude, the contamination levels are higher for areas close to the mountain systems: the Carpathians, the Crimean and Ural mountains, the Caucasian ridge, the Tien-Shan, the Altai, and the Eastern Siberian and Transbaikal systems. East of the Yenisei River, owing to the complex orography — the presence of many mountain systems occupying a large part of the territory — the latitude-zone differentiation is less marked. The latitude-zone distribution and the local deviations from it are closely related to the observed patterns of precipitation distribution [2].

The distribution of the ^{137}Cs concentration according to geographic and climatic zones is shown in Table 1. These data indicate the connection between the contamination level and the annual amount of atmospheric precipitation. A more detailed analysis has shown that the relation between the ^{137}Cs concentration and the annual average precipitation (P, mm) is expressed, for individual zones of the nonmountain areas of the country shown in Table 1, by the following formulas:

Tundra and forest—tundra	$Q = 0.25 + 0.14P$
Forest zone	$Q = 0.3 + 0.14P$
Forest—steppe and steppe	$Q = 0.45 + 0.12P$
Semidesert and desert	$Q = 0.55 + 0.35P$

Translated from Atomnaya Énergiya, Vol. 42, No. 5, pp. 355-360, May, 1977. Original article submitted December 6, 1976.

TABLE 1. Surface Density (concentration) of ^{137}Cs in Various Geographic Zones

Zone	Soil, vegetation	Participation, mm/yr	Concen., $\mu Ci/km^2$
Tundra and forest—tundra	Tundra gley and swampy soils (mosses, lichens, bushes, low trees)	150-600	64
Coniferous forest (taiga)	Podzol and swampy soils (coniferous forests, swamps, meadows)	300-900	110
Mixed forest	Sod-podzol and gray forest soils (coniferous and broadleaf forests, meadows)	450-900	107
Forest—steppe zone	Chernozem, gray forest soils (alternation of steppe massifs and forest areas)	300-550	91
Steppe zone	Chernozem and chestnut-colored soils (steppe vegetation)	300-400	87
Semidesert	Light chestnut and brown soils (wormwood-type and halophytic vegetation)	100-200	70
Desert	Gray-brown soils, serozems (haloxylon)	75-150	59

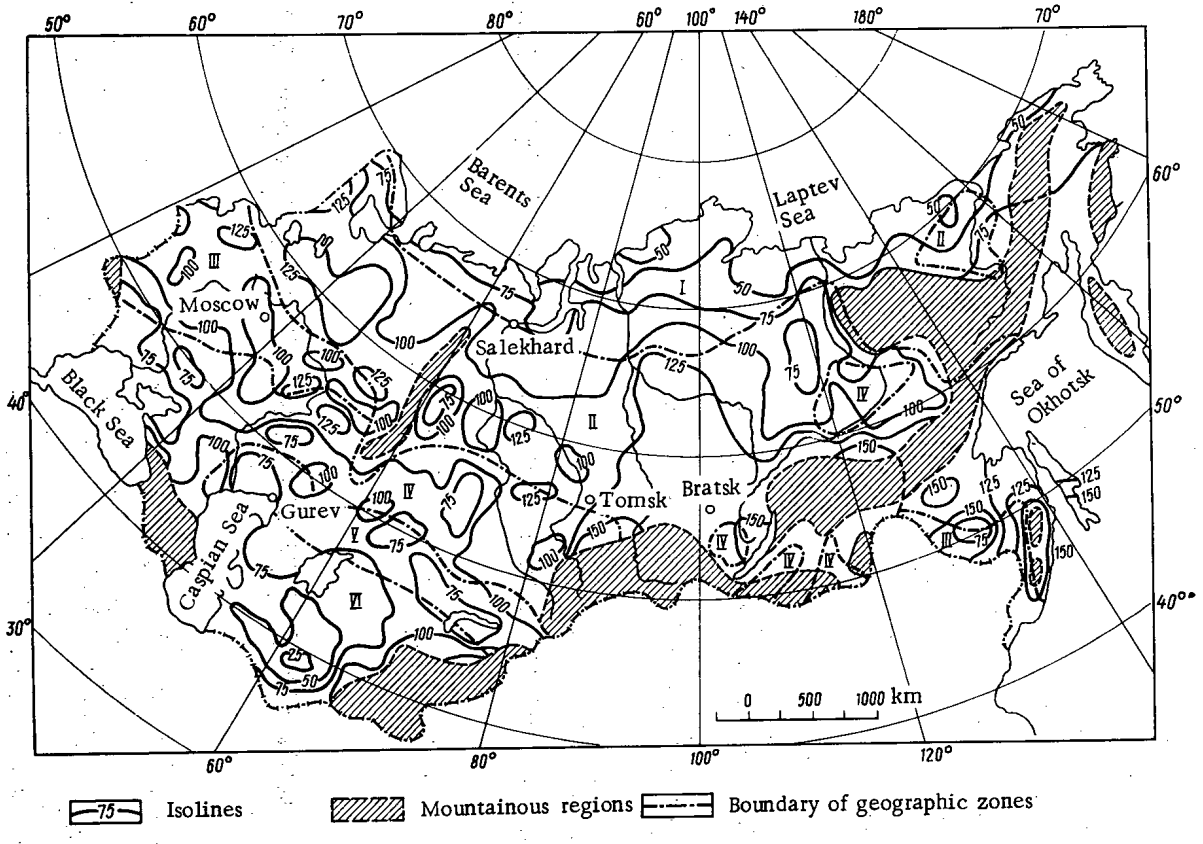

Fig. 1. Distribution of the concentration of ^{137}Cs over the territory of the USSR, $\mu Ci/km^2$: I) tundra and forest—tundra; II) coniferous forest; III) mixed forest; IV) forest—steppe and steppe; V) semidesert; VI) desert.

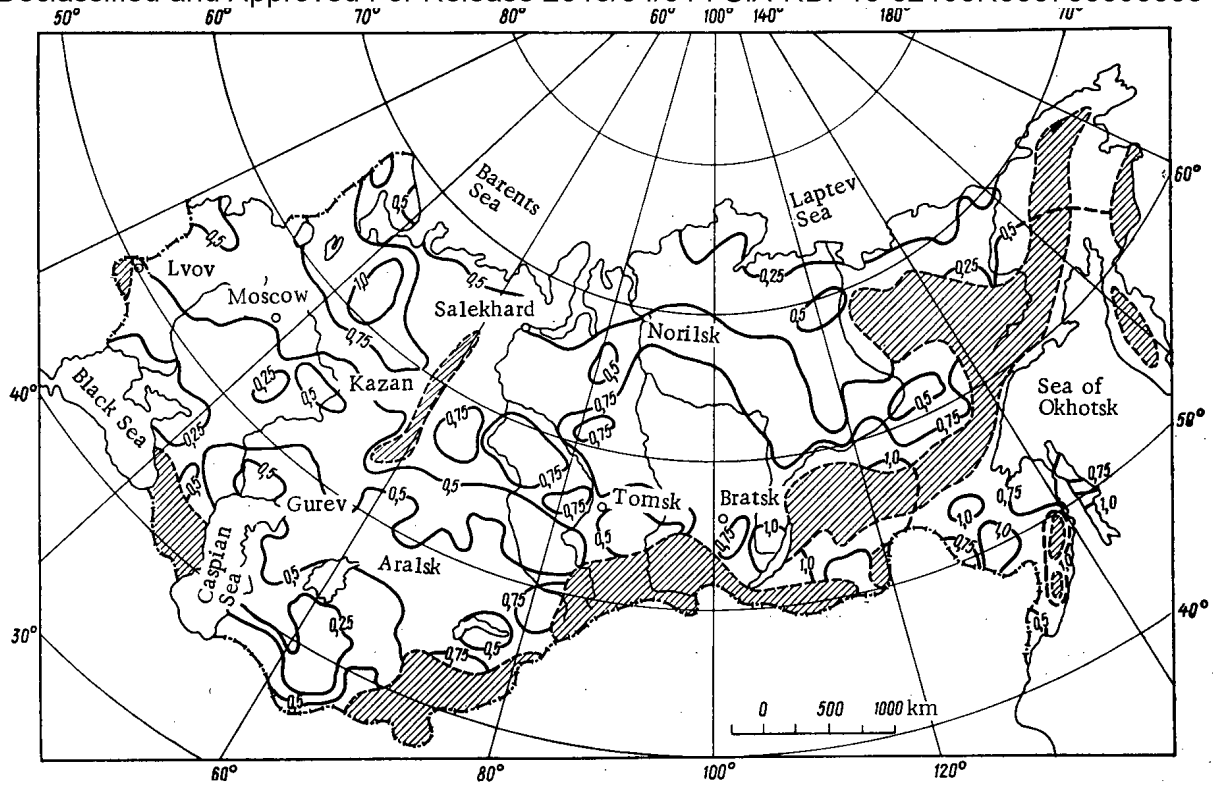

Fig. 2. ^{137}Cs γ-ray dose rate at a height of 1 m above the ground, μR/h (same legend as in Fig. 1).

(here $Q = q(P)/\bar{q}$ is the ratio of the ^{137}Cs concentration in a region with precipitation P to the average concentration in the entire zone).

In the equations given above, the constant term is equal to the fraction of the concentration due to dry fallout, and the regression coefficient characterizes the specific intensity of washing out of radioactive aerosols by the atmospheric precipitation. The dry-fallout fraction increases from the northern to the southern regions (from 25 to 55%). In the semidesert and desert zone the specific intensity of washing out of aerosols by the precipitation increases sharply.

^{90}Sr Contamination of the Soil and Vegetation Cover. An analysis of the ratio of ^{90}Sr to ^{137}Cs in the fallout [2] showed that the ^{90}Sr concentration can be found from the equation $q_{Sr} = 0.54\ q_{Cs}$ with an error of no more than 10%.

We investigated specimens of different types of USSR soils. The ratio of ^{90}Sr to ^{137}Cs for gray forest soils, chernozems, and chestnut soils was 0.55 ± 0.12. For gray-brown soils, serozems, and fixed sands it was 0.62 ± 0.15. The fairly large observed variations in the ratio (~25%) are due to the fact that the ^{90}Sr can be reliably determined in soil samples to a depth of about 10 cm but is not taken into account when it migrates into deeper horizons. The ratio in the soils is practically equal to the ratio in the fallout. Therefore the ^{90}Sr concentration should be assumed to conform to the relation given for the fallout. The average ^{90}Sr concentration calculated in this way for the territory of the USSR is equal to 50 μCi/km^2.

^{137}Cs γ-Ray Dose Rate. The distribution of the ^{137}Cs γ-ray dose rate at a height of 1 m for the territory of the USSR is shown in Fig. 2. In calculating the dose rate it was assumed that in the virgin lands the penetration of ^{137}Cs into the soil follows an exponential law. The penetration coefficient for 1972 was 0.6 ± 0.2 cm^2/yr. For this value of penetration coefficient the dose rate at a height of 1 m is related to the ^{137}Cs concentration by the equation P (in μR/h) = $6.5 \cdot 10^{-3} \cdot q$ (in μCi/km^2). The variations in dose rate as a result of oscillations in the value of the penetration coefficient amount to 15%.

Between the ^{137}Cs concentration map (see Fig. 1) and the dose-rate map (see Fig. 2) there are certain differences, due essentially to the fact that in cultivated fields the ^{137}Cs has penetrated the topsoil. As a result, the dose rate drops by a factor of as much

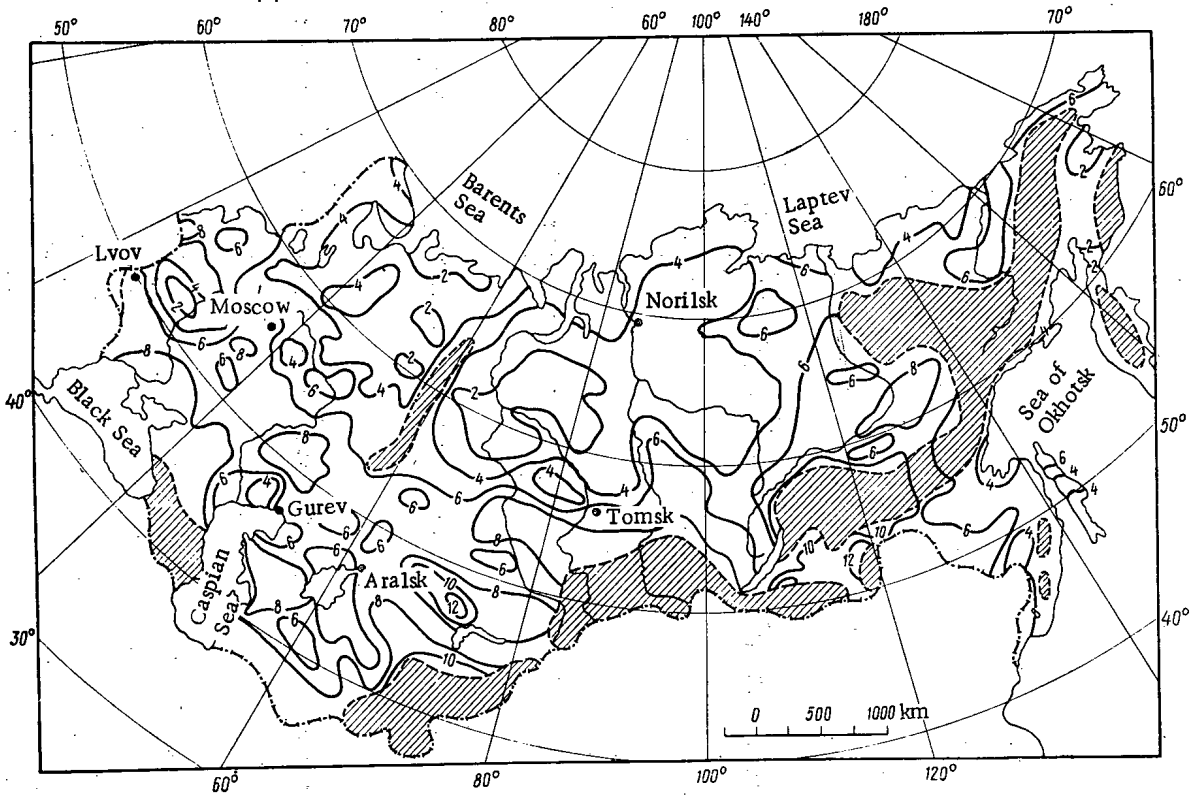

Fig. 3. Dose rate of γ rays from natural radioactive elements at a height of 1 m above the soil, μR/h (same legend as in Fig. 1).

TABLE 2. Average γ-Ray Dose Rate at a Height of 1 m above the Soil

Soils	Dose rate, μR/h	Coeff. of variation, %	Characteristic range of variation, μR/h
Tundra	3,5	43	2,0—5,0
Podzol	2,9	48	1,5—4,3
Sod-podzol	4,5	45	2,5—6,5
Gray forest soils	6,5	23	5,0—8,0
Chernozems	7,1	21	5,5—8,6
Chestnut soils	7,6	20	6,1—9,1
Brown desert—steppe soils	7,2	28	5,9—9,2
Gray-brown desert soils	7,7	18	6,4—9,2
Serozems	8,6	18	7,0—10,2

as 2.5. Therefore, where there is intensive agriculture, owing to the large areas taken up by plowed fields, the average dose rate is found to be considerably lower. The range of variation of the dose rate is between 0.10 and 1.25 μR/h. The average value of the dose rate when the plowed fields are taken into consideration is about 0.5 μR/h. As in the case of the concentration, there is a distribution into latitude zones.

The frequencies of the dose-rate values have a logarithmic-normal distribution. The marked asymmetry of the dose-rate distribution when there is a normal distribution of the concentration is due to the large number of low dose-rate values for plowed areas.

Dose Rate of γ-Rays from Natural Radioactive Elements. Natural radioactive elements constitute a constantly present source of γ rays. On the global and regional scales, the external irradiation is affected, as a rule, by the radioactivity of the soils. Except for mountainous regions, rock outcrops are limited in area, and therefore their γ radiation is local in character. The relative concentration of natural radioactive elements in soils is

TABLE 3. Numerical Values of the Shielding Coefficient

Geographic zone	^{137}Cs	Natural radioisotopes
Tundra and forest–tundra	0,40—0,80	0,60—0,90
Coniferous forest	0,50—0,85	0,70—0,95
Mixed forest	0,75—0,95	0,90—1,0
Forest–steppe and steppe	0,75—0,95	0,90—1,0
Semidesert	0,85—0,95	0,95—1,0
Desert	0,90—1,0	0,95—1,0

TABLE 4. Distribution of Cosmic-Ray Dose over the Terriotry of the USSR

Dose, Mrd/yr	Exposure dose rate, μR/h	Territorial extent, %
28—30	3,65—3,9	60
30—40	3,9—5,2	33
40—50	5,2—6,5	5,5
50—100	6,5—13	2,0
100—150	13—19,5	0,5

found to lie mainly within the following limits: $(0.5\text{-}3.5)\cdot10^{-4}$% for uranium, $(1\text{-}14)\cdot10^{-4}$% for thorium, 0.3-3.0% for potassium. A characteristic of the spatial distribution of natural radioactive elements in the soil is that on the regional level the relative concentrations increase from north to south. The relative concentrations in rocks do not, for the most part, exceed the maximum values of the relative concentrations in the soils. However, in some varieties of rocks the uranium and thorium content may be greater by as much as one order of magnitude than in the soils [1].

A map of the dose rate of γ rays from natural radioactive elements in the territory of the USSR, calculated on the basis of the uranium, thorium, and potassium content values determined by the aerial survey method [2], is shown in Fig. 3. The dose rate has a clearly marked latitude-zone distribution. Genetic types of soils closely related to the geographic and climatic zonality determine the spatial distribution of the dose field over the territory of the USSR (Table 2).

The frequency distribution of the dose rate within each genetic type of soil is satisfactorily approximated by the normal law. The amount associated with the range of dose-rate values (see Table 2) is 68%. This range was calculated on the basis of the normal distribution. There is a great deal of overlapping between the dose-rate values of different genetic types of soils; this corresponds to the gradual transition from one type of soil to another and is due to the effect of local factors, primarily the radioactivity of the parent rocks and the mechanical composition of the soils.

Table 2 does not take account of soil radioactivity data for the regions east of the Yenisei River. Here most of the territory is occupied by high plateaus and ridges which have a high proportion of outcrops (∿40%), so that it is difficult to distinguish the soil and rock radioactivity values. The isoline contours in this region often correspond to the boundaries of individual rock complexes. The lowest radioactivity is found in intrusive rocks of basic composition — basalts, andesites, and their tuffs (1.5-2.5 μR/h). The maximum value (9-14 μR/h) is found in areas of acid intrusive rocks (granites, granodiorites, quartz diorites) and metamorphic rocks.

Attenuation of External γ Radiation by Snow Cover. The snow cover can substantially reduce the external-radiation dose of field personnel and the general population. From the data of 550 weather stations concerning the moisture content in the snow cover in the territory of the USSR, averaged over many years [3], maps have been prepared to show the attenuation of the annual γ-ray dose rate from ^{137}Cs and natural radioactive elements [4].

The attenuation of the γ rays is characterized by the dose-rate shielding coefficient of the snow cover, $K(x) = P(I, x)/P(I)$, where x is the moisture content of the snow cover; $P(I, x)$ and $P(I)$ are the dose rates at a height of 1 m above the snow and above the soil, respectively. In calculating the shielding coefficient, the nature of radioisotope penetration into the soil was taken into account. The limits of variation of $K(x)$ over a 1-yr period for the main geographic zones of the country are shown in Table 3. These changes characterize the climatic nonuniformity of the zones considered. The greatest attenuation of the annual dose values is found in the tundra and the forest–tundra. The annual dose value decreases by a factor of 1.5 for natural radioactive elements and 2.5 for ^{137}Cs. In the southern regions of the country the γ-ray attenuation may be disregarded in practice.

Cosmic-Ray Dose. The cosmic-ray dose is caused mainly by the ionizing part of cosmic radiation. The contribution made by neutrons for geomagnetic latitudes of 40-50° in the 0-4-km altitude range is only 2-8% and is disregarded here.

TABLE 5. External Annual Radiation in the Territory of the USSR

Geographic zone	Natural radioactivity of soils and rocks	^{137}Cs	Cosmic rays	Atmospheric radon	Total dose
Tundra and forest–tundra	26,9*	3,3	28,3	1,5	50,0
	20,5	2,2	28,3	1,5	52,5
	39	4	54	3	100
Coniferous forest	27,7	5,5	28,5	1,2	62,9
	22,8	4,0	28,5	1,2	56,5
	40	7	51	2	100
Mixed forest	41,6	4,2	28,6	2,3	76,7
	37,4	3,4	28,6	2,3	71,7
	52	5	40	3	100
Forest–steppe and steppe	56,2	3,7	29,1	3,0	92,0
	50,5	3,0	29,1	3,0	85,6
	60	3	34	3	100
Semidesert	56,2	4,0	29,3	4,5	94,0
	53,3	3,6	29,3	4,5	90,7
	59	4	31	5	100
Desert	57,7	2,7	29,1	4,5	94,0
	57,7	2,7	29,1	4,5	94,0
	61	3	31	5	100

*The first line gives the average dose value in Mrd/yr; the second, the dose value taking account of the snow-cover shielding, Mrd/yr; the third line, the contribution to the total dose (taking account of the snow-cover effect), %

The annual doses for points which have a geomagnetic latitude of φ and an altitude of H above sea level can be calculated by the approximate formula [5]

$$D(\varphi, H) = a(\varphi) + b \exp [H/c(\varphi)].$$

If $D(\varphi, H)$ is expressed in megarads per year and H in kilometers, then b = 11,

$$a(\varphi) \begin{cases} 15 \text{ for } \varphi < 25°; \\ 15 + 0.118(\varphi - 25°) \text{ for } 25 < \varphi < 42°; \\ 17 \text{ for } \varphi > 42°; \end{cases}$$

$$c(\varphi) \begin{cases} 1.96 \text{ for } \varphi < 10°; \\ 1.96 \exp[-0.0028(\varphi - 10°)] \\ \qquad \text{for } 10 < \varphi < 50°; \\ 1.75 \text{ for } \varphi > 50°. \end{cases}$$

The formula given above enables us to estimate the annual doses with an error of no more than 5% in the 0-5-km altitude range.

The distribution of the cosmic-ray dose over the territory is characterized by the data of Table 4. An isodose map for the territory of the USSR, including the European part of the country (except for the Carpathians and the Caucasus) and the Western Siberian plain, the dose is 28-30 Mrd/yr, while the eastern mountainous part of the country has a dose of 30-50 Mrd/yr. The highest dose values are found in the area of the Pamir–Tien-Shan mountain system and the Caucasus, where the dose exceeds 100-150 Mrd/yr, with a maximum value of 200-350 Mrd/yr (∿700 Mrd/yr on Lenin Peak, Victory Peak, and Communism Peak). The dose rate may differ from the average by 3-10% because of variations in cosmic radiation.

Contribution Made by Various Sources to External Radiation in the Territory of the USSR. The maps shown above enable us to estimate the contribution made by γ-radiation from ^{137}Cs, natural radioactive elements, and cosmic rays to the external-radiation dose in the territory of the USSR.

In addition, γ rays are also emitted by radon decay products found in the atmosphere. In order to take this factor into account, we may assume that the average emanation coefficient is 10% and that the concentration of decay products in the air decreases exponentially with altitude and decreases by a factor of 2 at an altitude of 1 km [1].

The annual doses of external radiation for the geographic zones of the USSR are indicated in Table 5, from which it can be seen that the total dose of external radiation increases from the tundra to the desert zone by a factor of almost 2: from 52 to 94 Mrd/yr. The contribution made by the different components varies regularly for the different zones. Thus, in the first two zones most of the annual dose is due to cosmic rays. In the other zones the contribution of natural radioactivity is predominant. In the desert zone it is one and a half times as high as in the tundra and the coniferous forests. This difference is additional proof of the fact that the peaceful use of atomic energy has only a slight effect on the annual dose.

LITERATURE CITED

1. R. M. Kogan, I. M. Nazarov, and Sh. D. Fridman, Fundamentals of Gamma Spectrometry of Natural Environments [in Russian], Atomizdat, Moscow (1976).
2. L. Boltneva et al., in: Collection of Reports of the First Radioecological Conference, Starý Smrkovec, Czechoslovakia [in Russian], Vol. 3 (1972), p. 95.
3. Handbook of the Climate of the USSR, Part IV, Nos. 1-34 [in Russian], Gidrometeoizdat, Leningrad (1965-1970).
4. L. I. Boltneva, L. I. Kuznetsova, and I. M. Nazarov, in: Proceedings of the Institute of Applied Geophysics [in Russian], Gidrometeoizdat, Leningrad, No. 34 (1977), p. 57.
5. L. I. Boltneva, I. M. Nazarov, and Sh. D. Fridman, Izv. Akad. Nauk SSSR, Fiz. Zemli, No. 4, 66 (1974).

COMPLEX OF DEVICES FOR SAMPLING AND MEASURING TRITIUM IN ENVIRONMENTAL OBJECTS

L. I. Gedeonov, V. A. Blinov,
A. V. Stepanov, V. P. Tishkov,
A. M. Maksimova, and A. A. Antipov

UDC 546.110.23.002.637:543.05

Among the contaminants of technical origin in water systems are many which remain in the dissolved (ionic) state for a long time. Tritium may serve as an analog of their dispersal with bodies of water. At present, the tritium content in waters is sufficient for studying migration. Such research makes it possible to predict the behavior of industrial effluents in regions where new facilities are planned.

The use of nuclear energy has resulted in a marked global increase in the concentration of tritium over the past decades in almost all water systems, in rainfall, and in surface water. Thus, the mean monthly concentration of tritium reached 130 tritium units (t.u.) in U.S. river basins in 1966 [1], from 60 to 360 t.u. in various U.S. rivers in the winter of 1971-1972 [2], an average of 150 t.u. in the rivers of the prefectures of Japan in 1971 [3], and about 100 t.u. in the northern rivers of the USSR in 1972 [4].

Owing to dilution, the tritium concentration in large bodies of water is appreciably lower. Highly sensitive techniques must be employed to determine it. The highest sensitivity is ensured by methods employing scintillation and proportional counters. Analysis of work on tritium determination in natural bodies of water shows that when enrichment is employed the reproducibility of results is not good since there are no reliable methods of determining the degree to which the sample has been enriched with tritium if the initial concentration was low. An advantage of gas-filled proportional counters is that they ensure high sensitivity (without enrichment) and make absolute measurements.

Translated from Atomnaya Énergiya, Vol. 42, No. 5, pp. 361-364, May, 1977. Original article submitted August 11, 1976.

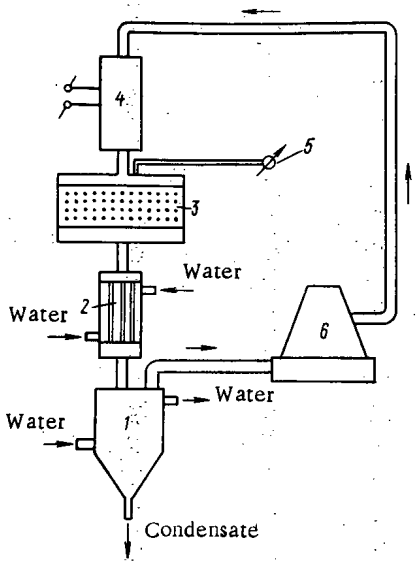

Fig. 1. Unit for regeneration of silica gel: 1) water collector; 2) condenser; 3) holder with silica gel; 4) oven; 5) thermocouples; 6) vacuum cleaner.

Apparatus for determining tritium in samples of water and atmospheric moisture were developed and described earlier [5]. Subsequently work was focused on improving the method.

The tritium concentration in hydrogen and water is determined in several stages: sampling of water or trapping of atmospheric moisture; oxidation of atmospheric hydrogen; obtaining hydrogen by decomposition of the sample; purification and introduction of the hydrogen into the counter with propane or incorporation of the hydrogen into the counting gas by means of synthesis; and measurement of the activity of the gas filling the counter.

The range of tritium concentration that can be measured is extremely wide. Accordingly, the complex of apparatus consists of independent units of two classes: the first, for measuring samples of "high" activity (with a tritium content exceeding $3 \cdot 10^3$ t.u.) and the second, for low activities (from $3 \cdot 10^3$ to 30 t.u.).

The previous method used to prepare samples for measurement had the following shortcomings: small quantity of hydrogen obtained, long time required to obtain it ($\sim$2 h), and a rather low degree of purity of the hydrogen which affects the process of synthesis and the results of the measurement.

In the new variant, samples of water are taken in glass ampules of up to 250 ml in volume which are sealed at the site of the sampling. This ensures long storage of samples, excludes the possibility of samples becoming enriched with tritium as a result of exchange with external sources, and if necessary permits measurement of further portions of water from the same sample. As in the previous variant, atmospheric moisture is trapped in previously dehydrated silica gel. It consists of an aluminum holder with two apertures, containing 2 kg of granulated silica gel. The air is drawn through an absorber by a vacuum cleaner at a rate such as not to allow water vapor to pass through. The principal parameters of the absorption unit are as follows: height of silica gel layer in absorption unit 10 cm; area of absorber 300 cm^2; air flow rate 0.5 m^3/min; resistance of absorber layer 30 mm Hg.

The sampling time is determined by the air temperature and humidity and is chosen so that the silica gel absorbs 250 ml of atmospheric moisture. The atmospheric moisture is extracted from the silica gel and the gel is regenerated by a stream of hot air circulating in a closed system (Fig. 1). Then, in preparing the sample for measurement the required quantity of water is mixed with calcium oxide and put into a stainless steel "reactor." When samples of water of high specific activity (above 3000 t.u.) are to be measured to obtain hydrogen a 0.2-ml sample of water is placed in a reactor consisting of a test tube of heat-resistant glass. To measure samples of low specific activity 20 ml of water is placed in the reactor.

When the reaction $CaO + H_2O \rightarrow Ca(OH)_2$ is completed, powdered zinc is added to the reactor. Completion of the reaction $Ca(OH)_2 + Zn \xrightarrow{t^\circ} ZnO + CaO + H_2$ excludes any isotopic effects. The time needed to obtain hydrogen is reduced to 5-10 min. Then the hydrogen is passed through a filter (a layer of silica gel and activated carbon), cooled by liquid nitrogen. Such purification enables us to obtain hydrogen free of impurities which poison the catalyst

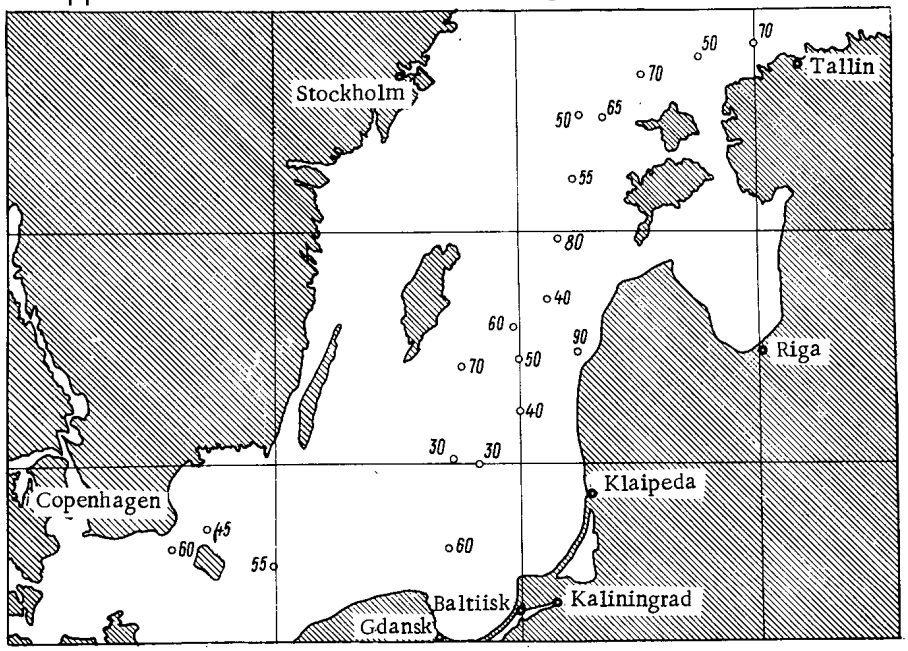

Fig. 2. Tritium concentration (in t.u.) in samples of water from the Baltic in 1975.

during synthesis of the filling gas for the counter and free of possible radioactive inert gases. Purified hydrogen is used in a mixture with propane to fill counters in measuring samples of high specific activity. When low concentrations of tritium are measured, the hydrogen enters into the synthesis system where it becomes part of the filling gas, butane. The latter is synthesized with the aid of a palladium catalyst from a mixture of butadiene and hydrogen obtained from the sample by the method described earlier [5]. The high purity of the gas ensures good reproducibility of the measurements.

The arrangement for measuring high tritium concentrations uses three proportional counters, differing only as to volume or form of shielding against the radiation background. Two of the counters have only passive shielding in the form of a 10-cm layer of lead and differ only in length and, consequently, in volume (302 and 604 cm^3). Such a combination is used in order to exclude the fringe effect. Hydrogen obtained from a single sample is introduced into both counters, up to the same partial pressure. Measurements in the counters yield the counting rates n_1' and n_2', respectively, for volumes V_1 and V_2 of hydrogen measured. The instrumental β spectrum recorded by a multichannel analyzer is used to introduce corrections for incomplete counts of the low-energy part of the spectrum and corrected counting rates n_1 and n_2 are obtained instead of n_1' and n_2'. Upon comparison with the absolute value of the activity due to the fringe effect, both counting rates are reduced by the same quantity and their difference is equal to the difference of the absolute values, whereby $a_0 = (n_1 - n_2)/(V_1 - V_2)$, where a_0 is the volumetric specific activity of the hydrogen from tritium. The third counter, of volume 302 cm^3, is inside a passive shielding and is surrounded by a ring of Geiger—Mueller counters operating in anticoincidence mode with the main counters. The efficiency of the latter is evaluated with a sample of known activity and was found to be ∿90% for standard measuring conditions.

More sensitive arrangements with proportional counters of volumes 3.1, 5, and 8 liters are installed in underground premises with shielding with a water equivalent of 120 m. Under these conditions there is no need of protection with the aid of an anticoincidence system. The mean background of the 3.1-liter counter is 11.1 ± 0.4 counts/min (with a confidence coefficient of 95% the deviation of a single measurement of the background is ±1.2 counts/min). A count that exceeds the background by 3 counts/min, which corresponds to ∿30 t.u., is considered a reliable result. Signals from the counter anode are amplified, sorted according to amplitude, and recorded. The entire apparatus is based on transistors and integrated micromodules. The schematic diagram of a similar arrangement was described earlier [5]. The background of the 302-cm^3 counter, with active shielding, is 3.4 counts/min.

The reproducibility of measurements on both arrangements was verified by repeated determinations of the tritium content of the same sample. The high-sensitivity 3.1-liter arrangement is characterized by a deviation of ±20% for a single measurement with a confidence

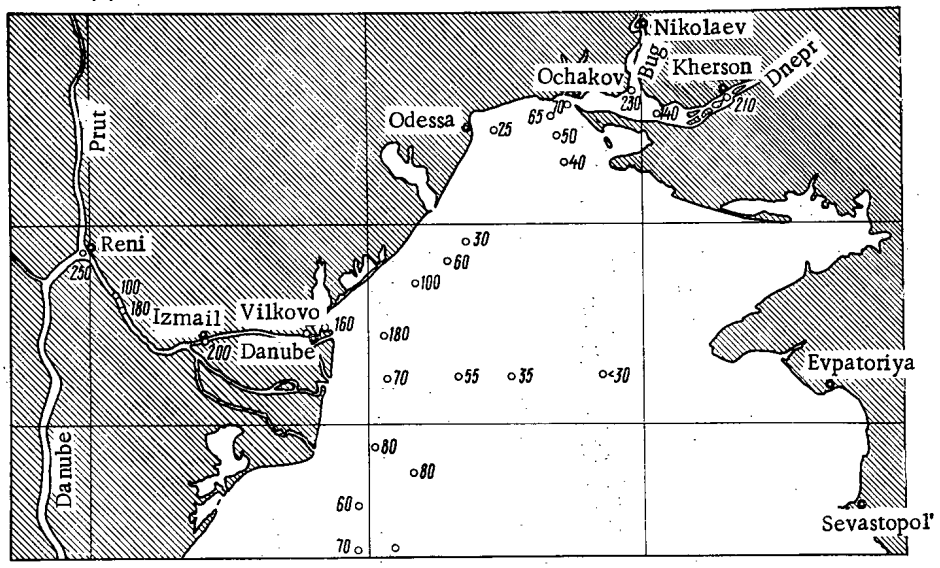

Fig. 3. The tritium concentrations (in t.u.) in samples of water from the lower course of the Danube and the northwestern part of the Black Sea.

coefficient of 95%. The arrangement for determining higher activities (with a 302-cm^3 counter) gives a deviation of ±8% with the same confidence coefficient.

The possibilities of ascertaining the spread of impurities in the environment with the aid of the apparatus described above were evaluated during the course of work on the Baltic Sea and in the lower courses of the Danube. Samples of water were taken at 20 points on the Baltic in 1975. After purification by a single distillation without enrichment, the tritium content of the samples was determined on a sensitive counter installed underground.

The sampling sites and the results obtained are shown in Fig. 2. The mean value of the results of all determinations was 56 ± 20 t.u. with a confidence coefficient of 95%. This differs little from the results of a 1972 analysis of five samples of water from the Baltic [4]. The results range from 30 to 90 t.u.

With a confidence coefficient of 95%, the deviation of a single result from the mean is 65% which is more than 3 times the spread characterizing the reproducibility in the determination of the lowest tritium concentrations and, as mentioned above, is ±20% for the same confidence coefficient. Only nine results obtained for Baltic samples deviate from the mean value by less than 20%, whereas all the others deviate more. Thus, with a confidence coefficient of more than 95% it can be said that these deviations reflect the variability of the concentrations in the Baltic and not the random error of the method.

The points at which the tritium concentration deviates significantly from the mean were not observed to be distributed systematically. This means that no effect of any local sources of tritium was noted. This is probably due to the fact that water from the land drains into the Baltic in various regions, freshening the seawater quite evenly. One may speak of some tendency towards lower values near sounds.

The picture is different at the mouths of the large rivers falling into the Black Sea (Fig. 3). The waters of the Danube bear a significant concentration of tritium, which is roughly the same over its entire lower course, surveyed over the Kilya branch. These levels are comparable to the tritium content in present-day atmospheric precipitation. In 1969-1970 the mean tritium concentration in precipitation was, e.g., 244 t.u. in Tbilisi, 247 t.u. in Odessa, and 133 t.u. in Rostov-on-Don [6]. The large mass of Danube waters is not diluted immediately, but only at a considerable distance from the delta is the concentration observed to drop to a minimum value which can be measured by our method without enrichment. Safe concentrations of tritium are involved here but the picture obtained here should also be characteristic of other dissolved impurities borne by the waters of the Danube, some of which may be toxic.

It is interesting that with a much smaller discharge from the Dnepr and the Bug the increase in the tritium concentration in the waters of the Black Sea near their mouths is traced

for a much smaller distance than at the mouth of the Danube. However, a halo of impurity spread is traced in this case, too.

The values of the tritium concentration in the Black Sea and the Danube cover a wide range. To take the mean in this case is to lose all the information about the differences in various parts of the halo of tritium spread. As mentioned above, the reproducibility of the results of measurements with the system described is characterized by an rms deviation of ±20%. This criterion can be used to evaluate the statistical reliability of the differences in the results of tritium concentration measurements in the Danube and the Black Sea. Almost all the differences observed are real.

Notwithstanding the increased tritium content in atmospheric precipitation and surface waters, there are still many vitally important objects with a tritium content that is measured in several t.u. or even fractions of a tritium unit. A serious problem is posed by the penetration of soluble poisonous impurities into the depths of the oceans and into subterranean waters. The study of these objects and processes calls for extremely sensitive techniques for tritium determination. It can be assumed that techniques employing proportional counters will prove useful.

LITERATURE CITED

1. M. Chesnutt et al., Radiol. Health Data Reports, 7, 377 (1966).
2. Radiation Data Reports, 13, No. 5, 8 (1972).
3. Nat. Inst. Radiolog. Sci., Chiba, Japan, NIRS-RSD, 34, No. 34 (1972).
4. T. N. Zhigalovskaya et al., in: Meteorological Aspects of Radioactive Pollution of the Atmosphere [in Russian], Gidrometeoizdat, Leningrad (1975), p. 223.
5. L. I. Gedeonov et al., in: Proceedings of the IAEA Symposium: "Environmental Surveillance around Nuclear Installations," Vienna (1974), Vol. 1, p. 235.
6. V. N. Soifer et al., in: Polluted Natural Media [in Russian], No. 3(42), Gidrometeoizdat, Moscow, p. 85.

EXPERIMENTAL INVESTIGATION OF ALGORITHMS FOR THE DIRECT DIGITAL CONTROL OF THE NEUTRON FIELD IN AN IRT-2000 REACTOR

E. V. Filipchuk, P. T. Potapenko,
A. P. Kryukov, A. P. Trofimov,
V. G. Dunaev, N. A. Kuznetsov,
and V. V. Fedulov

UDC 621.039.562

With the development of nuclear energy, the problem of the use of a computer for controlling the neutron field of large nuclear reactors has become increasingly urgent. Significant attention has recently been devoted to this problem. A review is given in [1] of methods of utilizing computers for reactor control in a number of foreign atomic power plants, and the problems of the synthesis of similar systems are discussed in [2]. It is being planned to use computers on a research reactor for the control and recording of the spatial distribution of the neutron field [3].

This article is devoted to an experimental investigation of various algorithms for the direct digital control of the neutron field of the Moscow Engineering Physics Institute IRT-2000 reactor. The legitimacy of a study of the distinctive features of spatial regulation on a research reactor has been shown in [4]. Research reactors can be successfully used as a physical model in the conduct of such experiments, control and processing problems can be

Translated from Atomnaya Énergiya, Vol. 42, No. 5, pp. 365-369, May, 1977. Original article submitted July 26, 1976.

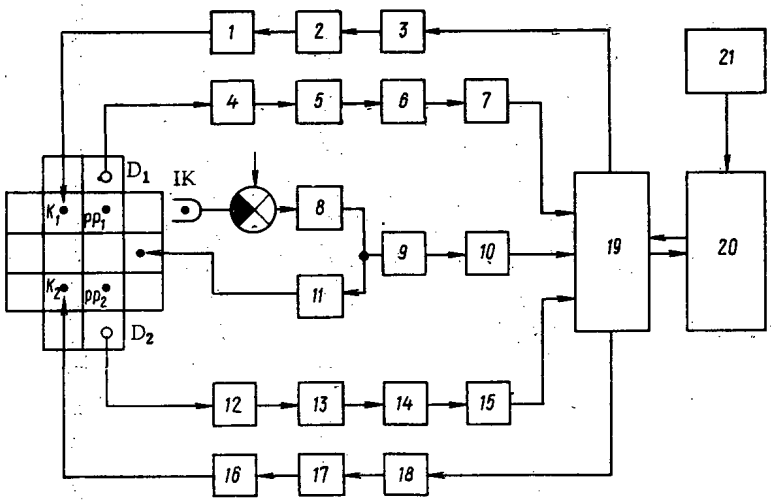

Fig. 1. Structural layout of the IRT-2000 reactor experimental control system: 1, 16) operating mechanisms with the logic unit; 2, 17) ÉMU-3A power amplifiers; 3, 18) TsAP-11/5 digital—analog converters; 4, 12) I-37 measuring amplifiers; 5, 13) passive correction circuits; 6, 14) I-102 normalizing amplifiers; 7, 15) F-203 voltmeters; 8) UR-8 mismatch amplifier; 9) integrating measuring amplifier; 10) Shch-1413 voltmeter; 11) standard automatic regulator; 19) input—output channel; 20) Nairi-S processor; and 21) "Consul" typewriter.

solved with their help, and experimental checks of the various algorithms and control system structures are made on the basis of real equipment [5].

The present trend in the application of computers for reactor control consists of the use of modular interconnected computer systems, which permits increasing the reliability and flexibility of the digital control system. Safety requirements result in the necessity of utilizing specialized computers which execute simple control functions but also possess high reliability at the lowest level of the automated control system hierarchy — direct digital control of the reactor. The legitimacy of such an approach is explained again by the fact that it is necessary to regulate the total power with very small cycles, which essentially excludes the possibility of using complex control laws.

It has proved possible on the basis of these ideas to use a Nairi-S computer for the experimental investigations. In order to couple similar input—output subsystems with the processor, a special logic unit for input—output control was constructed on the basis of integrated circuits; this unit was connected to an integrator by means of a coincidence circuit built with transistors. Such construction of the channel for input—output of information into the processor of the Nairi-S has permitted, without changing the command system of the machine, realizing control by analog—digital and digital—analog conversions, entry into memory, and the reading of information necessary for control. The indicated coupling unit permits providing for the input—output of discrete information over three channels, and, when necessary, over a larger number of channels with small additions, which significantly increases the computational power of the machine.

The complete structural layout of the experimental system for direct digital control and a diagram of the active zone of the IRT-2000 are given in Fig. 1. Type DPZ-11P emission detectors, which were successfully used earlier in experiments with automatic reactor control systems [4, 6, 7], arranged in expelled fuel elements were applied in the system as the neutron flux detectors D_1 and D_2. The boron rods K_1 and K_2 were used as actuating members of the control system, and the rods PP_1 and PP_2 were used to disturb the reactivity. In the course of carrying out the experiment on direct digital control of the reactor, the total power was stabilized by a standard automatic regulator (AR). Commercial measuring devices and converters, incorporated into the corresponding analog input and output subsystems, were used for connecting the reactor to the computer.

The analog input subsystem of the single control channel included a DPZ-11P detector, an I-37 current-measuring amplifier with a recording device, an I-102 normalizing amplifier,

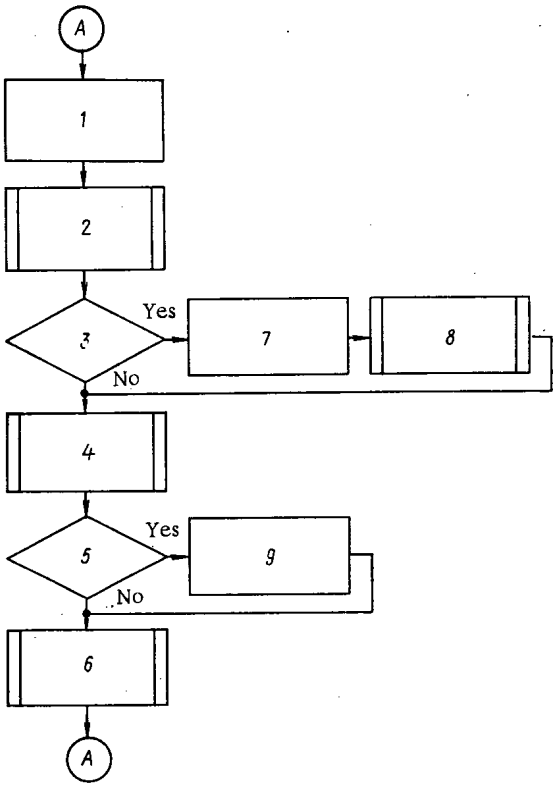

Fig. 2. Structural layout of the control program: 1) timer; 2) "Input" subprogram; 3) necessary input of new settings; 4) subprogram for calculation of the control actions; 5) check on violation of constraints; 6) "Output" subprogram; 7) digital—analog converter interrupt; 8) subprogram for input of settings; and 9) forming of the control action.

and an F-203 digital voltmeter, which was used as the analog—digital converter. A passive correction circuit was included between the measuring and normalizing amplifiers [6].

The analog output subsystem consisted of a TsAP-11/5 three-channel digital—analog converter, an ÉMU-3A power amplifier, a logic unit, which provides for different operating conditions of the motor, and a standard servo.

The total power imbalance signal, picked off the UR-8 mismatch amplifier of the standard AR system, was fed into the processor over a channel consisting of an integrating measuring amplifier and an analog—digital converter on an Shch-1413 voltmeter base. Input of information on the relative position of the AR rod was thereby provided.

The structure of the control program, which consists of several function subprograms, is given in Fig. 2. The subprogram "Input" interrogates the appropriate analog—digital converter, converts the double-decade output code of the voltmeter into the auxiliary code used by the machine, and enters the measured value into memory. The subprogram "Output" provides for control of the digital—analog converter ("zero" default, addressing) and converts the information applicable for output to the form necessary for the normal functioning of the converter.

A universal information-processing program calculates the control actions according to various algorithms and systematically alters the structure of the control system and the control law parameters. The functioning of the control program occurs in the following way. Indexing of the subprogram "Input" occurs according to a signal from the counter, which simulates the operation of a timer. After conclusion of input and the conversion operations control is transferred to the settings input program. If according to a requirement of the operator the input of new settings is necessary, an interrupt occurs in the digital—analog converter and the machine proceeds to the readiness state.

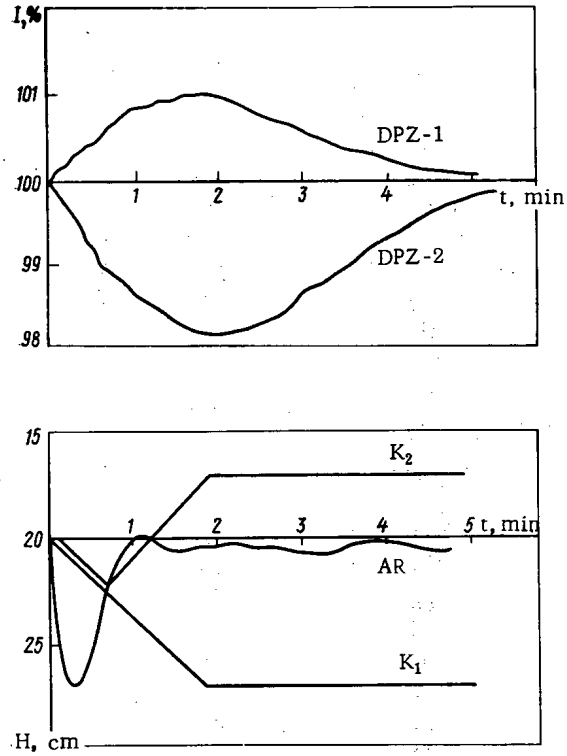

Fig. 3. Variation of the DPZ-1 and DPZ-2 currents and the positions of the control rods H in the course of compensating for a reactivity disturbance.

An adjustment is set by the operator from a console (a "Konsul" typewriter), after which control is transferred to the information-processing unit for calculation of the control action. The possibility of changing the control law form and parameters is similarly provided for in the program. Further, control is transferred to the constraint-checking unit, and finally the action decided upon enters with the aid of the subprogram "Output" the input of the appropriate digital—analog converter. Then control is transferred to the timer, and the cycle is repeated during the cycling time. The memory code of the Nairi-S machine was used as the master program.

One should emphasize that such hardware and software design permits successfully simulating the operation of a real control computer in combination with a real configuration of analog input and output subsystems.

The experiments conducted were concerned with investigations of system dynamics, the determination of adjustments, and checking the efficiency of the system under different standard disturbances. Linear and relay systems with in-phase and out-of-phase channel operation were similarly investigated with different control laws. As a result, the following basic quantitative characteristics have been obtained:

1. At a power of 2000 kW the current of each DPZ was approximately 2 μA.

2. The signal at the input of the F-203 analog—digital converter after correction and the I-102 normalizing amplifier was hundreds of millivolts, which made it possible to operate stably at the voltage limit of the voltmeter with three significant figures. At the same time stabilization of the DPZ currents with an error of 0.5% was ensured.

3. The analog output subsystem was adjusted so that based on safety ideas the rate of reactivity introduction was restricted to a value of 0.03 β/sec for the maximum control signal. The cycling time was 1 sec.

4. The active zone of the reactor possesses well-expressed spatial effects. Thus, upon a disturbance of the reactivity by the movement of the rod PP_1 upward by 5 cm, the current of DPZ-1 increased by 1.5-2%, and the current of DPZ-2 decreased by approximately the same amount. When rods K_1 and K_2 were simultaneously moved in different directions (the total

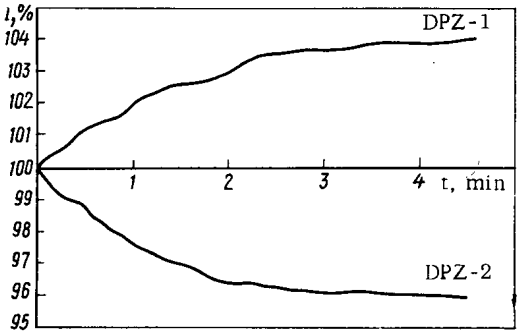

Fig. 4. Controlled alteration of the neutron field profile.

power is constant), it proved possible to achieve variations of 10-15% in the DPZ current.

Since the action of the standard power regulator compensates for the fundamental harmonic of the neutron field distribution, the dynamical properties of the direct digital control system are basically determined by the time constant of the emission detectors. Experiments with analog correction according to the procedure of [6] and with digital correction of the detectors (a correction based on the first difference was used, which is equivalent in continuous systems to a correction based on the derivative) showed that with proper adjustment the dynamical characteristics of the system are practically unchanged. However, when digital correction is used, it is necessary to take into account the additional load of the machine memory, which is especially significant when there is a large number of detectors.

The relay system with in-phase channel operation was selected as the base system after comparative analysis of the different structures for direct digital control. This structure possesses a number of advantages, among which one should note the simplicity of the analog output system, the great flexibility, and the simplicity of adjustment, which permits executing practically any control algorithms.

One of the most important problems in reactor control is regulation of the total power. It is possible that the necessity, for safety reasons, of an analog power regulator does not diminish for a reactor equipped with computer control. In this case one of the functions of the computer in the control process should be maintaining the AR rods in the most effective position. The following algorithm is a possible way to solve this problem. An error signal is formed in each channel from the sum of the local error, and it is possible to assume to the accuracy of the conversion processes that this signal is proportional to the position of the AR rods.

A transitional process affiliated with the compensation for the disturbance in the reactivity caused by the movement of rod PP_1 upward by 5 cm characterizes the operation of this system (Fig. 3). First the redistribution of DPZ currents is determined by the rapid-acting total power regulator. Further, a synchronous movement of rods K_1 and K_2 returns the AR rod to its original position, and in conclusion a redistribution occurs in the positions of the zone regulation rods in order to obtain the required field shape.

One should include high reliability and mobility in controlling the total power among the merits of this algorithm; the necessity of exact agreement of the settings which determine the field shape with the total power setting is a shortcoming. An algorithm which includes the normalization of the local signal of the neutron field to the average level is free of this disadvantage. In accordance with it a local error signal is determined by comparing the reference value of the field shape with the measured value. The main advantage of the algorithm consists of the independence of the error signal from the power. It has been experimentally confirmed that with appropriate adjustment of the channels a variation in the total power does not result in the actuation of the rods K_1 and K_2.

One should emphasize that in contrast to the schemes discussed earlier the algorithm which includes normalization of the error signal does not ensure regulation of the total power; therefore, the presence of an automatic power regulator becomes a necessary operating condition. In this case the introduction into the algorithm of the regulation of a signal proportional to the integral of the imbalance signal of the total power permits synthesizing a structure combining the advantages of the systems discussed earlier. Actually, this algorithm essentially ensures stabilization of the total power based on a signal from the mismatch amplifier of the standard regulator, maintaining at the same time a specified shape of the neutron field according to signals of the appropriate intrazone detectors. The power required for a specified field shape is determined by a unique setting.

It is important to note that the presence of automatic power regulator rods is not compulsory. An experimental check of the efficiency of a direct digital control system without a regular AR has shown that in this case acceptable quality of the processes is provided both under stabilization conditions (compensation of local disturbances) and in the case of a controlled redistribution of the neutron field. As an example, the transitional processes in the case of the controlled alteration of the field profile — the specification of heteropolar settings — are presented in Fig. 4.

The experiments conducted are only the first step in direct digital control of the neutron field of a reactor. However, the creation of new high-reliability installations with a computer operating in real time and their increasingly widespread introduction into the control systems of atomic electric power plants provide a basis for talking about the practical possibility of using a computer in a closed control loop. The results of the tests on the IRT-2000 reactor of the different structures and algorithms of direct digital control may be useful in the planning of real control systems for large energy reactors.

LITERATURE CITED

1. V. G. Dunaev and P. T. Potapenko, At. Tekh. Rubezhom, No. 12, 10 (1974).
2. E. V. Filipchuk et al., At. Energ., 39, No. 1, 12 (1975).
3. T. Apostolov, I. Uzunov, and A. Markov, in: Testing of the Operation and Use of Research Reactors [in Russian], Symposium of the Council for Mutual Economic Aid, Predyal (1974), p. 813.
4. E. V. Filipchuk et al., At. Energ., 39, No. 2, 90 (1975).
5. Ya. Bouzhik, A. Gadomski, and S. Lyatek, Kernenergie, 19, No. 6, 183 (1976).
6. L. G. Andreev et al., At. Energ., 40, No. 4, 335 (1976).
7. M. G. Mitel'man et al., At. Energ., 39, No. 4, 272 (1975).

TWO-ZONE SYSTEM PULSE METHOD

B. P. Shishin, Yu. A. Platovskikh, and T. S. Dideikin

UDC 621.039.51.12

In theoretical and experimental investigations [1-3] of the behavior of neutron pulses in multizone breeder systems, interest has centered on the principal eigenvalue λ_1, determining the neutron-pulse decay as $t \to \infty$. If the active-zone—reflector system is sufficiently subcritical, λ_1 depends entirely on the reflector properties and, if the system is only slightly subcritical, λ_1 depends predominantly on the active-zone properties [2-3]. In this work it is shown that under certain conditions the main part of the function representing the neutron-pulse decay with time is described by two time constants λ_1 and λ_2, where λ_2 depends mainly on the reflector properties and in particular on its adsorption cross section. Determining λ_1 and λ_2 is intimately connected with finding the reactivity in the given unsteady experiments.

The single-group diffusion approximation with the usual boundary conditions (equality of neutron fluxes and currents at the boundaries of the media and zero neutron flux at the boundary of the system) gives the following equations for the eigenvalues λ_n

$$D_1F_1[\omega_1(\lambda)] = D_2F_2[\omega_2(\lambda)],$$

where $F_1(\omega_1) = \omega_1 J_1(\omega_1 R_1)/J_0(\omega_1 R_1)$; $F_2(\omega_2) = \omega_2[I_1(\omega_2 R_1)K_0(\omega_2 R) + I_0(\omega_2 R_2)K_1(\omega_2 R_1)]/[I_0(\omega_2 R_2)\cdot K_0(\omega_2 R_1) - I_0(\omega_2 R_1)K_0(\omega_2 R_2)]$ for cylindrical geometry; $F_1(\omega_1) = \omega_1 \tan\omega_1 R_1$; $F_2(\omega_2) = \omega_2 \cot\omega_2 h$ for plane and spherical geometry. In the latter case the equation for λ agrees with the

Translated from Atomnaya Énergiya, Vol. 42, No. 5, pp. 370-372, May, 1977. Original article submitted July 13, 1976.

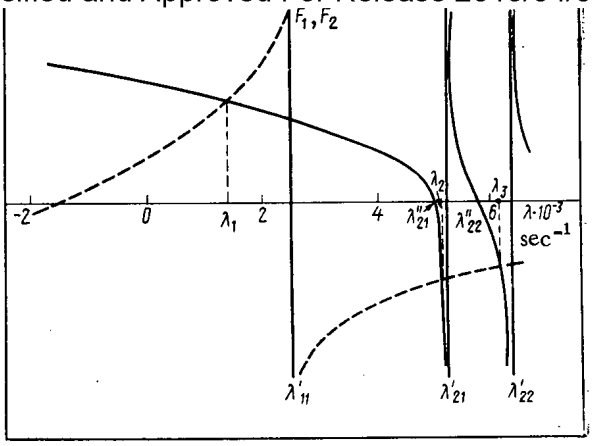

Fig. 1. Behavior of the functions F_1 (dashed line) and F_2 (continuous line).

corresponding equation of [2]. Here R_1 is the radius (or semithickness) of the active zone; R_2 is the external radius of the reflector; h is the reflector thickness; $\omega_1^2(\lambda) = [\lambda - \lambda_\infty - (\overline{vD})_1 B_Z^2]/(\overline{vD})_1$; $\omega_Z^2(\lambda) = [(v\overline{\Sigma_a})_2 + (\overline{vD})_2 B_Z^2 - \lambda]/(\overline{vD})_2$; λ_∞ is the time constant corresponding to an infinite medium with the properties of the active zone; $B_Z^2 = (\pi/H)^2$ is the geometric height parameter (for a finite cylinder of height H); the subscripts 1 and 2 on $\overline{v\Sigma_a}$, $\overline{vD}$, and ω refer to the active zone and the reflector, respectively; Σ_a is the thermal cross section. The value of $\overline{vD}$ determines the slope of the function $\lambda = \lambda(B^2)$ for each medium. To determine the limits on λ_1 and λ_2, the properties of the functions F_1 and F_2 are considered. F_1 and F_2 have the following properties: if λ is equal to λ'_{1n} and λ'_{2n} (the eigenvalues of media 1 and 2 with zero boundary conditions for the neutron flux at their boundaries), F_1 and F_2 have poles; if λ is equal to λ''_{1n} and λ''_{2n} (eigenvalues of each medium with zero boundary conditions for the derivative of the neutron flux at $r = R_1$), F_1 and F_2 have zeros between the poles. It is simple to estimate λ' and λ'' since they correspond to homogeneous media. F_1 is monotonic if $\lambda < \lambda'_{11}$ and F_2 is monotonic if $\lambda < \lambda''_{21}$ (Fig. 1). If $\lambda'_{11} < \lambda'_{21}$ (as in the experiments described below), the least (principal) eigenvalue λ_1 lies within the broad limits $\lambda''_{11} < \lambda_1 < \lambda''_{21}$ and depends on the height and breeder properties of the system. The second eigenvalue λ_2 is close to the pole of F_2 and is found within the limits $\lambda''_{21} = (v\overline{\Sigma_a})_2 + (\overline{vD})_2 \cdot [(\pi/2h)^2 + B_Z^2] < \lambda_2 < \lambda'_{21} = (v\overline{\Sigma_a})_2 + (\overline{vD})_2[(\pi/h)^2 + B_Z^2]$, i.e., between the eigenvalues of reflectors of thickness h and 2h. For a water reflector these limits are narrow.

Thus $\lambda_2 \approx (v\overline{\Sigma_a})_2$ and depends very little on the height and other properties of the active zone and also on the reflector dimensions. Therefore if the reflector height exceeds that of the active zone (as in several of the experiments) λ_2 is largely unaffected. The eigenvalue λ_1 corresponds to a monotonic eigenfunction of the neutron flux density with a maximum at the center of the active zone and λ_2, to an eigenfunction which has a maximum at the reflector and passes through zero close to the boundary of the active zone and the reflector. The formulas obtained for $\omega_1^2(\lambda)$ and $\omega_2^2(\lambda)$ correspond to a linear dependence $\lambda(B^2)$. Taking into account the nonlinearity of these dependences, significant at singularities for the active zone, leaves the conclusions qualitatively unchanged.

In the pulse experiments carried out on a two-zone reactor, the two neutron-density decay constants were found and the relation of these values to the change in the breeder properties of the reactor was established.

The experiments were carried out on a subcritical uranium—water pile surrounded by a supplementary water reflector. End reflection was practically absent. As a protection against thermal-neutron scattering in the pulse experiments the pile was coated with cadmium sheet below and at the sides. In addition, it was placed a distance of at least 1 m from the wall and floor of the chamber. Sampling measurements showed that the neutron-density decay constant in the water of the reflector for a dry active zone with porosity 80% was 4900 sec^{-1}. This value agrees with the constant in an isolated volume of the same order as the reflector volume, and hence scattering of the thermal neutrons makes a negligible contribution to the detector reading. Fast scattered neutrons were recorded in the 50-100-μsec range (this information was not considered).

In the experiments a neutron gas with a neutron-pulse length of 1 μsec was used. The commutation scheme developed allowed information from four SNM-13 neutron counters to be recorded simultaneously on an AI-256 analyzer [4]. The resolution time of the counter—analyzer

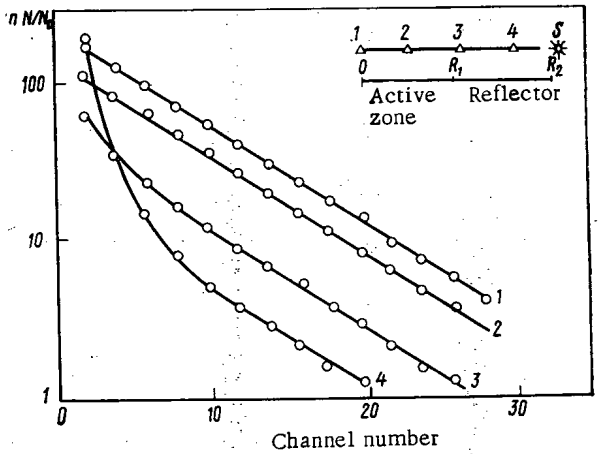

Fig. 2. Time dependence of neutron flux density, recorded by counters (Δ) in the active zone and reflector in pulse experiments (the figures on the curves correspond to the counter numbers; S is the neutron source).

TABLE 1. Results for Neutron Decay Constant

Expt.	State of active zone	State of reflector	Boron concn. in soln., g/liter	Subcriticality ρ/β	λ_1, sec^{-1}	λ_2, sec^{-1}
1	Dry	with H_2O	—	—	—	4900
2	with H_2O	The same	—	3,8	760	5000
3	with H_2O	"	—	4,9	950	5000
4	With boric acid solution	"	0,93	4,3	1420	5100
5	The same	"	0,93	7,9	2400	5000
6	"	With boric acid solution	0,22	3,6	1250	7300
7	"	The same	0,22	5,2	1670	7300
8	"	"	0,87	4,6	1520	13600
9	"	"	0,87	15,5	4490	13050

system was 10-12 μsec. The sites of the counters were at the center of the active zone, at half the radius of the active zone, in the reflector close to the active-zone—reflector boundary, and at the midpoint of the neutron reflector. The ratio of the active-zone or reflector volume to the volume of the SNM-13 counter was 10^4-10^5, and hence the counters had no practically significant effect on the processes in the active zone and the reflector. In the course of the experiments the active zone and the reflector were filled with water or boric acid solutions. The reflector was completely filled; this level remained unchanged in a series of experiments with constant contamination of the active zone with boron. The level of filling of the active zone was varied, thereby altering the degree to which the system was subcritical.

The AI-256 pulse time analyzer recorded the information from the four counters on the neutron-density decay in the reactor after the passage of a short pulse of fast neutrons. Typical results obtained from one of the experiments are shown in Fig. 2.

Analysis of the experiments shows that the neutron-density decay is described in the active zone basically by the function $\exp(-\lambda_1 t)$ and in the reflector by the sum of $\exp(-\lambda_1 t)$ and $\exp(-\lambda_2 t)$. In the whole series of experiments states with $\lambda_2 > \lambda_1$ were observed. The value of λ_2 was constant with constant reflector composition and different degrees of subcriticality of the reactor, but depended significantly on contamination of the reflector by boron; the value of λ_1 depended on the level of filling and boric acid concentration in the active zone and on the reflector properties (see Table 1).

The error in the measurements of λ_1 and λ_2 was ±3%. It follows from the experiments that the asymptotic decay constant λ_1 for the neutron density in the reactor indicates the breeder properties of the reactor, while λ_2 is a physical characteristic of the reflector. This puts in doubt the basis for the method of measuring the degree of subcriticality of two-zone reactors [5], in which the whole of the decay curve for the neutron pulse is used to determine the reactivity.

LITERATURE CITED

1. R. Sher, Nucl. Sci. Eng., 29, 302 (1967).
2. É. A. Stumbur et al., in: Theoretical and Experimental Problems of Unsteady Neutron Transfer [in Russian], Atomizdat, Moscow (1972), p. 282.
3. G. Wells, Trans. Am. Nucl. Soc., 9, 170 (1966).
4. S. P. Volkov and B. P. Shishin, Prib. Tekh. Eksp., No. 1, 95 (1975).
5. A. Walter and L. Ruby, Nukleonik, 8, 287 (1966).

TOTAL REACTION CROSS SECTIONS OF CERTAIN METALS AND GASES FOR VERY COLD NEUTRONS

N. T. Kashukeev, G. A. Stanev,
V. T. Surdzhiiski, and E. N. Stoyanova

UDC 539.125.5.162.2

Research on the storage of ultracold neutrons [1-4] has shown that there is a systematic discrepancy between theory and experiment. To investigate this, the interactions of neutrons with matter were studied at energies close to those of ultracold neutrons (UCN). The interaction of neutrons with certain materials was studied in [5] in the velocity range from 5 to 100 m/sec, and in [6, 7] in the range from 40 to 350 m/sec.

We describe the procedure and apparatus used to measure the interaction of very cold neutrons with certain metals and gases, and list the measured values of the neutron total reaction cross sections for velocities from 100 to 250 m/sec. The range of neutron velocities chosen is of interest since it is close to the range of ultracold neutrons, and also opens up the possibility of studying the interaction of neutrons with the nuclei of samples without the effects of coherent Bragg scattering and surface reflection from the samples. Calculations and experiments showed that the latter is unimportant.

Results of the investigation of the law of interaction of very cold neutrons with certain gases in the velocity range from 60 to 250 m/sec are presented. These results may turn out to be useful in investigating the propagation of ultracold and very cold neutrons in gases, and in the development of the theory of UCN gaseous converters.

Arrangement of Experiments to Study the Interaction of Very Cold Neutrons with Metals and Gases. The measurements were performed at the IRT-2000 reactor in Sofia on a 10-m horizontal channel especially fitted out for this purpose. The total interaction cross sections of samples for very cold neutrons were measured by the transmission method and the results were processed by the least-squares method.

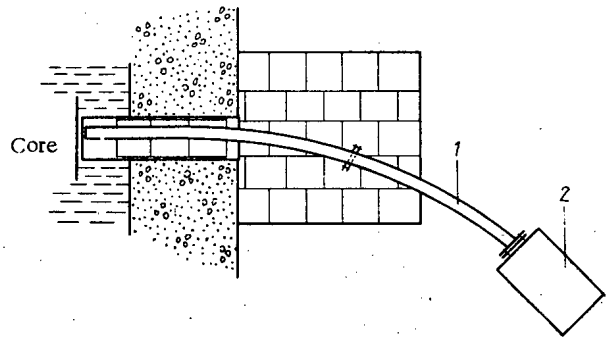

Fig. 1. Experimental channel to study interaction cross sections of metals and gases for very cold neutrons: 1) neutron guide; 2) chopper.

Institute of Nuclear Research and Nuclear Power, Bulgarian Academy of Sciences, Sofia. Translated from Atomnaya Énergiya, Vol. 42, No. 5, pp. 373-377, May, 1977. Original article submitted April 26, 1976.

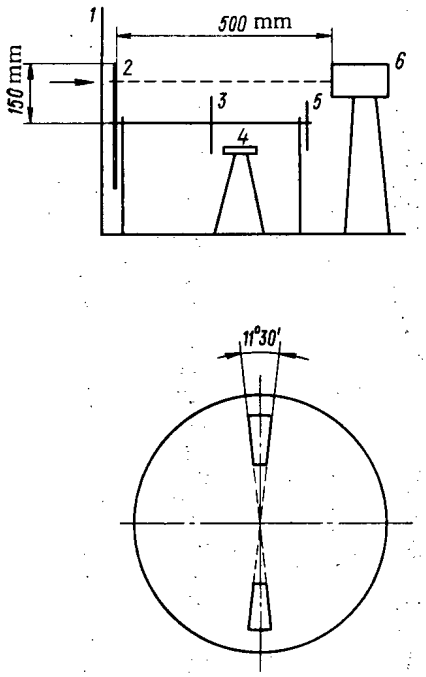

Fig. 2. Mechanical chopper for very cold neutrons: 1) protective screen; 2) flat rotor with two transmitting slits; 3, 4) system for receiving starting signal; 5) disk for attaching second rotor; 6) detector of very cold neutrons.

A beam of very cold neutrons was obtained at the exit of a curved reflecting neutron guide made of an electropolished stainless-steel tube (Fig. 1) inserted to the bottom of the channel. The neutron guide had a radius of curvature of 22 m, a diameter of 0.04 m, and an overall length of 7.37 m. The neutron guide consists of two parts which can be evacuated independently or filled with the gas under study.

The spectrum of the very cold neutrons was analyzed with a special mechanical chopper having a flat rotor with two transmitting slits and operating in a time-of-flight regime (Fig. 2). Experiments in the velocity range from 100 to 250 m/sec were performed with the rotor turning 2500 rpm, a flight path of 0.5 m, and 4 or 11.5° slits. Between the rotor and the detector there was a vacuum tube with a nonreflecting cadmium-plated surface which could be filled with the gas being studied. The very cold neutrons were detected with a helium-filled proportional counter made at Dubna for recording ultracold neutrons [3]. The detector signals were time analyzed with a 400-channel analyzer. Both parts of the analyzer memory were used; each part contains 200 channels each 102.4 msec wide.

The total flux of very cold neutrons incident on a sample was 50 pulses/cm^2•sec. Additional experiments to soften the spectrum or to increase the existing flux by using various converters were unsuccessful since the converters (graphite, aluminum, flowing distilled water) placed on the bottom of the neutron guide were not cooled.

Interaction Cross Sections of Metals. Experiments on the transmission of a beam of very cold neutrons through metal samples were performed for two different positions of the metal plates being studied.

1. A plate was rigidly fastened directly over the opening of the neutron guide in front on the protective screen of the chopper. The beam was measured with and without the sample and the results were compared.

2. A plate of suitable shape was fastened over one of the slits in the rotor and rotated with it. Two peaks were recorded simultaneously in the analyzer (Fig. 3) corresponding to the two slits — the spectra of the beam (1) without the sample and (2) with the sample.

The differences between the cross sections measured with the sample in the two positions were within the limits of error as can be seen from the results for copper and nickel (Table 1). Consequently, the two methods are equally suitable under the present conditions. In both cases the angle at which the detector is viewed from the sample is $\sim$10°.

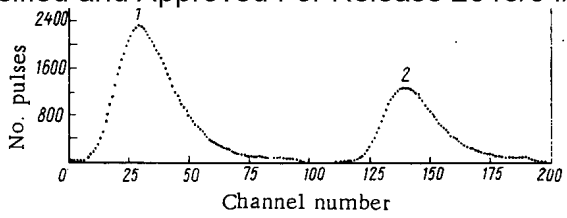

Fig. 3. Peaks corresponding to the two slits in the rotor of the mechanical chopper (silver, d = 0.128 mm, t = 120 mm).

TABLE 1. Neutron Interaction Cross Sections of Metals for v = 100 m/sec, b

Metals	σ_t^*	σ_a (BNL) †
Ag (1; 1) ‡	1356±120	1360
In (2; 1)	4080±370	4180
Cu (2; 1) technical	82±8	81
Cu (1; 1)	84±8	81
Cu (2; 1) electropolished technical	70±7	81
Ni (1: 1)	140±15	100
Ni (2; 1)	145±14	100
Fe (1; 1)	92±10	56
Mo (1; 2)	194±20	55
Mo (1; 3)	203±22	55

*Measured neutron total interaction cross section of sample.

†Neutron absorption cross sections of metals calculated from 1/v law.

‡The first number in parentheses denotes a stationary 1 or rotating 2 sample; the second is the number of plates in the sample.

Recycled neutrons were not observed in any of the measurements, as can be seen from Fig. 3, since there were no neutrons with velocities below 50 m/sec in the beam used.

The background was determined by averaging the number of pulses over all the channels in which the pulse counts were distributed statistically uniformly (no fewer than a hundred channels), and over the whole spectrum when measurements were made with both slits of the chopper rotor covered with cadmium screens. Both methods gave 0.004 pulses/sec per analyzer channel.

The statistical errors quoted for the measurements of the total cross sections were calculated for a neutron beam with an angular spread of 2° and an uncertainty of 0.05 m in the flight path because of the thickness of the detector. These estimates are considerably larger than the statistical spread of the results, since evidently the effective depth of penetration of neutrons into the detector is less than its thickness.

The range of neutron velocities for which the results are reported was chosen from a broader range of neutron velocities, since for this range the statistical errors were small. The results are less reliable for neutrons with somewhat lower velocities because of the very low intensity, and for neutrons of higher velocity because of the decrease of the spectrometer resolving power with increasing neutron velocity. A special channel was constructed to investigate the interaction of lower velocity neutrons.

In order to investigate the role of surface coherent effects for the velocity range studied, measurements were performed with different numbers of plates of the same metal. If these effects play any role in the present case, the results would depend on the number of plates, i.e., on the number of reflecting surfaces. Table 1 shows that two and three plates of molybdenum give practically identical results.

To investigate the absorption cross section and the incoherent scattering cross section, two groups of metals were studied: metals for which the thermal neutron absorption cross section is many times larger than the incoherent scattering cross section (Ag, In, Cu), and

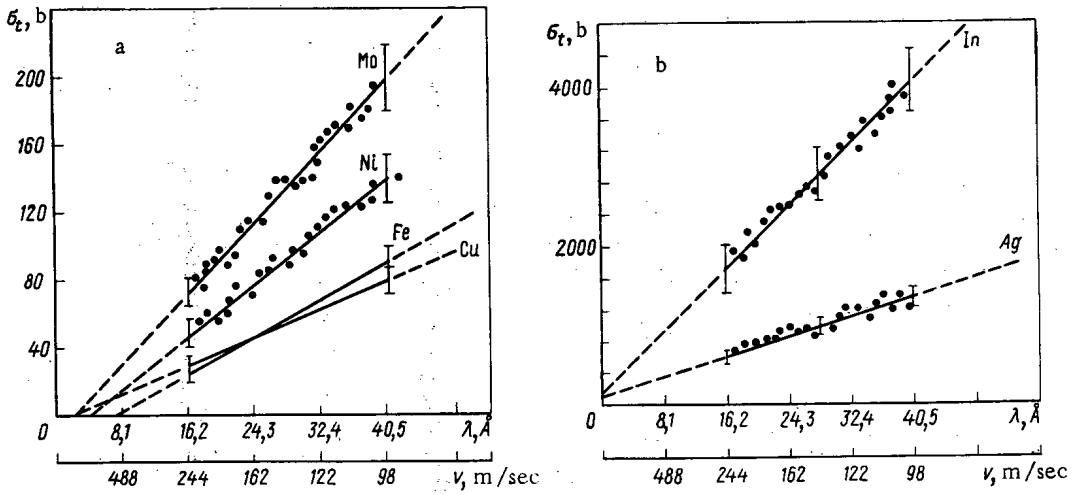

Fig. 4. Total interaction cross sections of certain metals for very cold neutrons as functions of neutron wavelength.

metals for which the incoherent scattering cross section is comparable with the thermal neutron absorption cross section (Ni, Fe, Mo).

Figure 4a and b shows the total interaction cross sections of certain metals for neutrons in the velocity range 100-250 m/sec as functions of the neutron wavelength. In both groups of metals this relation is linear; i.e., the interaction cross section obeys the 1/v law:

$$\sigma(v) = a + b/v. \qquad (1)$$

The total cross sections for weakly absorbing metals (Fig. 4a) become negative when extrapolated to $\lambda = 0$, but these values, like those for metals with large capture cross sections (Fig. 4b), lie within the limits of statistical errors. It is doubtful whether such an extrapolation should be made, however, because of the multiplicity of different interaction processes possible for neutrons with widely different wavelengths.

Table 1 lists values of the neutron total cross sections at 100 m/sec. The absorption cross sections for this velocity were calculated from the thermal values by using the 1/v law. For metals of the first group, the absorption cross sections are the same as the total interaction cross sections, while for metals of the second group there are substantial differences. Thus, the absorption cross sections of metals of the first group obey the 1/v law in the range from 100 to 2200 m/sec. If it is assumed that the absorption cross sections of metals of the second group obey the 1/v law in the 100-2200-m/sec range, then in the 100-250-m/sec range there is another interaction, in addition to absorption, whose cross section obeys the 1/v law.

Table 1 shows that the differences between the measured total cross sections and the absorption cross sections calculated by the 1/v law are not the same for the metals investigated: for Ag, In, and Cu there is no difference; for Ni and Fe the difference is the same (40 b); for Mo the difference is appreciable (140 b).

The additional interaction of neutrons with nickel and iron in the indicated velocity range is apparently related to the domain structure of the samples. For the molybdenum sample the reason for the observed difference is so far not clear. On the basis of further investigations it can be conjectured that the cause of the increase in the neutron total reaction cross section of molybdenum is the small-angle scattering of neutrons by inhomogeneities of the sample. However, this scattering should obey the 1/v law in the velocity range investigated, and is observed at appreciably larger angles, depending on the characteristics of the experimental arrangement.

It should be noted that the measured values of the total cross sections of copper and nickel are in good agreement with the values reported in [5-7] for this velocity range.

The data in Table 1 were obtained for metal samples of 99.95% purity. Some samples of copper, nickel, and iron of technical purity were investigated also; the results obtained do not differ significantly from those for the high-purity samples.

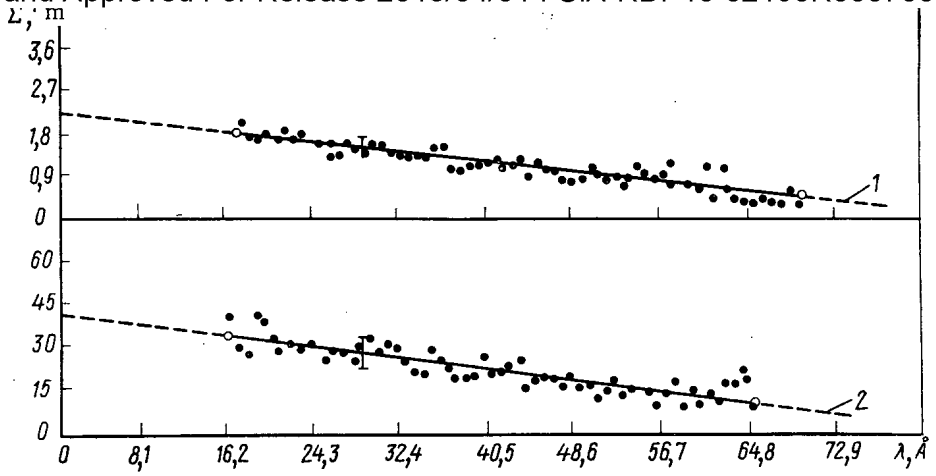

Fig. 5. Mean free path of very cold neutrons as a function of neutron wavelength: 1) tube between chopper rotor and detector filled with nitrogen; 2) outer portion of neutron guide filled with argon (gas pressure — 760 mm Hg).

Total Interaction Cross Sections of Gases for Very Cold Neutrons. Two methods of locating the targets were used in the investigations with gases. The gas filled a straight tube with nonreflecting walls located between the chopper rotor and the detector, or the outer portion of the neutron guide. In this case the geometry of the experiment is relatively good, but the results might be affected by a possible change in the coefficient of reflection of neutrons from the walls of the neutron guide when gas is present. Figure 5 shows the dependence of the neutron mean free path in nitrogen and argon at a pressure of 760 mm Hg on the neturon wavelength. The total interaction cross section varies with neutron velocity according to a hyperbolic law:

$$\sigma(v) = (c - d/v)^{-1}. \qquad (2)$$

The quantity u = 2d/NL, where N is the nuclear density of the gas and L is the length of the tube, has the same value as the mean-square velocity of the gas molecules.

It should be noted that the neutron total interaction cross sections of gases appear to deviate from (2) for lower neutron velocities.

Further studies will be made for different temperatures of the gas targets and for gases with substantially different molecular weights.

The authors thank A. V. Antonov, V. M. Iobashov, I. M. Frank, and Khr. Ya. Kristov for their stimulating interest in the work; V. V. Golikov, V. I. Lushchikov, A. V. Strelkov, and Yu. V. Taran for helpful discussions of the results.

LITERATURE CITED

1. F. L. Shapiro, JINR Preprint R3-7135, Dubna (1973).
2. L. V. Groshev et al., JINR Preprint R3-5392, Dubna (1970).
3. L. V. Groshev et al., JINR Preprint R3-7282, Dubna (1973).
4. I. M. Frank, JINR Preprint R3-7810, Dubna (1974).
5. A. Steyerl and H. Vonach, Z. Phys., 250, 166 (1972).
6. W. Dilg and W. Mannhart, Z. Phys., 266, 157 (1974).
7. R. Lermer and A. Steyerl, Phys. Stat. Sol. (a), 33, 531 (1976).

RESULTS OF TESTING CARBIDE FUEL ELEMENTS IN THE BOR-60 REACTOR

V. A. Tsykanov, V. M. Gryazev,
E. F. Davydov, V. I. Kuz'min,
A. A. Maershin, V. N. Syuzev,
I. S. Golovnin, T. S. Men'shikova,
Yu. K. Bibilashvili, R. B. Kotel'nikov,
V. S. Mukhin, and G. V. Kalashnik

UDC 621.039.542.344

A great deal of attention has been given recently to the investigation of carbide fuel for fast power reactors with higher thermal conductivity and a larger number of heavy atoms than oxide fuels; this makes it possible to reduce the doubling time, increase the multiplication factor, and thereby make the operation of fast reactors more efficient. In this paper we present some results of a study of the behavior of carbide fuel and carbide fuel elements under irradiation; these were used in the BOR-60 reactor to a burnup of 10% of the heavy atoms (h.a.).

Characteristics of Bundles and Fuel Elements. Each of the four irradiated bundles contained 19 fuel elements. In two bundles there were three fuel elements each with a sodium–potassium layer. In the other fuel elements, the gap between the jacket and the core was filled with helium. The construction of the bundles and the fuel elements has been described earlier [1]. The density of the fuel pellets was 90-96% of the theoretical value, and the carbon content was 4.7-5.1% by mass. If we take account of the oxygen and nitrogen content, the mole ratio (C + O + N)/U ranged from 0.98 to 1.08. The cores were constructed by pressing and baking, and also by hot pressing of the original carbide powders obtained by gas

TABLE 1. Parameters for the Testing of Fuel Elements with Carbide Fuel

Maximal irradiation regime	Bundle			
	I	II	III	IV
Burnup, % h.a.	3,5	5,1	7,1	10,4
Fluence of neutrons · 10^{-22}, neutrons/cm²				
for E > 0 MeV	2,1	3,5	5,1	7,6
for E > 0.1 MeV	1,7	2,8	4,1	6,1
Linear power, W/cm	550	550	560	700
Temp. of jacket, °C	600	600	650	680
Calculated temp. at center of fuel element with helium layer, °C*	1120	1120	1160	1300
Operating time at power, h	5760	8570	11500	13600

*The thermal conductivity of the fuel was taken to be 0.15 W/cm·deg C; the conductivity of the contact between fuel and jacket was taken to be 1 W/cm²·deg C.

TABLE 2. Balance of Volume Variation in Fuel Elements under Irradiation up to a Burnup of 10.4% h.a., Expressed as % of the Initial Volume within the Fuel-Element Jacket along the Active Part

Part of fuel element	Before irradiation	After irradiation	Change in volume
Jacket	100/100	104,6/105,2	+4,6/5,2
Core,	88,6/85,8	104,6/105,2	+16,0/19,4
including:			
fuel	73,8/79,7	75,2/81,1	+1,4/1,4
pores	4,8/5,1	17,9/23,9	+13,1/19,7
cracks	0/0	0,6/0,7†	+0,7/0,7
central cavity	10,1/0	10,9/0	+0,8/0
Gaps,	11,2/14,0	0/0	—11,2/14,0
including:			
radial	6,3/9,1	0/0	—6,3/9,1
axial	4,9/4,9	0/0	—4,9/4,9

*The data in the numerator refer to fuel elements with a plug core, those in the denominator fo fuel elements with pellet cores.
† Estimate.

Translated from Atomnaya Énergiya, Vol. 42, No. 5, pp. 378-382, May, 1977. Original article submitted October 4, 1976.

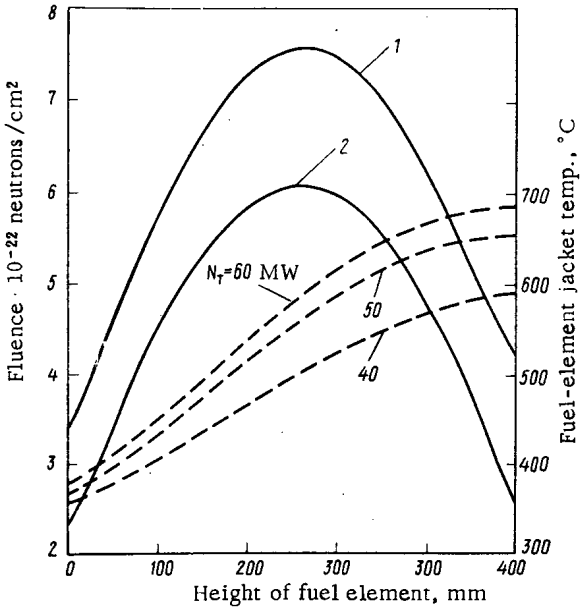

Fig. 1. Distributions of neutron flux for E > 0 (1) and >0.1 MeV (2) and maximum fuel-element jacket temperature as functions of active-zone height.

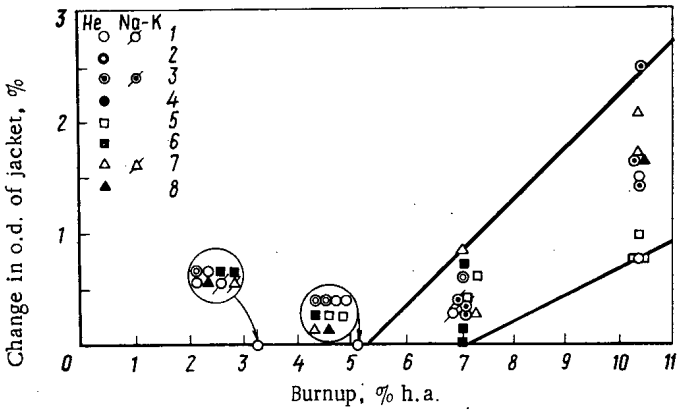

Fig. 2. Variation of outer diameter of the fuel-element jacket as a function of burnup: 1, 2, 3, 4) gas carbidization: pellets, plugs, pellets with covering, and with UC—PuC, respectively; 5, 6, 7, 8) carbothermal reduction: pellets, plugs, hot-pressed pellets, and pellets with covering, respectively.

carbidization of powdered uranium and carbothermal reduction of uranium dioxide [2-4]. Two fuel elements had a mixed fuel containing ∿15% PuC by mass. The diametral gap between the pellets and the jacket varied from 0.12 to 0.4 and from 0.2 to 0.6 mm, respectively, for the fuel elements with a helium layer and those with a sodium—potassium layer. The ^{235}U enrichment was 90%. The jacket was made of 0Kh16N15M3B stainless steel, with an outer diameter of 6.9 mm and a wall thickness of 0.4 mm. In five fuel elements the fuel pellets had a chromium—niobium-based covering.

Test Parameters. All the bundles were tested in the fifth row of the active zone of the BOR-60 reactor (Table 1). The distributions of the neutron flux and of the maximum jacket temperature for different reactor power levels are shown as functions of active-zone height in Fig. 1.

Condition of the Fuel Elements. The condition of the fuel elements and bundles after the test was satisfactory. All the fuel elements remained airtight. The change in the outer diameter of the jacket was observed after 5% h.a. burnup, and at the maximum burnup value of 10.4% h.a. it amounted to 0.8-2.5% (Fig. 2).

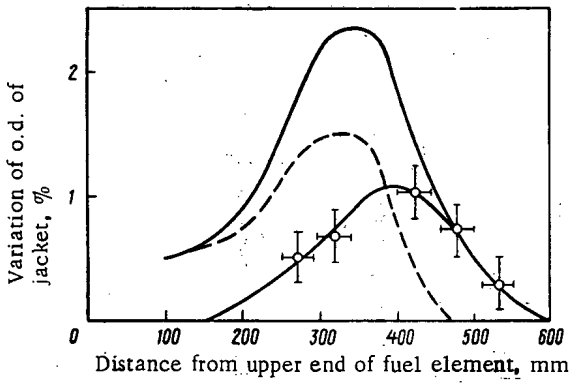

Fig. 3. Variation in outer diameter (solid curve), plastic deformation (dashed curve), and diametral swelling of jacket (solid curve with circles) as functions of fuel-element active-zone height.

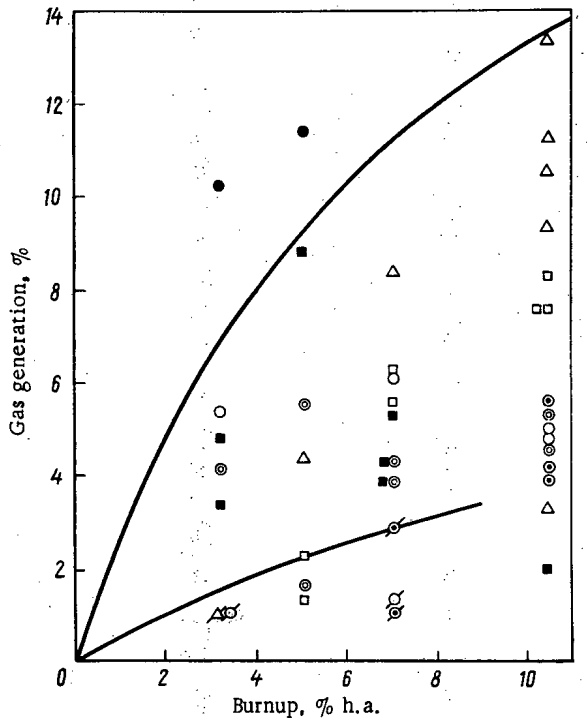

Fig. 4. Variation of relative flow rate of gaseous fragments from fuel as a function of burnup (same legend as Fig. 2).

Estimates made on the basis of the change in the density of the steel jacket by the method of hydrostatic suspension showed that for a fast-neutron fluence of $6 \cdot 10^{22}$ neutrons/cm^2 ($E > 0.1$ MeV) the increase in the diameter as a result of jacket swelling [for isotopic swelling $\Delta d/d = (1/3)\Delta V/V$] was (0.8-1.0) ± 0.2% (jacket temperature 500°C). The remainder of the change in the jacket diameter was apparently caused by a deformation of the steel under the pressure of the swollen fuel.

The plastic deformation of the jacket, calculated as the difference between the total change in diameter and the diameter increment due to the swelling of the jacket material at a burnup value of 10.4% h.a., was 0-1.5%, i.e., constituted up to 60% of the total change in the jacket diameter. The change in the outer diameter due to the swelling of the jacket material and to plastic deformation of the jacket along the height of the active part of a fuel element used to a burnup of 10.4% h.a. is shown in Fig. 3.

The relative flow rate of fission-fragment gases from the fuel element under the jacket at a core temperature of less than 1300°C was 2-12% and 1-3% for fuel elements with helium and sodium—potassium layers, respectively (Fig. 4), and increased somewhat with increased burnup.

Balance of Volume Variation in Fuel Elements under Irradiation. Data on volume changes for the irradiation of fuel elements with different carbide cores are given in Table 2.

Deformation of the Jacket. Experimental data on the deformation of the fuel-element jackets were investigated by the method of regression analysis. We studied the variation of the relative deformation with the different forms of free spaces in the fuel element, with

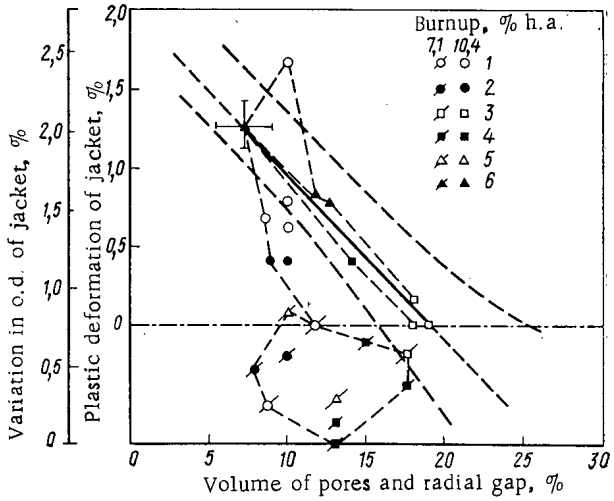

Fig. 5. Variation of the outer diameter and plastic deformation of fuel-element jackets as functions of the porosity of the fuel and the radial gap: 1, 2) UC, gas carbidization: pellets and plugs; 3, 4, 5, 6) UC, carbothermal reduction: pellets, plugs, hot-pressed pellets, and plugs, respectively; +) confidence interval 0.9; ---) boundaries of region of reliable values.

the presence of an axial cavity, and with the properties of the techniques by which the carbide and the core were obtained. The analysis was carried out for fuel elements irradiated to burnup values of 7.1 and 10.4% h.a. To construct the regression models, we used the most efficient step method [5]. For fuel elements irradiated to a burnup value of 10.4% h.a. we found that the jacket deformation depended only weakly on the effective fuel density (effective density is the ratio of the fuel mass to the volume inside the jacket along the active part of the fuel element) and did not observe any effect produced by the central cavity and the techniques by which the carbide and the cores were obtained. The best correlation was found for the sum of the values for the fuel porosity and the radial gap (Fig. 5). It follows from Fig. 5 that in order to obtain zero plastic deformation (the dot—dash line) for given irradiation conditions, the total volume of the pores in the fuel and the radial gap must be ∿20%.

Variation in Fuel Structure. The typical structure of the irradiated fuel (Fig. 6) indicates that there is no marked grain growth; this is in agreement with the calculated estimate for a relatively low fuel temperature (1300 and 1150°C for pellet and plug cores, respectively). In most of the investigated cross sections of the fuel elements, we found cracking of the core after irradiation.

The main change in the carbide-fuel structure under irradiation consists in the formation of pores. The dependence of this process on the irradiation temperature, the burnup, and, probably, the granularity and chemical composition of the fuel is very complicated. At a temperature above 1000-1100°C the fuel forms pores with a diameter of more than 0.1 μ, which are visible with an optical microscope and are homogeneously distributed through the grain at a burnup value of up to 5% h.a. An increase in temperature and burnup leads to the preferential formation of large pores along the boundaries of the grains, and in a number of cases to a merging of the pores on the boundaries oriented perpendicular to the thermal gradient (Fig. 6b). At a temperature of ∿1300°C and a burnup of 10% h.a. we found that the interconnected porosity changed to isolated porosity (Fig. 6c). Metallographic investigation of the irradiated fuel did not reveal any phases containing fission products, apparently as a result of their high degree of dispersion due to the relatively low irradiation temperature.

The uranium dicarbide present in the superstoichiometric fuel in the form of numerous inclusions was dissolved under irradiation. This may be due to the fact that the oxygen stabilizing the dicarbide is bound by the fragment elements [6]. The 0.4% decrease in the monocarbide lattice parameter (Fig. 7) for 10% h.a. burnup indicates considerable solubility in it of the fission products (zirconium, molybdenum, etc.).

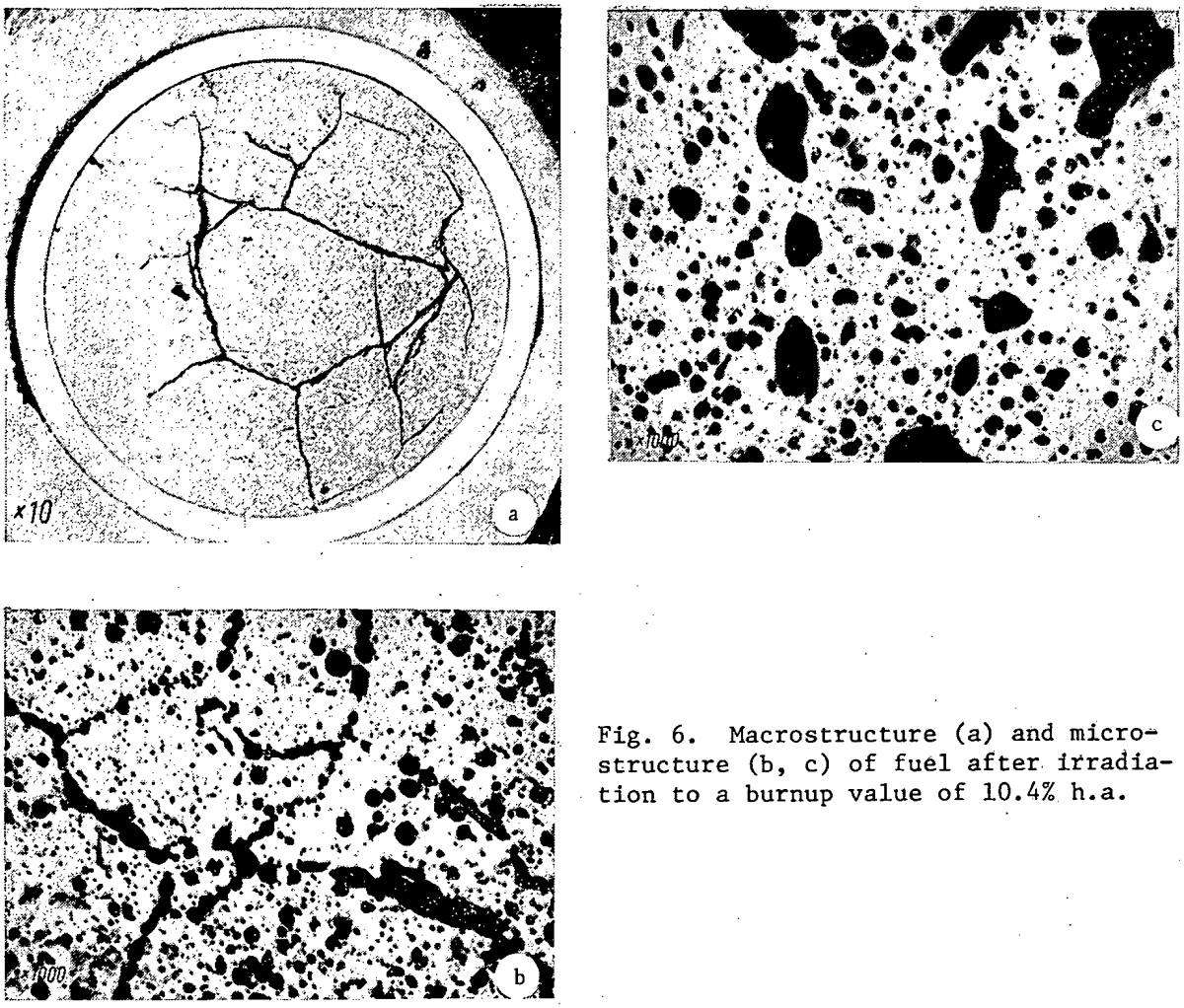

Fig. 6. Macrostructure (a) and microstructure (b, c) of fuel after irradiation to a burnup value of 10.4% h.a.

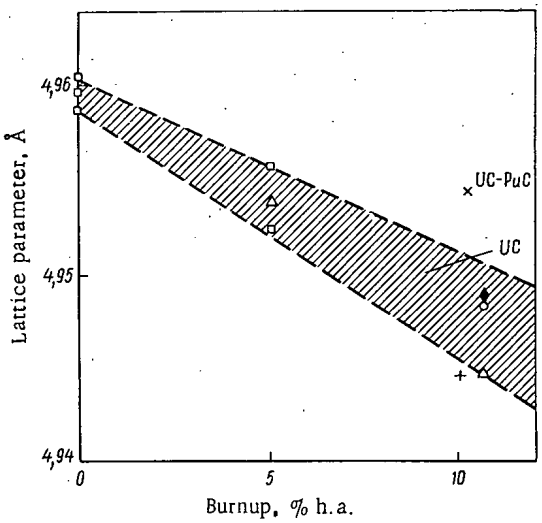

Fig. 7. Variation of the uranium monocarbide lattice parameter as a result of irradiation: ○) gas carbidization; □) carbothermal reduction; Δ) hot pressing; ×, +) simulators with 0.3 and >0.5% O; ◆) UC + Cr.

Swelling of the Fuel. The swelling of the fuel was determined on the basis of the change in density and in the geometric dimensions of the fuel briquettes. When the core center temperature was 1200 ± 50°C, the average rate of swelling was 1.5 ± 0.2 and 1.2 ± 0.4% per 1% burnup on the basis of the density change and the geometric-dimension change, respectively.

TABLE 3. Carbonization of the Jacket in the Case of Fuel Elements with a Helium Layer (burnup 10.4% h.a.)

Jacket characteristics	Carbon content of fuel, % by mass			
	4,7	4,82	4,9	4,95
Max. depth of the zone of interaction, μ	150	120	150	150
Microhardness kg/mm²:				
interaction zone	350	500	360	350
outside zone of interaction	260	300	300	300
Av. carbon content of jacket, % by mass	—	0,14	0,14	0,16

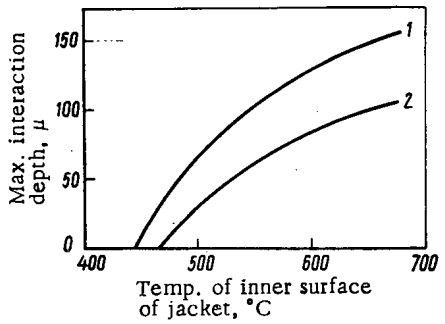

Fig. 8. Variation of depth of the zone of interaction in fuel elements with a helium layer as a function of temperature: 1) carbothermal reduction; 2) gas carbidization.

On the basis of data on the change in the dimensions of the fuel column in the axial and diametral directions, we estimated the degree of anisotropy of the swelling, which was found to be 1.3. The average value of the anisotropy coefficient indicates that the core swells somewhat more in the radial than in the axial direction.

Compatibility of the Fuel and Jacket. The carbonization of the jacket — one of the problems involved in the use of carbide fuel — is most dangerous when there is a heat-conducting liquid metal layer between the fuel and the jacket. When a helium layer is used, the carbonization is slight; we found that the carbon content of the fuel in the range from 4.7 to 4.95% by mass did not substantially affect this process (Table 3).

In fuel elements with mixed uranium—plutonium fuel irradiated to burnup values of 3 and 5% h.a., the depth of the zone of interaction did not exceed 20 μ. The variation of the depth of the zone of interaction in fuel elements with a helium layer (burnup value 10.4% h.a.) as a function of temperature is shown in Fig. 8.

In fuel elements with a sodium—potassium layer that were irradiated to burnup values of 3.3 and 7.1% h.a., the maximum depth of the interaction zone was found to be 100-150 and <50 μ for a carbon content in the fuel of 5.1 and <5.0% by mass, respectively [1]. The use of coverings (preferably with a chromium and niobium base) on the fuel pellets practically prevents the carbonization of fuel-element jackets with either a helium or liquid metal layer, and the depth of the zone of interaction does not exceed 30 μ.

Thus, the test in the BOR-60 reactor showed the real possibility of achieving 10% h.a. burnup values in fuel elements with carbide fuel at a maximum linear power of 550-700 W/cm and a jacket temperature of up to 680°C. A study of the behavior of carbide fuel elements at higher levels of thermal load and temperature, as well as the search for an optimal fuel-element structure, will be a problem for further investigations.

LITERATURE CITED

1. E. F. Davydov et al., At. Energ., 39, No. 1, 33 (1975).
2. G. A. Meerson et al., At. Energ., 9, No. 6, 387 (1960).
3. F. G. Reshetnikov et al., At. Energ., 35, No. 6, 377 (1973).
4. I. S. Golovnin et al., At. Energ., 30, No. 2, 211 (1971).
5. N. Draper and H. Smith, Applied Regression Analysis, Wiley (1966).
6. R. B. Kotel'nikov et al., At. Energ., 39, No. 4, 255 (1975).

MEASUREMENT OF THE EFFECTS OF THE REACTIVITY OF MATERIALS IN A FAST REACTOR

V. R. Nargundkar, T. K. Bazu,
K. Chandramoleshvar, P. K. Dzhob,
and Rao K. Subba

UDC 621.039.519

The Plutonium Reactor for Neutronic Investigations in Multiplying Assemblies (PURNIMA) [1-3] was designed to study the physical parameters of the KPFR reactor [4]. The fuel element (Fig. 1) of this assembly consists of high-density PuO_2 pellets in a stainless-steel jacket. An 18-cm-high column of pellets is bounded on both ends by 8-cm-thick molybdenum and reflectors. The fuel elements are rigidly fixed on top in a supporting grid. The core has the form of an asymmetric hexahedron. The core is surrounded by a 17-cm-thick copper reflector and a 23-cm-thick steel shield. In the shut-down state the core is completely withdrawn from the region surrounded by the reflector.

The effectiveness of a fuel element as a function of its position in the core was measured in order to estimate its possible use in a scram system such as in the IBR reactor [5, 6]. Measurements of the effects of the reactivity of samples of various materials in the core were also compared for their possible use as scram elements in the KPFR reactor. The same analysis was performed when the samples were placed at a definite location inside the copper reflector in order to estimate the effectiveness of the materials as control elements in the KPFR reactor.

Measurement Procedure. The following detectors were used to measure neutron multiplication in the subcritical system:

a fission counter containing 10 mg of ^{235}U having the shape of a fuel element and located at the core center;

a neutron counter with 1.6 g of ^{235}U surrounded by paraffin and located at the outer edge of the steel shield;

a neutron counter with 180 mg of boron located inside the copper reflector.

Six Pu—Be sources of strength $\sim 10^7$ neutrons/sec, also made in the shape of fuel elements, were introduced to increase the counting rate in the core. A schematic plan of the location of the detectors and sources is shown in Fig. 2.

Multiplication was measured by using a previously calibrated standard rod [7]. The effective delayed neutron fraction was assumed equal to 0.002. The subcriticality of the reactor Δk under operating conditions when the core is surrounded by the copper reflector is given by the relation

$$\Delta k = \rho_{shim} \frac{C_{shim}}{C_{shim} - C_{core}},$$

Department of Neutron Physics, Bhabha Atomic Research Center, Trombay, India. Translated from Atomnaya Énergiya, Vol. 42, No. 5, pp. 383-386, May, 1977. Original article submitted November 15, 1976.

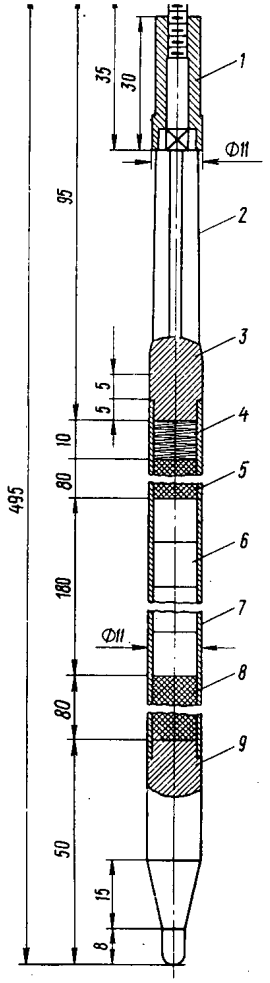

Fig. 1. Fuel element: 1) nut; 2) 1°12' cone; 3) steel upper plug; 4) steel spring; 5) molybdenum; 6, 8) PuO_2 pellets; 7) 0.3-mm-thick steel jacket; 9) steel lower plug.

where ρ_{shim} is the effectiveness of the standard rod, C_{shim} is the counting rate under operating conditions when the standard rod is introduced into the core, and C_{core} is the counting rate under operating conditions when the standard rod is withdrawn. The effectiveness of any sample under investigation was determined from the expression

$$W = (\Delta k)_T - (\Delta k)_0.$$

Here $(\Delta k)_T$ and $(\Delta k)_0$ are, respectively, the values of the subcriticality in the absence of the standard rod with and without the sample under study.

In measuring the effectiveness of fuel rods, the core was removed from the reflector and transferred to the loading device. The fuel element was replaced by a copper "dummy" and the core was returned to its original location. The uncertainty in the measurement of reactivity in this operation was found previously experimentally to be ±0.05β.

A dismountable rod in the shape of a standard fuel element with a removable upper plug was used to estimate the effectiveness of the material under investigation. The sample being studied was 18 cm high, the same as the column of pellets. It was placed between the upper and lower molybdenum plugs, each 8 cm high. In this way the effectiveness of the whole rod including the molybdenum plugs was determined.

It was not necessary to transport the core to measure the effectiveness of control rod materials. To shift samples, the core was dropped down to a position ensuring reactor shutdown. In this case the return of the core to the initial state introduces an error of ±0.01β. Most of the test samples were of standard control rod size, 4 cm in diameter and 18 cm high. The samples were fixed vertically in a straight-through channel in the copper neutron reflector by special holders. The effectiveness of the samples was determined relative to an empty channel.

Experimental Results. Table 1 lists data on the effectiveness of fuel elements relative to the state without a fuel element as a function of the distance from the core center (Fig. 3).

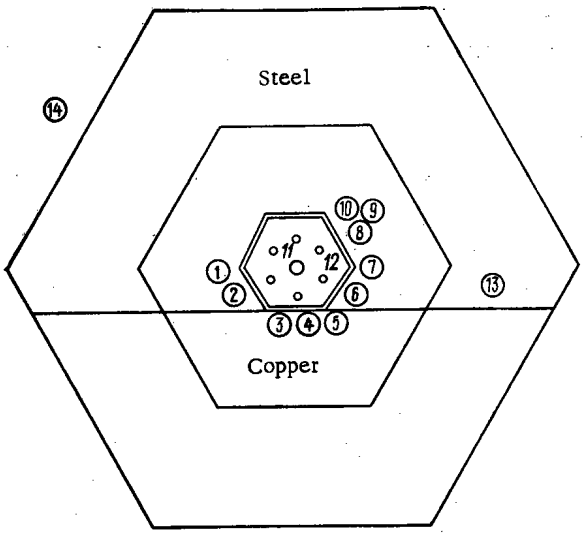

Fig. 2. Schematic diagram of PURNIMA I assembly: 1-4, 6, 7) safety rods; 5) measuring channel for samples; 8) coarse control; 9) fine control; 10) standard rod; 11) fission counter for in-core measurements; 12) Pu—Be neutron source; 13) BF_3 counter; 14) fission counter.

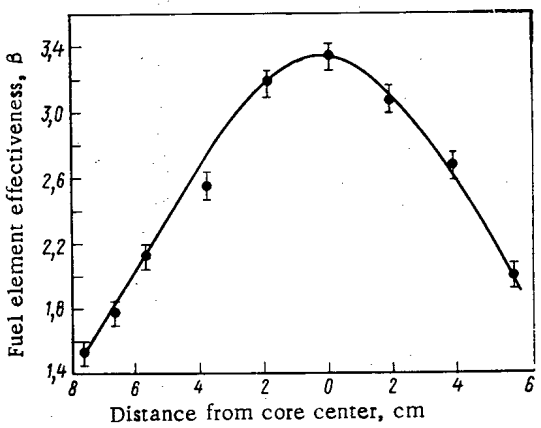

Fig. 3. Effectiveness of PuO_2 rod as a function of its distance from the center of the PURNIMA I core assembly.

Since the measurement was performed with respect to the state with a copper fuel element, the values were obtained by taking account of the corresponding effectiveness of the copper fuel element. It is easy to see that the effectiveness of a fuel element $(3.33 \pm 0.1)\beta$ at the core center falls to $(1.53 \pm 0.06)\beta$ at the periphery. The theoretical effectiveness of a peripheral fuel element is 1.61β [8], in good agreement with the experimental value. The effectiveness of a fuel element at a distance of 3.8 cm, characterizing the average distance from the core center, is $(2.71 \pm 0.08)\beta$, and is in good agreement with the value 2.77β calculated for the average effectiveness of a fuel element by starting from the critical loading for 180 fuel elements.

For most of the nonfissionable heavy metals the effectiveness at the core center is $(0.45 \pm 0.05)\beta$. This indicates that in the present case the reactivity is changed because of a decrease in neutron leakage in the axial direction, and that the absorption of neutrons in the samples is small. A higher effectiveness at the core center for plastic, natural uranium, and a copper—beryllium alloy results from a decrease in axial neutron leakage and an increase in fission density in the sample itself or in neighboring fuel elements as a result of a change in the neutron spectrum.

The measured values of the effectiveness of samples of various materials are shown in Table 2. The values of the effectiveness of a copper sample at the core center and at the periphery are $(0.41 \pm 0.05)\beta$ and $(0.51 \pm 0.05)\beta$, respectively. For molybdenum, these values are $(0.52 \pm 0.05)\beta$ and $(0.59 \pm 0.05)\beta$. The increase in effectiveness from the center toward the periphery is due to the good scattering properties of the materials. For natural uranium

Elements in PURNIMA I Core as a Function of Radial Position

Distance from core center, cm	Effectiveness of fuel element in units of: β	rel.	Distance from core center, cm	Effectiveness of fuel element in units of: β	rel.
0	3,33±0,10	1,00	5,7	2,04±0,06	0,61
1,9	3,13±0,10	0,94	6,6	1,76±0,06	0,53
3,8	2,71±0,08	0,81	7,6	1,53±0,06	0,46

Core Center and Periphery

Material of sample	Mass, g	Effectiveness in units of β	
		at center	at periphery
PuO_2	142	3,33±0,10	1,53±0,06
Plastic	13,8	0,99±0,05	0,75±0,05
Natural uranium	257	0,98±0,05	—
Be–Cu alloy (18% Be by vol.)	65	0,76±0,05	—
UO_2	138	0,72±0,05	0,59±0,05
Molybdenum	141	0,52±0,05	0,59±0,05
Stainless steel	106,6	0,47±0,05	—
ThO_2	121	0,46±0,05	—
Copper	123,6	0,41±0,05	0,51±0,05
Thorium	156	0,40±0,05	—

TABLE 3. Effectiveness of Standard-Sized Control Rod Simulators Relative to Air

Material	Mass, kg	Effectiveness in units of β	Effectiveness, 10^{-2} β/g·mole
Be (height H = 20 cm)*	0,470	1,42±0,04	2,72
Natural uranium (H = 16.8 cm, diameter 3.5 cm)	3,000	1,00±0,04	7,85
Molybdenum	2,295	1,07±0,03	4,51
Copper	1,990	1,05±0,03	3,37
Graphite	0,410	1,04±0,03	3,05
Stainless steel	1,785	1,01±0,03	3,16
Elmet (tungsten alloy H = 20 cm)*	4,500	1,00±0,03	1,05
Mild steel	1,770	0,84±0,03	2,62
Aluminum	0,605	0,68±0,03	3,05
Titanium	1,015	0,62±0,03	2,83
Boron carbide	0,324	−0,29±0,04	−4,93
Plastic	0,272	−0,35±0,04	−12,9
Teflon	0,210	−0,99±0,03	−47,0

*Nonstandard size.

dioxide and plastic, the effectiveness is decreased from (0.72 ± 0.05)β and (0.99 ± 0.05)β at the core center to (0.59 ± 0.05)β and (0.75 ± 0.05)β at the periphery, respectively. The decrease in effectiveness of uranium dioxide is accounted for by the decrease in fission density, and of plastic by the absorption of reflected and moderated neutrons at the core periphery.

The measured values of the effectiveness of control rod simulators 18 cm long and 4 cm in diameter (Table 3) show that the beryllium and natural uranium samples give a maximum effect for the given dimensions. The large negative effect of the Teflon sample is due to the absorption of reflected and moderated neutrons.

CONCLUSIONS

It has been established that the effectiveness of fuel elements is quite adequate to permit their use as fast safety rods. This conclusion agrees with the experience accumulated in the course of the design and operation of the IBR reactor. The ejection of rods from the KPFR reactor core can be aided by compressed springs. It has been shown that the reactivity can be decreased by the rapid withdrawal of one beryllium or plastic rod, as provided for in the KPFR reactor. Standard-sized beryllium or natural uranium rods can be used as conventional control and safety elements. The large negative effect of Teflon permits its use as a supplementary material in scram systems to increase the effect of reactivity.

The authors thank M. Srinivasan and K. S. Pasupasi for help in performing the experiment.

LITERATURE CITED

1. P. Iyengar et al., in: Proceedings of the Indo—Soviet Seminar on Fast Reactors, Kalpakkam, India (1972), p. 249.
2. P. Iyengar, in: Proceedings of the IAEA Symposium on Irradiation Facilities for Research Reactors, Teheran (1972), p. 375.
3. V. Nargundkar et al., PURNIMA-PuO_2 Fueled Zero Energy Fast Reactor (to be published).
4. P. Iyengar, Workshop on Intense Neutron Sources, BNL, May (1973).
5. I. I. Bondarenko and Yu. Ya. Stavisskii, At. Energ., 7, No. 5, 417 (1959).
6. G. E. Blokhin et al., At. Energ., 10, No. 5, 437 (1961).
7. S. Das and M. Srinivasan, Atomkernenergie, 27, 18 (1976).
8. P. Iyengar et al., BARC/I-134 (1971).

THE EFFECT OF A HIGH-FREQUENCY CURRENT IN A HELICAL WINDING ON THE DISCHARGE IN THE TO-1 TOKAMAK

L. I. Artemenkov, N. V. Ivanov,
A. M. Kakurin, and A. N. Chudnovskii

UDC 621.039.623

A number of studies [1-9] have been made in recent years of the possibility of using an inverse feedback arrangement to stabilize helical instabilities in a plasma filament of a tokamak. The present article describes the results of the first stage of such an investigation, carried out on the TO-1 tokamak. This stage involved the study of the effect on the discharge of a current of a given frequency flowing through a helical winding in a TO-1 chamber, giving main consideration to probe measurements of the poloidal magnetic field at the chamber walls.

The TO-1 tokamak device is of relatively small size with specific characteristics: instead of using a conducting casing, it maintains the plasma filament in equilibrium by means of a system of control windings [10]. The vacuum chamber is made of 1-mm-thick stainless steel and has large and small radii of 60 and 18 cm, respectively. The radius of the diaphragm is 12.5 cm.

The helical winding of the TO-1 (Fig. 1) is a helical quadrupole with m = 2, n = 1, and left-hand rotation. The winding consists of four plane stainless-steel strips fastened within the chamber at four equally spaced points around the circumference. The strips, which are 3 mm thick and 50 mm wide, are positioned in the shadow of the diaphragm at a distance of 35 mm from the wall of the chamber and are not separated from the plasma by a dielectric.

No experimental observations have been made of any effects due to the shunting of the uninsulated helical winding across the plasma at frequencies in the range 1-200 kHz, for various amplitudes of winding current, and for various regimes of the tokamak discharge pulse. The shunting involves the danger of the possible presence in the shadow of the diaphragm of a plasma of comparatively high concentration which in principle could have a fairly large conductivity and dielectric permittivity. At frequencies that are several tens of megahertz higher, the effect of shunting the uninsulated conductor by the plasma at the boundary of the tokamak has been experimentally discovered [11].

The main portion of the work was carried out on hydrogen at an initial gas pressure in the chamber of $8 \cdot 10^{-4}$ mm Hg. The toroidal magnetic field intensity was varied within the

Translated from Atomnaya Énergiya, Vol. 42, No. 5, pp. 387-390, May, 1977. Original article submitted July 2, 1976.

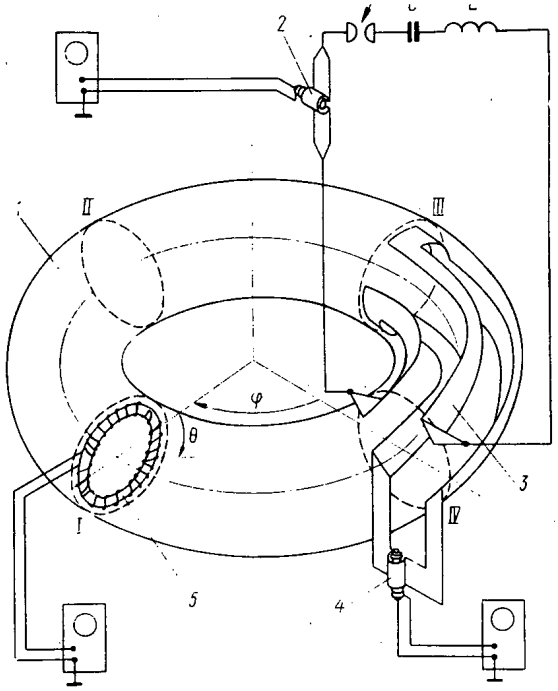

Fig. 1. Schematic diagram of the arrangement of the helical winding and magnetic probes in the chamber of the TO-1 tokamak: 1) toroidal chamber; 2, 4) detectors of the current in the helical winding; 3) helical winding; 5) magnetic Fourier probe.

range 4-8 kOe. The discharge pulse lasted 100-150 msec and was rectangular in shape, with an amplitude of 15 kA.

At a given instant in time, relative to the beginning of the discharge pulse of the tokamak, an external circuit was used to excite a train of 10-15 cycles of damped oscillations of the current in the helical winding. The frequency of these oscillations was 20 kHz and their initial amplitude was 1.5 kA. The excitation of the current in the helical winding was accompanied by the appearance of signals of the magnetic probes measuring the alternating magnetic field near the wall of the chamber. The magnetic probes were positioned at two cross sections of the chamber, indicated in Fig. 1 by numerals I and II. They were designed for a spatial harmonic analysis of the perturbation of the magnetic field at the given cross sections, and were a set of four coils wound on a ring-shaped form surrounding the plasma filament. The density of turns in the winding of each coil varied along the form according to a harmonic law; i.e., it was proportional to $\sin m(\theta - \theta_0)$, where m = 2, 3, 4, 5. With the probe construction used, it was possible to arbitrarily vary the phase of the winding θ_0. In addition to the Fourier probes, the same cross sections of the toroidal chamber contained local probes for recording the distributions of the poloidal and toroidal components of the alternating magnetic field at the wall of the chamber along the small circumference of the torus.

The nature of the response of the magnetic probes to the appearance of the current in the helical winding depended qualitatively on the regime of the tokamak's discharge pulse; more precisely, on the stability safety factor q. For rather large values of this factor ($q \geq 6$ along the diaphragm) the oscillograms of the signals of the local magnetic and Fourier probes for m = 2 showed (see Fig. 2) damped oscillations similar to the oscillogram of the signal from the detector of the current in the helical winding; the alternating magnetic field being detected had only a poloidal component. Its amplitude was a linear function of the current in the helical winding (Fig. 3). In a given discharge mode, the switching on of a high-frequency pulse of current in the helical winding had no significant effect on the temporal behavior of the signals from the Fourier probes with m = 3, 4, and 5.

A comparison of the signals from the magnetic probes at the two cross sections of the tokamak chamber showed that the form of the induced alternating magnetic field was that of a

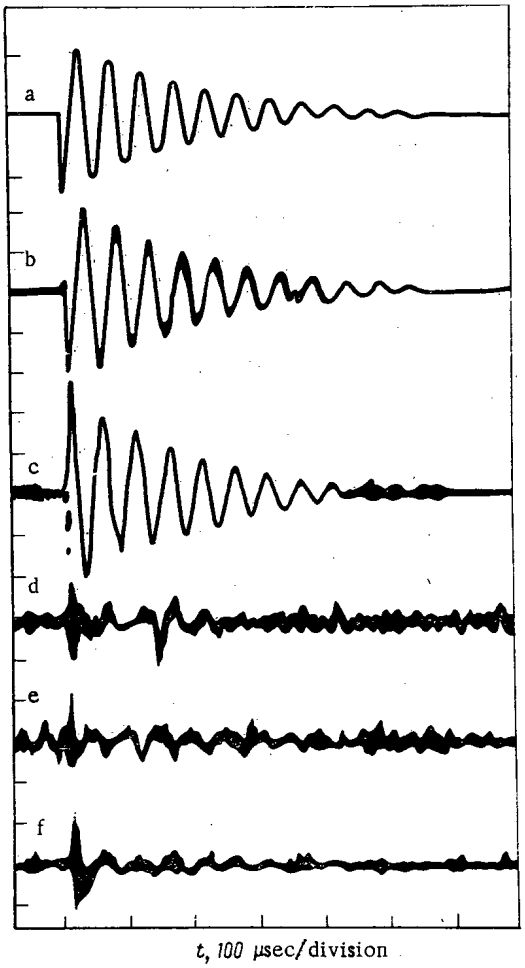

Fig. 2. Oscillograms of the derivative of the current in the helical winding: a) of the signals of the local magnetic probe and b) of the Fourier probes with m = 2 (c), m = 3 (d), m = 4 (e), and m = 5 (f) at the first cross section of the chamber (the sensitivity of the derivative of the current was 10^8 A/sec, and the probe sensitivity was $2 \cdot 10^5$ Oe/sec per division).

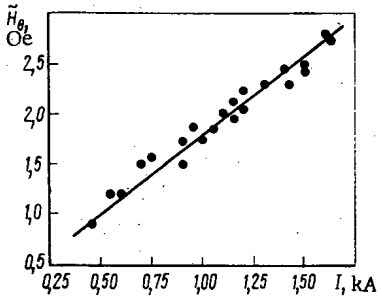

Fig. 3. Amplitude of the alternating poloidal magnetic field at the wall of the tokamak chamber, as a function of the amplitude of the high-frequency current in the helical winding.

standing wave with constant phase and periodically varying oscillation amplitude around the small circumference of the torus (Fig. 4). The geometrical position of the nodes and antinodes of the induced standing wave in each of the two cross sections remained the same for various discharge pulses, depending only on the direction of the toroidal magnetic field of the tokamak for a fixed direction of discharge current. The phase of the measured alternating field lags behind that of the current in the helical winding. The phase shift, which after the the breakdown stage reaches a large value in the regime under consideration, has a tendency to decrease steadily during the discharge pulse. At an instant 7.5 msec after the beginning of the pulse, the phase shift with current present in the helical winding was 40°; its value 57.5 msec after the start of the pulse was about 18-20°.

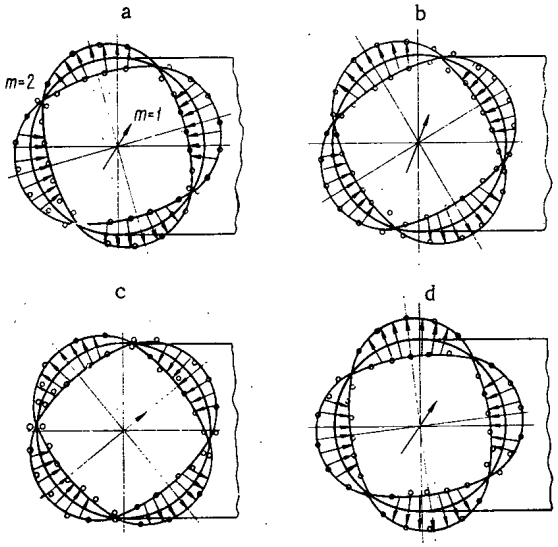

Fig. 4. Spatial structures of the m = 1 and m = 2 harmonics of the alternating magnetic field for two opposite directions of rotational transformation of the tokamak magnetic field. Left: in the direction of rotation of the helical winding, at (a) the first and (b) the second cross section of the chamber. Right: at (c) the first and (d) the second cross section of the chamber.

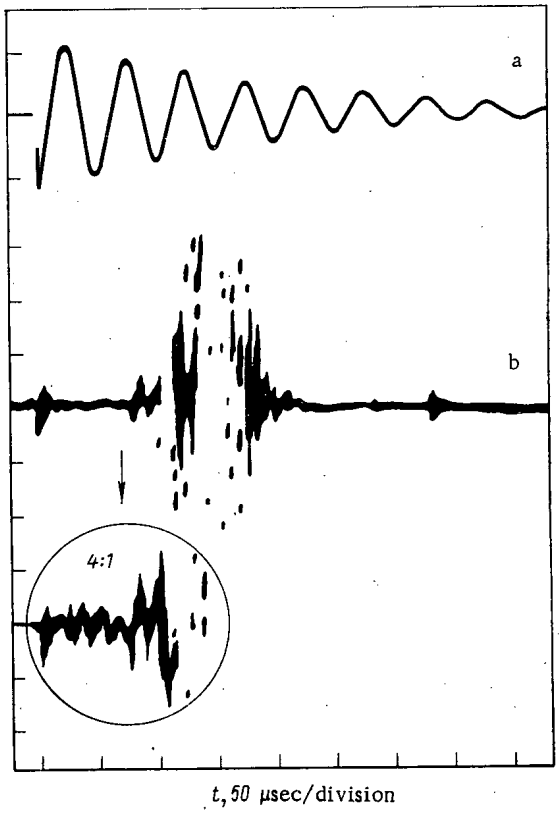

Fig. 5. Oscillograms of (a) the derivative of the current in the helical winding and (b) the derivative of the signal of the local magnetic probe. The sensitivity of the derivative of the current is 10^8 A/sec per division, and that of the probe is $5 \cdot 10^6$ Oe/sec per division.

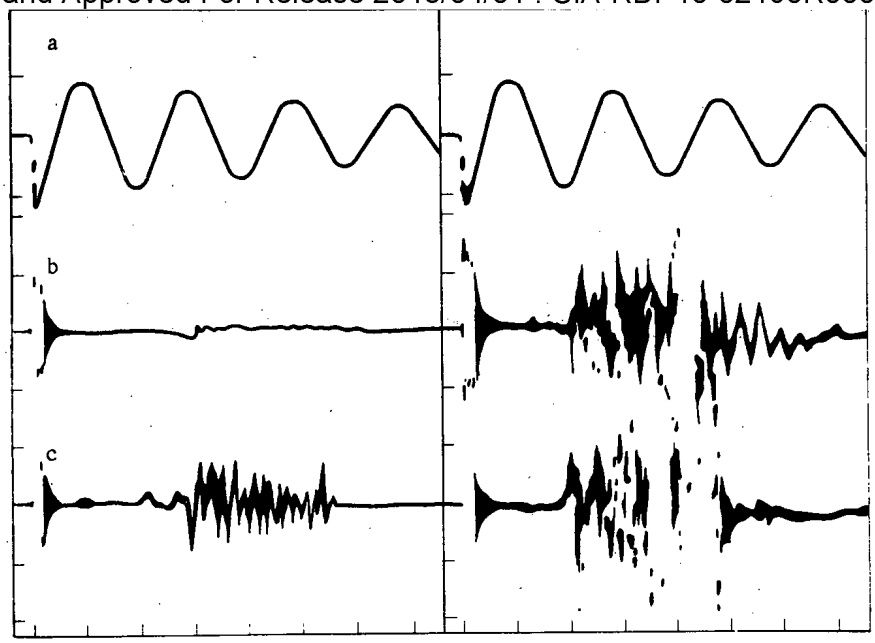

Fig. 6. Oscillograms of (a) the derivative of the current in the helical winding, (b) the derivative of the Fourier probe for m = 2, and (c) for m =3. The sensitivity of the derivative of the current is 10^8 A/sec per division, and for the probe signal it is 10^7 Oe/sec per division. The left-hand and right-hand oscillograms pertain to discharges with weakly and strongly developed instabilities in the disruption, respectively.

In addition to the m = 2 spatial harmonic detected by the Fourier probes, an m = 1 induced harmonic was also detected in each of the two cross sections, which could be interpreted as a periodic displacement of the filament due to the transverse component of the alternating magnetic field produced by the helical winding in the tokamak chamber as a consequence of its toroidal character.

As was shown above, the magnetic probes used in the experiments were located in only two cross sections of the tokamak chamber, separated from each other by an angle of 90° relative to the principal axis of the torus. There is therefore not enough data at the present time to make a detailed analysis of the structure of the field perturbation along the large circumference of the torus, and we must confine ourselves to making a few observations.

According to Fig. 4, the position of the nodes and antinodes of the standing wave of the m = 2 perturbation are different in the two cross sections of the chamber; they are rotated through a certain angle, where the rotation is in the same direction as the direction of the rotational transformation of the tokamak magnetic field for two of its opposite values. The change in the spatial phase of the standing wave at one quarter of the circumference of the torus is too small to be explained by the perturbation of only one helical spatial harmonic and is an apparent indication of the excitation of several harmonics with different toroidal wave numbers. It should be noted that this is not an unexpected conclusion, because the helical winding of the TO-1 has a finite spatial extension along the circuit of the torus and, along with the n = 1 harmonic, can effectively couple to the other toroidal spatial harmonics.

At lower values of the stability safety factor ($q \approx 4$ at the diaphragm) the high-frequency current pulse in the helical winding led to the excitation of a helical instability in the plasma. This was indicated by a sudden increase, amounting to several tens of oersteds, in the amplitude of the perturbation of the poloidal magnetic field (see Fig. 5). Meanwhile, the Fourier probes simultaneously detected several spatial harmonics of the magnetic field perturbations with frequencies which were different from that of the current in the helical winding. The excitation of the helical instability was accompanied by the appearance of negative and positive voltage peaks and disruptions of the tokamak discharge current.

In such a regime, for the same initial conditions and amplitude of current in the helical winding, instabilities of different intensity developed in different tokamak discharge pulses.

The m = 3 helical mode appeared to develop predominantly for a rather weakly developed instability accompanied by small peaks in the voltage and a 10-15% drop in the discharge current. For a strongly developed instability having large voltage peaks and total disruption of the current in a few milliseconds, the growth in the m = 2 and m = 3 modes was about the same (see Fig. 6).

We can draw the following conclusions on the basis of this work. A helical winding which is not insulated from the plasma by a dielectric, and which is located within the discharge chamber of a TO-1 tokamak, is not shunted by the plasma and therefore can be used to study helical instabilities of plasma filaments.

The effect on the tokamak discharge of a short high-frequency current pulse produced in the helical winding by a separate source depends on the stability safety factor q. For $q \approx 6$-8, switching on the high-frequency current excites a perturbation in the poloidal magnetic field with the spatial structure of a standing wave and a frequency of the current in the helical winding. For $q \approx 4$, the same action results in the development of a strong helical instability and the disruption of the discharge.

LITERATURE CITED

1. A. I. Morozov and L. S. Solov'ev, Zh. Tekh. Fiz., 34, 1566 (1964).
2. V. V. Arsenin and V. A. Chuyanov, At. Energ., 25, No. 2, 141 (1968).
3. V. V. Arsenin, At. Energ., 28, No. 2, 141 (1970).
4. V. V. Arsenin, At. Energ., 33, No. 2, 691 (1972).
5. Yu. P. Ladikov-Roev and Yu. M. Samoilenko, Zh. Tekh. Fiz., 47, 2062 (1972).
6. R. Lowder and K. Thomassen, Phys. Fluids, 16, 1497 (1973).
7. J. Hugill, Plasma Phys., 16, 1200 (1974).
8. K. Bol et al., in: Proceedings of the Fifth International Conference on Plasma Physics and Controlled Nuclear Fusion Research, Tokyo (1974). IAEA, Vienna (1975), Vol. I, CN-33/A 4-2.
9. F. Karger et al., ibid., CN-33/PD-2.
10. L. I. Artemenkov et al., in: Proceedings of the Fourth International Conference on Plasma Physics and Controlled Nuclear Fusion Research, Madison (1971). IAEA, Vienna (1971), Vol. I, CN-28/C-3.
11. N. V. Ivanov and I. A. Kovan, in: Proceedings of the Fifth International Conference on Plasma Physics and Controlled Nuclear Fusion Research, Tokyo (1974). IAEA, Vienna (1975), Vol. I, CN-33/A 9-5.

X-RAY DETECTORS BASED ON CADMIUM TELLURIDE

V. F. Kushniruk, L. V. Maslova,
O. A. Matveev, V. S. Ponomarev,
S. M. Ryvkin, A. I. Terent'ev,
Yu. P. Kharitonov, and A. Kh. Khusainov

UDC 539.107.45

The most promising material for detectors of γ-quanta and x-ray radiation is cadmium telluride, which satisfies the majority of requirements for producing spectrometric detectors having a high detection efficiency and not requiring cooling [1, 2].

There has recently been considerable success in obtaining pure crystals of cadmium telluride [3] and in making spectrometric detectors for γ-quanta and x-ray radiation [4, 5]. Calculations, based on the parameters of existing crystals [4], indicate that an improved energy resolution can be expected in x-ray and γ-ray spectrometry at energies of ≤ 60 keV.

Translated from Atomnaya Énergiya, Vol. 42, No. 5, pp. 391-394, May, 1977. Original article submitted August 6, 1976.

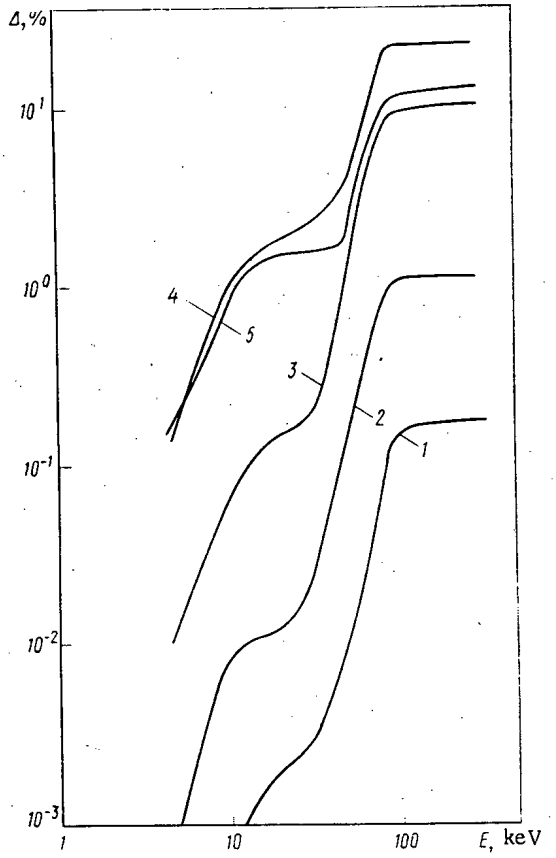

Fig. 1

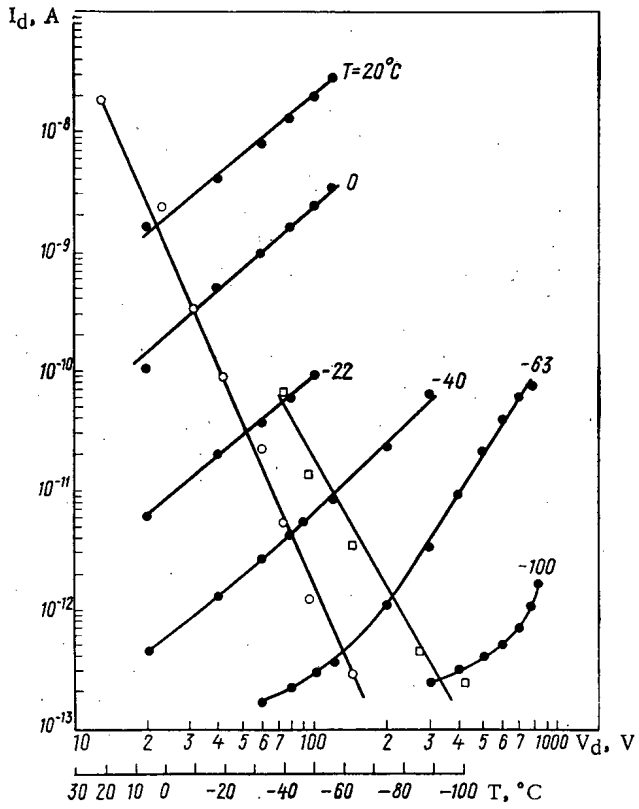

Fig. 2

Fig. 1. Dependence on the energy of the detected radiation of the detector energy resolution, as determined by fluctuations in charge collection, for values of d/λ_- and d/λ_+ equal, respectively, to: 1) 0.001, 0.01; 2) 0.01, 0.1; 3) 0.1, 1; 4) 2, 20; 5) 4, 40 (d is the thickness of the crystal).

Fig. 2. Volt–ampere characteristics of a detector at temperatures from +20 to –100°C. Temperature dependence of the detector current for voltages: 100 (○) and 300 (□) (detector working area 10 mm², crystal thickness 2 mm).

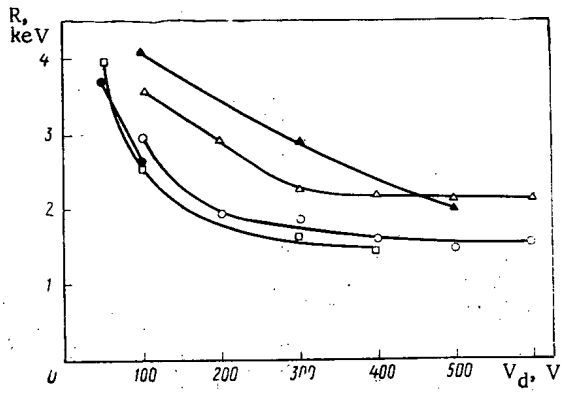

Fig. 3. Dependence on the operating voltage of the detector energy resolution at temperature values of –100 (▲), –75 (△), –58 (○), –40 (□), and –22°C (●) at energy 59.6 keV from a preparation of ^{241}Am.

Calculated values of the energy resolution of detectors, as a function of the radiation energy, are shown in Fig. 1 for several values of the trapping mean free path of electrons ($\lambda_- = \mu_-\tau_-E$) and holes ($\lambda_+ = \mu_+\tau_+E$), where μ and τ are, respectively, the mobility and lifetime of the charge carriers and E is the electric field strength in the detector. The calculations are carried out on the model used in [6], which assumes that irradiation occurs from the negative electrode. The crystals were assumed, in these calculations, to have parameter values $\mu_-\tau_- = (2\text{-}3)\cdot10^{-3}$ cm²/V and $\mu_+\tau_+ = (1\text{-}6)\cdot10^{-4}$ cm²/V (cf. [4]). The asymmetry in the mobility of electrons and holes in cadmium telluride crystals, characterized by a ratio $\mu_-/\mu_+ \approx 10$, is the reason why the detector resolving power depends so strongly on the

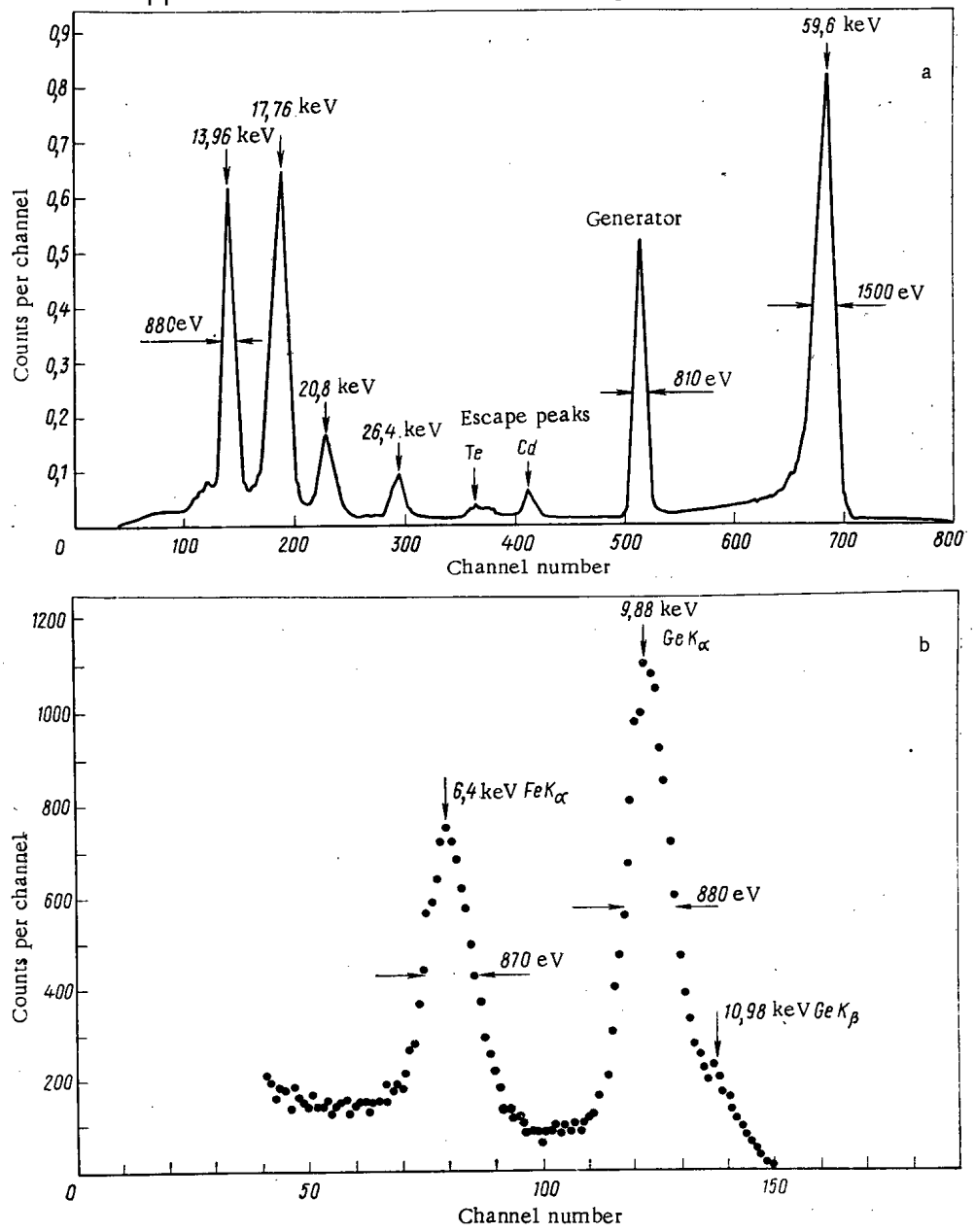

Fig. 4. a) Energy spectra of γ quanta from a preparation of ^{241}Am; b) x-ray radiation from Fe and Ge, excited from a ^{109}Cd source (operating voltage 400 V, temperature −40°C, detector area 10 mm^2, thickness 1.5 mm).

hardness of the radiation. As can be seen from Fig. 1, detectors constructed from these crystals have a resolution of $\lesssim 1\%$ at energies below 60 keV, for an electric field strength $\sim 10^3$ V/cm.

However, the line width observed in actual detectors noticeably exceeds the predicted value, and this is caused both by charge collection fluctuations and by current noise. The latter phenomenon plays a decisive part in the spectrometry of x-ray quanta and so improvements in x-ray detectors depend, at present, on reducing the current noise. Since detectors based on cadmium telluride are constructed in the metal−semiconductor−metal form [4, 5] with nonrectifying contacts and the current is determined by the crystal resistivity, it is clear that the detector current can, in principle, be reduced either by cooling or by making an n−i−p configuration. The latter method is the more radical. However, the preparation of an n−i contact has met with considerable difficulty [6, 7]. The construction of an n−i−p configuration, sustaining large voltages (an electric field strength of $\gtrsim 10^4$ V/cm is required) with small leakage currents ($\lesssim 10^{-9}$ A), is a complex matter and demands the solution of a number of fundamental problems.

Cooling the detector to intermediate temperatures (−50°C) enables a substantially enhanced energy resolution to be achieved, by lowering the current noise and raising the working voltage. The characteristics of the detectors are then improved so much that detectors with these parameters have been successfully applied in currently important problems, e.g., in nuclear geophysics, geology, the mining industry, medicine, and other fields.

The detector and the field-effect transistor of the first amplifier stage were cooled by a thermoelectric refrigerator, the current to which was used to regulate the detector temperature in the range +20 to −100°C.

A family of volt−ampere characteristics of one detector, for various temperatures, is shown in Fig. 2. Also shown is the temperature dependence of the detector current, at two operating voltages. It can be seen that the current exhibits an ohmic dependence over a wide temperature range and falls off exponentially when the temperature is lowered, at fixed operating voltage. At a temperature around −40°C the current has already become extremely small ($\leqslant 10^{-10}$ A at the operating voltage) and this enables the detector noise level to be sufficiently low. In view of this, further cooling is not advised.

The dependence of the detector energy resolution on the operating voltage, for various temperatures, shows (Fig. 3) that the best results are obtained also at temperatures of −40 to −60°C. Further temperature reduction leads to a noticeable deterioration in the resolving power, which is reasonable since in this case the charge carriers are trapped in the fine-structure levels. The optimum operating temperature for the detectors is therefore typically −40°C.

The energy spectra of γ-quanta from a preparation of ^{241}Am (Fig. 4a) and of x-ray radiation from Fe and Ge, excited from a ^{109}Cd source (Fig. 4b), have been obtained with one of the detectors being investigated at a temperature of −40°C and operating voltage of 400 V. In addition to the five γ-lines of ^{241}Am, with energy resolution 1500 and 880 eV for the lines with energy 59.6 and 13.96 keV, there are also clearly visible, in Fig. 4a, two maxima corresponding to escape peaks of Cd and Te (36.4 and 32.1 keV), the energy equivalent of the detector and electronics noise from the generator peak being 810 eV. The energy spectra of Fe and Ge in the x-ray K_α series have a line width of 880 eV and are well resolved. This indicates the possibility of element analysis of substances with atomic number $Z \geq 25$.

Over the temperature range used in the investigations (from +20 to −100°C) the detector characteristics are stable with time; i.e., no crystal polarization is observed. It should be mentioned that as well as cadmium telluride crystals, detectors from which possess a normal dependence of energy resolution on electric field and temperature, there are crystals for which the resolving power is constant over a wide range of operating voltages while the efficiency of charge collection in them increases with increasing voltage [8]. When detectors from this type of crystal are cooled, the resolving power shows an insignificant improvement. For example, a detector described in [8] had a resolution of 2.9 keV at energy 59.6 keV, for the optimum temperature −40°C and an operating voltage 1100 V ($E \approx 6 \cdot 10^3$ V/cm), which is 10 times larger than the calculated value. The causes of the observed anomaly are being investigated.

Thus, for crystals which possess a normal dependence of the resolution on operating voltage, at room temperature, a small degree of cooling considerably improves the detector characteristics. Since compact refrigeration units have now been developed, which enable temperatures of −40 to −60°C to be obtained with small power requirements (∼10 W) [9], the detectors described may be used for element analysis of substances, using an aperture and field apparatus.

The authors would like to thank G. N. Flerov for his constant interest in the work.

LITERATURE CITED

1. E. N. Arkad'eva, O. A. Matveev, Yu. V. Rud', and S. M. Ryvkin, Zh. Tekh. Fiz., 36, 1146 (1966).
2. E. N. Arkad'eva, L. V. Maslova, et al., Fiz. Tekh. Poluprovodn., 2, 279 (1968).
3. O. A. Matveev, E. N. Arkad'eva, and L. A. Goncharov, Dokl. Akad. Nauk SSSR, 221, No. 2, 325 (1975).
4. E. N. Arkad'eva, L. V. Maslova, O. A. Matveev, S. V. Prokof'ev, S. M. Ryvkin, and A. Kh. Khusainov, Dokl. Akad. Nauk SSSR, 221, No. 1, 77 (1975).
5. P. Siffert, J. P. Ponpon, and A. Cornet, Onde Electr., 55, No. 5, 281 (1975).
6. N. V. Agrinskaya, E. N. Arkad'eva, M. I. Guseva, et al., Fiz. Tekh. Poluprovodn., 6, 473 (1972).

7. E. N. Arkad'eva, M. I. Guseva, O. A. Matveev, and V. A. Sladkova, Fiz. Tekh. Poluprovodn., 9, 853 (1975).
8. L. V. Maslova et al., Proceedings of the Second International Symposium on Cadmium Telluride, Strasbourg, France, June 30-July 2, 1976.
9. E. A. Kolenko, Thermoelectric Cooling Devices [in Russian], Nauka, Moscow (1967).

USE OF ARGON IONS FOR THE PREPARATION OF NUCLEAR FILTERS

S. P. Tret'yakova, G. N. Akap'ev,
V. S. Barashenkov, L. I. Samoilova,
and V. A. Shchegolev

UDC 539.082.79

For making nuclear filters from polymers, the contemporary practice is to use heavy charged particles (fission fragments of uranium, curium, and californium nuclei) or accelerated xenon ions [1, 2], which create a great deal of radiation damage in the irradiated material. The energy of these particles varies over the range 0.5-1 MeV/nucleon and corresponds to a range of 10-20 μ (Fig. 1) in materials such as Dacron or polycarbonate.

It is of great practical interest to consider the possibility of using beams of lighter ions, such as argon, capable of being produced in the U-300 cyclotron and other accelerators. The energy of accelerated argon ions may reach 6 MeV/nucleon in this cyclotron, which corresponds to a range of ∿70 μ in plastic materials, much greater than that of xenon ions, in which the energy never exceeds 1 MeV/nucleon (Fig. 1).

For making nuclear filters, one uses the selective etching of a polymer after its degradation by charged particles; the mode of etching depends on the degree of degradation and the diameter of the channel in which degradation has occurred [2]. For every polymer there is a minimum (threshold) value of the specific energy loss at which selective etching of the kind envisaged may be carried out [2, 3]. For Dacron the value is ∿3.0-3.5 MeV•cm²/mg, which is much lower than the specific energy loss for argon ions (in the kinetic energy range $E \lesssim 5$ MeV/nucleon).

The diameter of the through channel etched out in the plastic [4] is given by the equation

$$D(t) = D_0\{1 - \exp[-a(t_0 - t)]\} + b(t_0 - t),$$

where t is the etching time; D_0, a, b, t_0 are coefficients found experimentally. For pores with diameters of over 0.1 μ the principal role is usually played by the last term in this equation alone, and the value of D is to a good approximation proportional to the etch time [5], i.e.,

$$D(t) \approx 2Vt,$$

TABLE 1. Irradiation of Dacron Film with Argon Ions

Thickness of aluminum absorbed, μ	Energy of Ar ions, MeV/nucleon	Specific energy losses of Ar ions in Dacron, MeV · cm²/mg	Range of Ar ions in Dacron, μ
0	5,0	16,0	70
18	3,4	19,5	44
27	2,3	22,0	29
36	1,3	27,2	16
40,5	0,7	29,7	11

Translated from Atomnaya Énergiya, Vol. 42, No. 5, pp. 395-397, May, 1977. Original article submitted May 10, 1976.

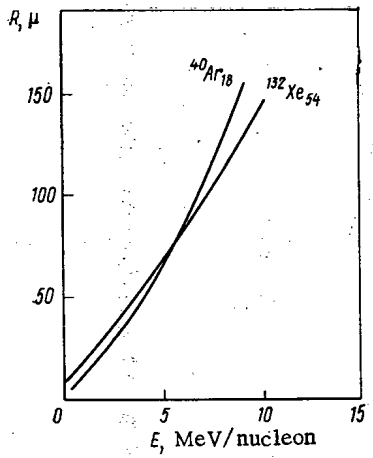

Fig. 1

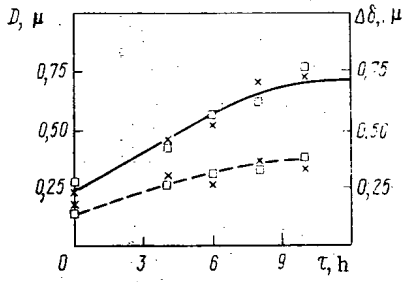

Fig. 2

Fig. 1. Range of argon and xenon ions in Dacron as functions of their energy.

Fig. 2. Pore diameter and change in the thickness of the Dacron film as functions of the period of ultraviolet irradiation: ×) pore diameter; □) reduction in film thickness Δδ; ---) etch time 26; ——) 49 min.

where V is the rate of etching the plastic. In making filters with pores less than 0.1 μ in diameter still more careful allowance for effects depending on the film thickness, the initial density, and other factors must be made. The dependence on the type of ion then becomes far more important.

In this paper we shall consider the preparation of filters with pore diameters exceeding 0.1 μ.

A study of the rate of etching the polymer polycarbonate (macrofoil) along the track as a function of the energy of the ion [4] showed that on increasing the specific energy loss (dE/dx) this etch rate first increased and then remained constant. Dacron is a compound of the same class as macrofoil and the properties of these plastics are fairly similar to one another; for Dacron we shall therefore expect the same dependence of etch rate on dE/dx. Since in order to increase the degradation of the polymer additional irradiation with ultraviolet light is frequently employed, it is important to study this relationship subject to the corresponding conditions.*

For this purpose a Dacron film 12 μ thick was irradiated with argon ions accelerated in the U-300 cyclotron, their energy being reduced by means of aluminum foils of corresponding thickness (Table 1). The exposure to ultraviolet radiation was varied from 4 to 15 h.

After ultraviolet irradiation the Dacron film was etched in a 20% NaOH solution at 50 ± 1°C to various pore diameters, using the equipment and technique described in [2].

The results of the experiments regarding the effect of ultraviolet exposure time on the diameter of the through channel along the particle trajectory for a constant value of dE/dx = 27.2 MeV•cm²/kg are presented in Fig. 2. The value of D was measured by a gasdynamic method [2]. For samples obtained after a 10-h irradiation, control measurements were also made with a microscope. Very similar values of D were obtained by these two methods (Table 2).

We see from Fig. 2 that the dependence of the pore diameter on the dose of ultraviolet radiation passes out to a plateau after roughly eight hours irradiation, twice as great as in the case of xenon ions [2].

Using an electron microscope, we obtained a photograph representing the cross section of the channels in a nuclear filter (Fig. 3). It is easy to see the cylindrical shape of these; the channel image passing out beyond the plane of the section is due to the fact that the

*Additional treatment with ultraviolet radiation after ion irradiation of the film not only increases the etch rate along the trajectory of the ion but also imparts a regular cylindrical shape to the filtering channels [2]. Ultraviolet radiation was not used in [4].

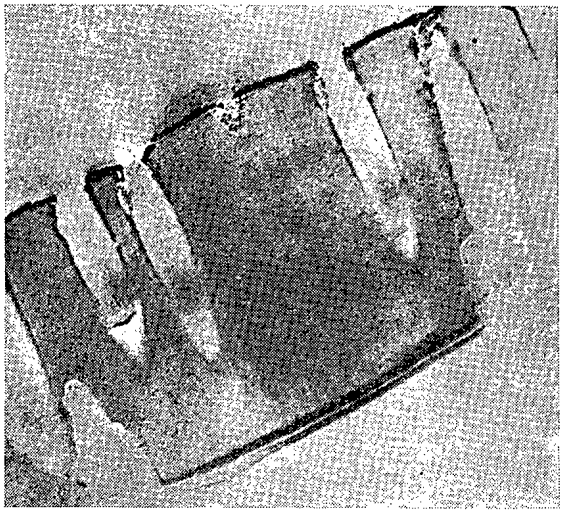

Fig. 3. Electron micrograph of the cross section of a nuclear filter with a pore diameter of 0.952 μ (×10,500).

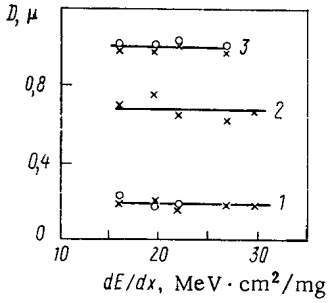

Fig. 4

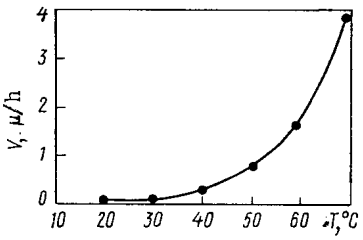

Fig. 5

Fig. 4. Diameter of filter pores as a function of the specific energy loss of the argon ions for various periods of ultraviolet irradiation and etching: ×, 0) data obtained for 8- and 10-h ultraviolet irradiation; 1, 2, 3) etch times, respectively, 15, 51, and 75 min in 20% KOH solution.

Fig. 5. Rate of change of filter-channel diameter as a function of the temperature of the NaOH solution.

argon ions irradiating the film entered it at an angle slightly differing from a right angle.

In order to discover the effect of the specific energy loss of the ion on the pore etch rate and correspondingly the pore-diameter dispersion, we chose films irradiated with argon ions of different energies. All the samples studied were irradiated with ultraviolet light for 8 and 10 h. The pore diameter was determined by the gasdynamic method.

We see from Fig. 4 that, for the ultraviolet exposure times indicated, the diameter of the etched channel does not depend on the change in the specific energy loss of the ion in the range of argon energies studied (0.7-5.0 MeV/nucleon).

We also studied the effect of the temperature of the etching solution on the etch rate of the filter channels. The temperature was varied over the range 20-70°C (accuracy ±0.5°C). Ultraviolet irradiation lasted 10 h. For measuring the pore diameters we used the gasdynamic method; however, the pore diameters of some of the filter samples were also checked under the electron microscope. The data presented in Table 3 are in excellent agreement with the results of the measurement.

The influence of the temperature of the NaOH solution on the rate of change of pore diameter may be seen from Fig. 5; the etch rate rises sharply at temperatures exceeding 60°C.

TABLE 2. Diameters of the Pores Measured by the Gasdynamic Method and in the Electron Microscope

D g-d, μ	D el. m., μ	D g-d, μ	D el. m., μ
0,09 0,16	0,10 0,15	0,40 0,80	0,40 0,75

TABLE 3. Effect of the Mode of Etching on the Pore Diameter

Mode of etching		D g-d, μ	D el. m., μ
°C	min		
30 40 59	120 60 30	0,24 0,32 0,9	0,20 0,28 0,82

The quality of the filters obtained by means of argon ions is in no way inferior to that of those obtained by means of xenon ions.

LITERATURE CITED

1. Nuclepore, Specifications and Physical Properties, Nuclepore Corporation, Plesanton, Calif. (1973).
2. G. N. Akap'ev et al., JINR Preprint B-114-8214, Dubna (1974).
3. E. Benton, Rep. VS NRDL-TR-68-14 (1968).
4. I. Tripier et al., in: Proceedings of the Eighth International Conference on Nuclear Photography and Solid-State Trace Detectors, Vol. 1, Bucharest, July 10-15 (1972), p. 290.
5. D. Hagegan, ibid., p. 213.

SOME RELIABILITY ASPECTS OF REACTOR EMERGENCY PROTECTION SYSTEMS

A. I. Pereguda and A. A. Petrenko

UDC 621.039.58

The emergency protection (EP) systems of a reactor are considered as a queuing system containing majorant schemes and fault-monitoring devices. Streams of demand with an intensity of μ_i ($i = 1, \ldots, k$) are fed into the input of this system. Because of a fault in the EP system the demand may receive a refusal of service. The intensity of refusals by the EP system devices, connected in an m out of n circuit, is determined from the transcendental equation

$$\frac{\mu_0 Q}{k\mu_i Q_i} = 1 - \frac{\sum_{\gamma=0}^{\infty} [(m+1)_\gamma (m-n+1)_\gamma/(m+1)(m+2)_\gamma \gamma!]}{B(m+1;\ n-m)} \sum_{\varkappa=0}^{\infty} \frac{(1/\alpha)_\varkappa [-\lambda_j (m+\gamma+1) Q_i^\alpha]^\varkappa}{k!(1+1/\alpha)_\varkappa},$$

where μ_0 is the mean number of transmitted demands per unit time; Q is the operating time of the EP system, defined as the time between reactor rechargings; Q_i is the operating time of the protection device in an interval of time; λ_j is the intensity of refusals by the device; and α is the parameter of the Weibull distribution.

If λ_j is so small that its value cannot be attained in the realization of an EP system, periodic monitoring must be introduced. Then the probability that there will be no unserved demands is given by the formula

$$P_0(Q) = \exp\left\{-\mu\left[1 - \frac{1-\exp(-\lambda_j T)}{\lambda_j (T+\theta)}\right] Q\right\},$$

where T is the monitoring period and θ is the duration of the preventive maintenance.

Presentation of the protection channel with periodic monitoring enables us to obtain the relation

$$\hat{\lambda} = \lambda T/Q + 2\theta/TQ,$$

where $\hat{\lambda}$ is the intensity of refusals by the relevant device.

Thus, setting $\hat{\lambda} = \lambda_j$ and knowing Q as well as the true intensity λ of refusals by the device, we can find the duration θ of the preventive maintenance if we bear in mind that

$$T_{\text{opt}} \approx \sqrt{2\theta/\lambda},$$

where T_{opt} is the optimal monitoring period.

The method presented can be used when designing and modernizing the existing control and protection system of a reactor.

Translated from Atomnaya Énergiya, Vol. 42, No. 5, pp. 398-402, May, 1977.

THERMAL OPENING OF IRRADIATED URANIUM OXIDE FUEL ELEMENTS OF A BR-5 REACTOR WITH FUEL SEPARATION BY DISSOLUTION

G. P. Novoselov and S. E. Bibikov

UDC 621.039.5

Experiments to verify a thermal method of opening irradiated fuel elements and separating the fuel from the steel by dissolution in nitric acid were carried out with fuel elements from a BR-5 reactor. The elements were 300 mm long and 5 mm in diameter, and consisted of a can of 1Kh16N16M3B steel filled with UO_2 pellets with 80% enrichment in ^{235}U. After irradiation with a fluence of $1 \cdot 10^{22}$ neutrons/cm^2, the fuel elements were stored for 1 year; the burn-up attained was 1.42 at. %.

To determine the quantity of gaseous fission products in the cans, the fuel elements were heated in a vacuum furnace until the internal pressure burst the cans. The quantity of ^{85}Kr in the samples taken was measured by a scintillation γ-ray spectrometer. The Kr yield from the fuel was 0.32% of the initial content of 5.2 Ci/kg. The temperature at which the cans burst dropped and the yield of gaseous fission products rose as the burn-up increased.

The steel cans of the fuel elements were melted off at 1450-1700°C. As a result, fragments of UO_2 pellets and a steel ingot were obtained. Up to 70% of the fuel was free of steel and the remainder of the fuel was disseminated throughout the surface layer of the ingot. The fuel was separated from the steel either by dissolution in nitric acid or oxidation in air, after which the ingots were dissolved for analysis.

The data of analysis show that the total radioactivity of the fuel before and after the can was melted off is due mainly to ^{144}Ce and ^{144}Pr, whereas there was 1/10 as much ^{135}Cs, ^{90}Sr, ^{106}Ru, and ^{106}Rh and 1/100 as much ^{95}Zr and ^{95}Nb.

When the fuel elements had been opened thermally, the steel contained from $7 \cdot 10^{-3}$ to $5 \cdot 10^{-2}$ mass % U. Comparison of the γ-ray spectra of the steel before and after the can was melted off shows that ^{54}Mn and ^{58}Co form in the steel during irradiation and the other fission products enter the steel during the melting process (Fig. 1).

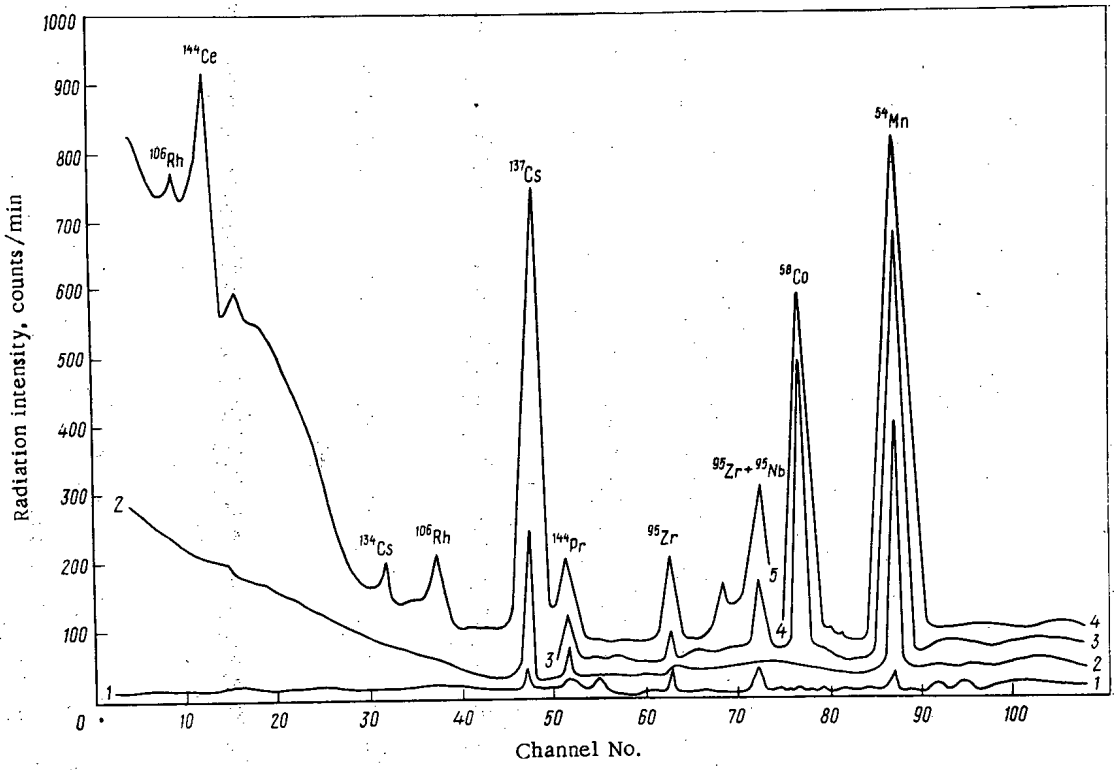

Fig. 1. Spectra of products of thermal opening of fuel elements: 1) aerosols; 2) sublimates; 3) steel after melting off; 4) steel before melting off; 5) fuel.

The sublimates on the condenser were observed to contain from $8 \cdot 10^{-5}$ to $5.7 \cdot 10^{-4}$ g U [$(1-7) \cdot 10^{3}$% of the original content]. The most intense radiation in the sublimates is that of ^{137}Cs (2.3% of the original); the content of other fission products ranges from roughly 10^{-2} to 10^{-5}%.

The aerosol filter was found to hold from $2 \cdot 10^{-7}$ to $4 \cdot 10^{-5}$ g U ($3 \cdot 10^{-6}$ to $\sim 5 \cdot 10^{-4}$% of the original); the quantity of ^{144}Ce, ^{144}Pr, ^{95}Zr, and ^{95}Nb is $(1-3.5) \cdot 10^{-4}$% of the original, and that of ^{137}Cs and ^{54}Mn reaches $2 \cdot 10^{-2}$ and $0.6 \cdot 10^{-2}$% of the original. The distribution of the uranium fission products after thermal opening of fuel elements is shown in Fig. 1.

LITERATURE CITED

1. G. P. Novoselov and A. T. Ageenkov, Proceedings of the Thirty-Sixth International Conference on Industrial Chemistry, Brussels (1966), Paper No. 11/755.
2. G. P. Novoselov and A. T. Ageenkov, At. Energ., 26, No. 3, 230 (1969).
3. J. Goode et al., Trans. Am. Nucl. Soc., 1, No. 15, 87 (1972).
4. V. K. Markov et al., Uranium. Methods of Determination [in Russian], Atomizdat, Moscow (1964).
5. Report ORNL-2929 (1960).
6. Report WARD-185 (1960).
7. M. Bleiberg et al., in: Proceedings of the IAEA Symposium: "Radiation Damage in Reactor Materials," Vienna (1963), p. 319.
8. W. Lewis, Trans. Am. Nucl. Soc., 7, No. 1, 24 (1964).

CALCULATION OF DIFFERENTIAL EFFICIENCY OF REACTIVITY CONTROLLER BY THE MONTE CARLO METHOD

Yu. P. Sukharev

UDC 621.039.51:621.039.567

An algorithm is proposed for the calculation of the differential efficiency of a reactivity controller in a three-dimensional reactor by the Monte Carlo method. The algorithm is based on the calculation of the terms in the perturbation-theory formulas by means of direct and conjugate estimates of the neutron importance and flux on the surface of the perturbation region of the controller on the assumption that the sources are constant in the equations for the flux and the importance.*

Calculation of the terms in the perturbation-theory formulas reduces to estimating the functionals

$$R = \int f(x) F(x) F_k^+(x) dx \tag{1}$$

by the Monte Carlo method; each of the functionals can be calculated by constructing the random quantity

$$\hat{\xi} = \sum_{j=1}^{N} \frac{\gamma \Sigma_t(x_j)}{\Sigma_a(x_j)} \sum_{i=1}^{L} \frac{\chi(E_i) Q(\mathbf{r}_i)}{4\pi K_{\text{eff}} \Sigma_t(\mathbf{r}_i, E_{i-1})} W_i \tag{2}$$

and averaging it over the histories of the neutrons, beginning from the point $x_0 = \{\mathbf{r}_0, \Omega_0, E_0\}$ of the perturbation region with the distribution $f(x)$ and consisting of two branches: $\beta = (\mathbf{r}_0, \Omega_0, E_0), (\mathbf{r}_1, \Omega, E_1), \ldots, (\mathbf{r}_0, \Omega_N, E_N)$ and $j = (\mathbf{r}_0, -\Omega_0, E_0), (\tilde{\mathbf{r}}_1, \tilde{\Omega}_1, \tilde{E}_1), \ldots, (\tilde{\mathbf{r}}_L, \tilde{\Omega}_L, \tilde{E}_L)$.

The importance $F_k^+(\mathbf{r}_0, \Omega_0, E_0)$ is estimated from the β branch and the neutron flux $F(\mathbf{r}_0, \Omega_0, E_0)$ from the γ branch. Functional (1) is calculated by integration over all the initial currents of the history in the perturbation region.

To solve the problem, we organized a random walk of neutrons, described by the direct transfer kernel during determination of the importance, and a conjugate random walk for estimation of the flux. The right-hand side of the inhomogeneous equations for the neutron importance and flux is a $\delta(x - x_0)$ function, $x = \{\mathbf{r}, \Omega, E\}$. In Eq. (2)

* The algorithm was developed under the supervision of V. G. Zolutkhin.

$$W_i = W_{i-1}\frac{\Sigma^+(\mathbf{r}_i, E_{i-1})}{\Sigma_i(\mathbf{r}_i, E_{i-1})};\ W_1 = \frac{\int_{E_0}^{E^*} g(E)\,\Delta\Sigma(E)\,dE}{g(E_0)};$$

$$\Sigma^+(\mathbf{r}, E) = \sum_{A,i}\rho_A(\mathbf{r}')\,\sigma^+_{A,i}(E, \mathbf{r}') = \sum_{A,i}\rho_A(\mathbf{r})\int_E^{E^*}\int_{4\pi}\sigma_{A,i}(E')\,g_{A,i}(E'\Omega'\to E\Omega)\,dE'\,d\Omega', \quad (2)$$

where E* is the maximum energy considered in the problem; Q(r) is the distribution function of sources of fission neutrons; $g(E_i)$ is the fraction of neutrons of energy E_i in the reactor spectrum; and $\Delta\Sigma$ is the change in the total macroscopic cross section or scattering cross section. The remaining symbols have the customary meanings.

The proposed algorithm was realized in a program on an M-220A computer and checked by calculations of the differential efficiency of the moving reflector of a critical assembly.†

†H. Takahashi, Nucl. Sci. Engng., 41, 259 (1970).

PENETRATION OF γ RAYS THROUGH MATTER. GREEN'S FUNCTION OF PLANE-PARALLEL PROBLEM WITH AZIMUTHAL SYMMETRY

L. D. Pleshakov

UDC 539.171.015

This paper considers the problem of the penetration of γ rays to a great distance from plane sources with azimuthally symmetric angular and arbitrary energy distributions.

A kinetic equation was obtained for Green's function describing the flux density of scattered γ rays at large distances from the source; this equation proves to be a differential equation of the hyperbolic type.

An asymptotic solution was found for the case when the attenuation factor is approximated by polynomials of the first, second, and third degree and the relation $E_0 < E_{min}$ is satisfied (E_{min} is the energy corresponding to the minimum attenuation factor). If the attenuation factor is approximated by a second-degree polynomial

$$\mu(\lambda) = \mu_0 + \mu_1(\lambda-\lambda_0) + \mu_2(\lambda-\lambda_0)^2,$$

then Green's function is of the form

$$I_p(x, \lambda, y_0) = \frac{b\lambda_0^2}{\mu_0\lambda}\frac{\left[\frac{\mu_1}{\mu_0}\left(\lambda-\lambda_0-\frac{y_0}{c_1}\right)\right]^{\frac{\bar b}{\mu_1}-1}}{\left[1+\frac{\mu_2}{\mu_1}\left(\lambda-\lambda_0-\frac{y_0}{c_1}\right)\right]^{\frac{\bar b}{\mu_1}+1}}\ \frac{(\mu_0 x)^{\frac{\bar b}{\mu_1}}}{\Gamma\left(\frac{\bar b}{\mu_1}+1\right)}\exp(-\mu_0 x)\left\{\frac{\bar b}{\mu_1}\int_0^1 dv\, v^{\frac{\bar b}{\mu_1}-1}\times\right.$$

$$\left.\times\exp\left[-\mu_0 x\left(1-v+\frac{\mu_1}{\mu_0 c_1}v\right)y_0\right]\right\}\left[1+O\left(\frac{1}{x}\right)\right];$$

$$\left(\lambda-\lambda_0-\frac{y_0}{c_1}\right)>0,$$

where λ is the wavelength of the radiation; x is the distance from the source to the point of detection; $\bar b$ is the eigenvalue found by solving the problem about the penetration of γ rays to a large distance*; b and c_1 are known constants; Γ(x) is the γ function of $y_0 = \theta_0^2/2$; and θ_0 is the angle of γ-ray emission from the source.

As an example of the use of Green's function, we found the distribution function of the energy flux density for plane and point isotropic sources.

It was shown that the distribution functions of the energy flux density at large distances from a plane perpendicular and a point isotropic source agree to with in the factor $\Phi(z, \lambda_0)/4\pi x^2$ (z is the nuclear charge of the matter through which the radiation passes).

*U. Fano, J. Res. Nat. Bur. Standards, 51, 95 (1953).

It was shown that the factor $\Phi(Z, \lambda_0)$ can not only be found theoretically but can also be expressed in terms of the ratio of energy build-up factors of the plane perpendicular and point isotropic sources which can be taken from experiment or calculated by the momentum method.

A comparison is made of the factor Φ calculated theoretically and in terms of the ratio of the energy build-up factors.

NEUTRON TRANSPORT IN HALF-SPACE WITH SOURCES

V. P. Gorelov and V. I. Il'in

UDC 621.039.51.12:539.125.52

This paper considers the distribution of neutrons in a half-space with sources. The solution is found in the form of a series in the complete set of eigenfunctions of the transport equation [1]. The approximations used for the coefficient of the expansion of the solution for the eigenfunctions of the continuous part of the spectrum lead to finite analytic expressions that are convenient for calculations.

We considered the Milne problem with quadratic anisotropy. To solve the initial equation for original transport equation, the expansion coefficient of the solution for the eigenfunctions of the continuous part of the spectrum is approximated by the expression

$$A(\nu, f_2) = A(f_2)(1-\nu)$$

(where ν is the eigenvalue of the continuous part of the spectrum and f_2 is the anisotropy parameter), satisfying the well-known properties of the vanishing of $A(\nu, f_2)$ at the point $\nu = 1$ and the divergence of the derivative of the total neutron flux at the interface [1]. In the process, for the boundary-value problem we replace the exact boundary conditions by Marshak conditions for the moments of the distribution function [2]. This allows simple analytic expressions to be obtained for the extrapolated length of $H(f_2)$ and the angular distribution of the radiation emerging from the half-space.

Calculations show that the formulas derived give good accuracy. The results for $H(f_2)$ confirm that the extrapolated length depends weakly on the anisotropy factor f_2.

It was noted that the expressions obtained for the neutron spectrum and the extrapolated length contain a nondiffusive term in explicit form and give the dependence on f_2, while remaining simpler than other known results [1, 3, 4].

The paper solves the problem of a half-space with anisotropic neutron sources by the method of generalized eigenfunctions [1]. The spectral coefficient in this case is approximated by

$$A(\nu, \mu_0) = A(\mu_0)(1-\nu)\left\{P\frac{C\nu}{2(\nu-\mu_0)} + \lambda(\nu)\,\delta(\nu-\mu_0)\right\},$$

where $\lambda(\nu) = 1 - (C\nu/2)\ln[(1+\nu)/(1-\nu)]$; arc cos μ_0 is the angle of incidence of neutrons from the source; $\delta(\nu)$ is the Dirac delta function; $A(\mu_0)$ is an unknown coefficient found from the boundary conditions; and the index p denotes that the relevant integrals are taken in the sense of the Cauchy principal value [5].

The form chosen for the spectral coefficient $A(\nu, \mu_0)$ conveys the salient features, known from the exact solution, of its vanishing at the point $\nu = 1$ and the existence of a pole at the value $\nu = \mu_0$.

Replacement of the exact boundary conditions by the conditions for the moments of the distribution function,

$$\int_0^1 \mu^{2k+1}\psi(0, \mu)\,d\mu = \mu_0^{2k+1}, \quad k = 0, 1,$$

enables the necessary equations to be obtained for determining the unknown constants.

The analytic form of the spectrum of radiation emerging from the half-space and the expression for the albedo of the half-space with neutron capture have been obtained. Calculations

of the latter show that the results arrived at are in good agreement with the exact value [6]. The computational formulas convey nondiffusive effects and are quite simple in form.

The quadratic anisotropy limitation is not fundamental and the consideration can be generalized to more complex scattering laws.

LITERATURE CITED

1. K. M. Case and P. F. Zweifel, Linear Transport Theory, Addison-Wesley (1967).
2. G. I. Marchuk, Theory and Methods for Nuclear Reactor Calculations, Plenum Publ. (1964).
3. L. N. Romanova, in: Some Mathematical Problems of Neutron Physics [in Russian], Mosk. Gos. Univ. (1960), p. 8.
4. N. V. Ptitsyna, ibid., p. 28.
5. F. D. Gakhov, Boundary Value Problems, Pergamon (1966).
6. C. Crosjean, in: Proceedings of the Second International Conference, Vol. 16, Geneva (1958), p. 431.

LETTERS TO THE EDITOR

MEASUREMENT OF THE SENSITIVITY OF NEUTRON DETECTORS WITH SILVER EMITTER DURING LONG SERVICE IN REACTOR

I. Ya. Emel'yanov, Yu. I. Volod'ko,
V. V. Postnikov, V. O. Steklov,
and V. I. Uvarov

UDC 621.039.517

Beta-emission neutron detectors (BEND), especially BEND with silver emitters, are used extensively to monitor the neutron flux density in reactors [1, 2]. The technology used in the manufacture of cables with magnesian insulation is often employed in the fabrication of BEND. This technology makes it possible to organize the series production of BEND with practically no limitations as to the length of the sensitive part of the detector.

Tests have been made with BEND with silver emitter, constituting a segment of a KDMS(S) cable (TUMI 098-69), manufactured by the technology used in making cables with magnesian insulation. The cable has an Sr-999 silver core (GOST 7222-54) of 0.55-mm diameter, insulation of analytically pure magnesium oxide (GOST 4526-67), and a sheath of Kh18N10T corrosion-resistant steel 0.5 mm thick. The outside diameter of the cable is 3.0 mm.

On-site radiation testing of BEND was carried out in an IVV-2 reactor up to a thermal-neutron fluence of $2.4 \cdot 10^{21}$ neutrons/cm^2 at $\sim$650°C, as well as in the reactors of the first and second blocks of the Beloyarsk atomic power plant up to a fluence of $1 \cdot 10^{21}$ neutrons/cm^2 at $\sim$300°C. The tests showed that the mean BEND current is proportional to the reactor power and the mean neutron flux density, up to a power close to the nominal power of the first and second Beloyarsk reactors and the IVV-2, i.e., at a thermal-neutron flux of up to $1 \cdot 10^{13}$, $2 \cdot 10^{13}$, and $1 \cdot 10^{14}$ neutrons/cm$^2 \cdot$sec, respectively. The proportionality is maintained during long use up to the given values of the thermal-neutron fluence. The BEND specimens (seven in the IVV-2 reactor, four in the second Beloyarsk reactor, and more than 30 in the first Beloyarsk reactor) retained a sufficiently high insulation resistance during the tests. Thus, at nominal reactor power it was no worse than 10^6 $\Omega \cdot$m.

Along with the specimens of BEND consisting of a straight segment of cable-detector, five-section BEND were also tested to monitor the energy distribution over the height of the first Beloyarsk reactor. The BEND sections, at $\sim$80°C, consisted of segments of cable-detector twisted into a cylindrical spiral. The signal from each section was transmitted to recording equipment by a KNMS(S) cable [3]. The five-section BEND retained signal linearity and a sufficiently high resistance of insulation during use in a reactor for more than 2 years. The tests confirmed the long service life of cable-type BEND with silver emitter. However, precise data about the variations in the sensitivity of BEND sensitivity as a function of the thermal-neutron fluence are also required in order to monitor the energy distribution in the reactors. To obtain such data the IVV-2 reactor was provided with two experimental ports holding, respectively, 7 and 9 BEND specimens. The cable-detector length irradiated was 0.7 m. At nominal reactor power the temperature of the BEND specimens was $\sim$80°C, the mean density of the thermal-neutron flux was $4.7 \cdot 10^{13}$ neutrons/cm$^2 \cdot$sec, the mean density of the fast-neutron flux (E > 1 MeV) was $1.2 \cdot 10^{13}$ neutrons/cm^2.sec, and the mean γ-ray dose rate was $1.0 \cdot 10^5$ rd/sec.

In addition to determining the sensitivity, we periodically checked the linearity of the BEND and measured the resistance of their insulation under various intensities of irradiation. For precision monitoring of the neutron flux density, over a period of 1.5 yr we measured the activity of a 2.0-mm-diameter wire made of Sr-999 silver. The wire was irradiated in an experimental port along with a number of BEND specimens for 10 min at a reactor power close to the

Translated from Atomnaya Énergiya, Vol. 42, No. 5, pp. 403-404, May, 1977. Original article submitted February 13, 1976.

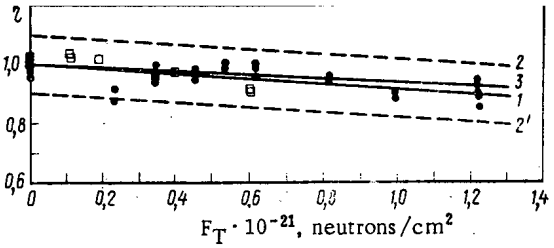

Fig. 1. Sensitivity of BEND vs thermal neutron fluence F_T: 1) curve corresponding to formula given in text; 2, 2') confidence limits with a confidence coefficient of 0.98; 3) calculated curve; first (●) and second (□) experimental ports.

TABLE 1. Resistance of BEND Insulation at Various Values of Flux Density and Thermal-Neutron Fluence

φ_T, neutrons/cm²·sec	F_T, neutrons/cm²											
	10^{18}	$0{,}93\cdot10^{20}$	$1{,}9\cdot10^{20}$	$2{,}3\cdot10^{20}$	$3{,}4\cdot10^{20}$	$4{,}0\cdot10^{20}$	$4{,}6\cdot10^{20}$	$5{,}3\cdot10^{20}$	$6{,}1\cdot10^{20}$	$8{,}2\cdot10^{20}$	$9{,}9\cdot10^{20}$	$1{,}2\cdot10^{21}$
$4{,}7\cdot10^{12}$	—	$6{,}4\cdot10^{8}$	—	—	—	—	$5{,}3\cdot10^{8}$	—	—	—	—	$5{,}8\cdot10^{8}$
$9{,}6\cdot10^{12}$	$2{,}3\cdot10^{8}$	—	—	—	—	—	$4{,}2\cdot10^{8}$	—	—	—	—	—
$1{,}4\cdot10^{13}$	$1{,}6\cdot10^{8}$	—	—	—	—	—	$3{,}8\cdot10^{8}$	—	—	—	—	$4{,}2\cdot10^{8}$
$2{,}2\cdot10^{13}$	$1{,}2\cdot10^{8}$	$1{,}4\cdot10^{8}$	—	—	—	—	$2{,}7\cdot10^{8}$	—	$1{,}6\cdot10^{8}$	—	—	—
$2{,}6\cdot10^{13}$	—	—	$1{,}0\cdot10^{8}$	—	$3{,}8\cdot10^{8}$	—	$2{,}2\cdot10^{8}$	—	$2{,}0\cdot10^{8}$	—	—	$3{,}0\cdot10^{8}$
$3{,}1\cdot10^{13}$	—	—	$2{,}5\cdot10^{8}$	—	—	—	$3{,}1\cdot10^{8}$	—	$2{,}0\cdot10^{8}$	—	—	—
$4{,}2\cdot10^{13}$	$n{,}1\cdot10^{8}$	$9{,}5\cdot10^{7}$	$7{,}8\cdot10^{7}$	—	$3{,}6\cdot10^{8}$	$4{,}8\cdot10^{8}$	$1{,}9\cdot10^{8}$	$2{,}3\cdot10^{8}$	$2{,}1\cdot10^{7}$	$8{,}4\cdot10^{8}$	$1{,}7\cdot10^{8}$	$1{,}7\cdot10^{8}$

nominal value. After exposure in this port for 3-5 min activity with half-lives of 24.4 and 2.4 min decayed practically completely in one hour above the active zone. The residual activity with a half-life of 259 days is not high (the γ-ray dose rate at a distance of 0.1 m is less than 100 μR/sec) and practically does not change during the measurements, thus making for convenient work with a tracer and more accurate results of the measurements.

All the specimens retained their efficiency at a thermal-neutron fluence of $1.2\cdot10^{21}$ and $8.8\cdot10^{20}$ neutrons/cm² in the first and second experimental ports. The tests showed that the BEND readings remain linear in the neutron flux to within ±2% at an indicated radiation intensity up to the values of the thermal-neutron fluence attained.

The results of the measurements, given in Fig. 1, were processed by the least-squares method. Finally, we obtained an empirical formula characterizing the relative variations in the sensitivity of the β-emission neutron detectors with silver emitter as a function of the thermal-neutron fluence F_T:

$$\eta = 1 - 0.08 \cdot F_T \cdot 10^{-21}.$$

Figure 1 gives the curve corresponding to this formula and the confidence limits for a confidence coefficient of 0.98. It also gives the calculated curve of the variations in the BEND sensitivity as a result of burn-up of the emitter material and an increase in the thermal-neutron fluence. As seen from Fig. 1, the calculated curve is close to the experimental. At a fluence of 10^{21} neutrons/cm² the calculated variations in the sensitivity are 6%, whereas the formula above yields 8%.

The resistance of the BEND insulation depends little on the irradiation intensity at constant temperature [2]. A slight drop in the insulation resistance was observed in the given experiment as the irradiation intensity increased; this is evidently due to a relatively small rise in temperature which occurs in the process, regardless of well-organized heat removal from the specimens. In the course of the data processing, the geometric mean of the resistance of the BEND insulation was found separately from specimens placed in each port. These values for various intensities of irradiation and neutron fluence are listed in Table 1. It can be seen that at a constant irradiation intensity the BEND insulation resistance does not display any tendency to change with an increase in the neutron fluence, up to $1.2\cdot10^{21}$ neutrons/cm², and is $\sim10^{8}$ Ω·cm.

Knowing the neutron fluence for each detector, we can make allowance for variations in its sensitivity by means of the given relation. The detector sensitivity variations due not to burn-up of the emitter material but to changes in the insulation resistance [2] can evidently be disregarded, at least for a fluence of up to $1.2 \cdot 10^{21}$ neutrons/cm^2 since there are no significant changes in the resistance.

The results of the given studies confirm the usefulness of cable-type β-emission neutron detectors with silver emitter for precision monitoring of energy distribution during long periods of use in the active zone of a reactor with a power load.

LITERATURE CITED

1. I. Ya. Emel'yanov et al., At. Energ., 30, No. 3, 275 (1971).
2. I. Ya. Emel'yanov et al., At. Energ., 37, No. 1, 72 (1974).
3. I. Ya. Emel'yanov et al., in: Problems of Atomic Science and Engineering. "Reactor Construction" Series [in Russian], No. 4 (11), Izd. TsNIIatominform, Moscow (1974), p. 51.

LOCAL CONTROL OF PROFILE AND MAGNITUDE OF ENERGY RELEASE OF LOOP CHANNELS

F. M. Arinkin and G. A. Batyrbekov

UDC 621.039.51.519

This paper gives the results of studies on the possibilities of controlling the neutron field and energy release over the height and diameter of an experimental channel of a water-moderated—water-cooled reactor by means of an annular chamber with gaseous neutron absorber ^{3}He.

Chamber 1 (absorbing shield) consists of two stainless-steel coaxial tubes 2, welded into the common end plate and flange. Along its height the chamber is divided into seven isolated sections 3 with an autonomous gas supply system (Fig. 1). The number and dimensions of the sections were chosen in accordance with the conditions of nuclear safety of the experiment (the reactivity of one section did not exceed 0.7 β_{eff}, the fraction of delayed neutrons) and acceptable control of the energy-release profile along the channel height. The height of the active part of the ^{3}He-filled chamber was 580 mm, which is slightly less than that of the active zone (600 mm). The chamber is connected to cut-off valves and manometers via a collector with a tank for ^{3}He by a system of tubes 4. The chamber was installed in the central cavity of a critical assembly measuring 140 mm in diameter [1], formed by a shaped plunger 5 made of CAV alloy. The chamber was provided with 3-mm inside and outside gaps for coolant ducts. In the middle of the chamber was an experimental channel of 96-mm diameter into which a model fuel assembly was inserted. The assembly consisted of uranium dioxide tablets enriched to 90%, measuring 12 mm in diameter and 4-6 mm in height, and packed in a tungsten can with a wall thickness of 1 mm. The assembly contained seven model fuel elements arranged along the channel axis and had a height of 400 mm with a clearance of 60 mm between tablets.

For nuclear safety the chamber and all the tubing were tested for a long time at a pressure of 1.5 times the working pressure. Upon being filled with gas, the sections were cut off from the collector by the cut-off valves; this eliminated the possibility of ^{3}He leaking from all the sections simultaneously if the main tube burst. When the assembly was in an automatic control mode, the automatic control rod (AC) was inserted almost completely (450 mm) so that in the event of leakage of ^{3}He from the system complete insertion of AC would activate the scram system.

Translated from Atomnaya Énergiya, Vol. 42, No. 5, pp. 404-407, May, 1977. Original article submitted March 9, 1976.

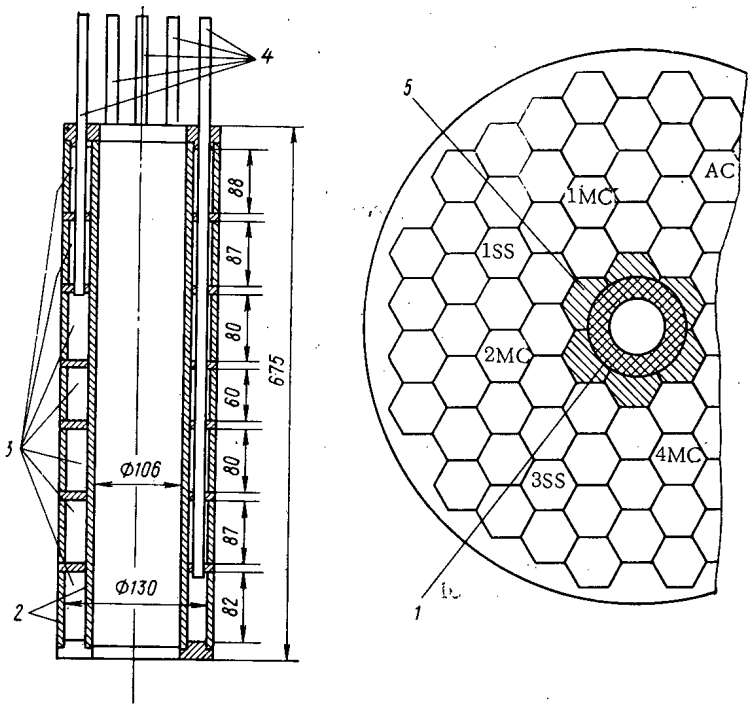

Fig. 1. Diagram of chamber and recorder chart of active-zone load (all dimensions in mm).

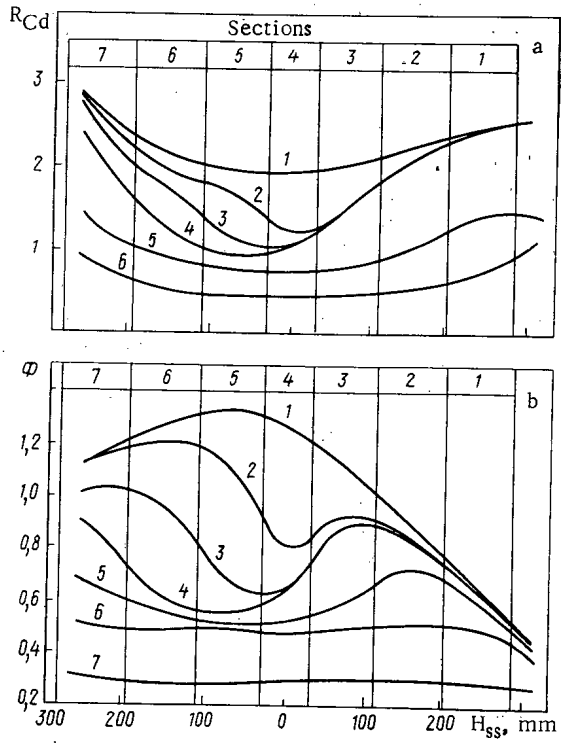

Fig. 2. Distribution of (a) R_{Cd} and (b) thermal-neutron flux Φ along the height of the experimental channel: a) cadmium ratio for $(\Sigma_a d)_n^m$, where m is the number of the curve; n is the number of the section: $(\Sigma_a d)_4^{2-5} = 1.163$; $(\Sigma_a d)_5^{2-5} = 0.831$; $(\Sigma_a d)_6^{4,5} = (\Sigma_a d)_3^5 = 0.665$; $(\Sigma_a d)_2^5 = 0,416$; $(\Sigma_a d)_7^5 = 0.582$; $(\Sigma_a d)_{1-7}^6 = 1.828$; the other sections for all curves $\Sigma_a d = 0$ for $\Sigma_a d = 1.828$, and P = 1114.6 kPa; b) thermal-neutron flux: $(\Sigma_a d)_4^{2-6} = (\Sigma_a d)_2^7 = 1.163$; $(\Sigma_a d)_5^{3-6} = 0,831$; $(\Sigma_a d)_3^{4-6} = 0.665$; $(\Sigma_a d)_7^5 = 0.249$; $(\Sigma_a d)_2^6 = (\Sigma_a d)_1^7 = 0,419$; $(\Sigma_a d)_7^6 = 0.582$; $(\Sigma_a d)_{3-6}^7 = 1.828$; $(\Sigma_a d)_7^7 = 1.496$; in the other sections, for all curves $\Sigma_a d = 0$.

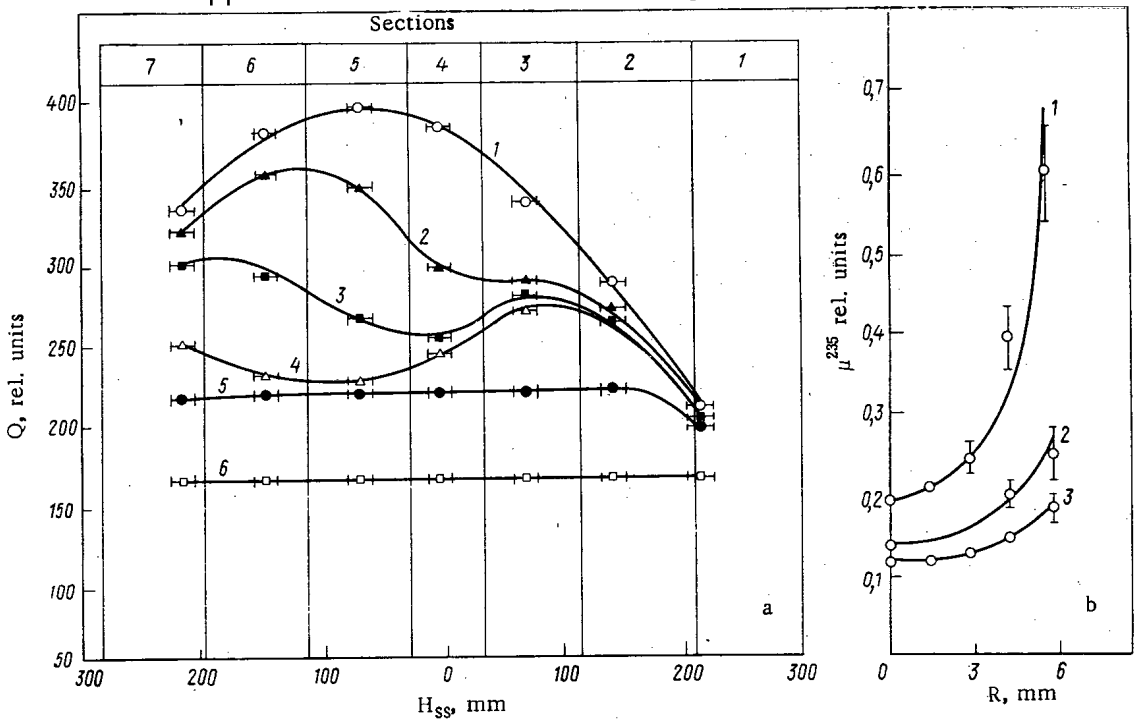

Fig. 3. a) Distribution of energy along height of fuel assembly and b) uranium fission density (μ^{235}) along radius of fuel-element model: a) $(\Sigma_a d)^{2-5}_4 = 1.163$; $(\Sigma_a d)^{3-5}_5 = 0.831$; $(\Sigma_a d)^{4\cdot5}_6 = (\Sigma_a d)^{5}_3 = 0.665$; $(\Sigma_a d)^{5}_7 = 0.249$; $(\Sigma_a d)^{6}_2 = (\Sigma_a d)^{6}_7 = 0.582$; $(\Sigma_a d)^{6}_{3-6} = 1.828$; in the other sections, for all curves $\Sigma_a d = 0$; b) $\Sigma_a d = 0$ (1); 0.996 (2), and 1.828 (3).

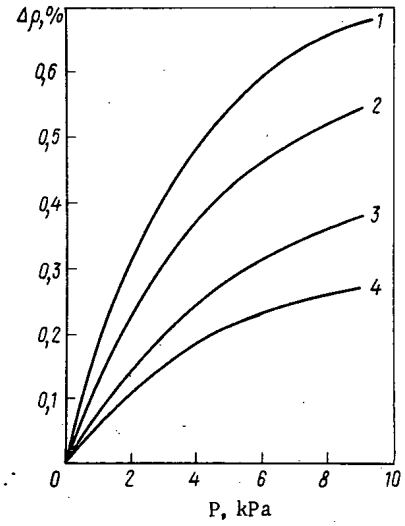

Fig. 4. Negative reactivity of individual sections of chamber as function of ^{3}He pressure: 1, 2) sections 4 and 5 (in the other sections $\Sigma_a d = 0$); 3, 4) sections 5 and 4 (in the other sections $\Sigma_a d = 1.328$, P = 911.9 kPa).

In studying the properties of the chamber, we employed the concept of shield "blackness," determined by $\Sigma_a d$ (where Σ_a is the macroscopic cross section for the absorption of thermal neutrons by a working substance of thickness d). The essence of the method of control proposed consists in measuring the shield blackness over height by varying the pressure of ^{3}He in separate sections.

The purpose of the experiment was twofold: to study the possibility of controlling the distributions of the neutron flux and energy release along the radius and the height of the experimental channel; and to study the effect of the chamber on the physical characteristics of the active zone and to analyze the safety aspects of work with such devices.

The distributions of the energy release in the fuel assembly, of the thermal-neutron flux, and the cadmium ratio R_{Cd} in the experimental channel were measured as a function of the ^{3}He pressure, as were the reactivity introduced into the active zone by the chamber as a whole and by the individual sections as well as the interference between the sections.

The energy distribution along the height of the fuel assembly was determined by calorimetric methods [2]. The energy microdistribution inside the fuel elements was also measured; upon integration, this gave the total energy release in each element [3]. The thermal-neutron flux and R_{Cd} were measured with ^{197}Au and ^{63}Cu detectors. In regions with a large neutron-flux gradient we resorted to autoradiography of the detecting material (in the given case, strips of ^{63}Cu) onto x-ray film which was subsequently analyzed on a microphotometer [4].

Figure 2 shows the distribution of the thermal-neutron flux and R_{Cd} on the empty experimental channel as a function of $(\Sigma_a d)_n$, where n is the number of the section counted from the top. Curve 1 corresponds to the case when the ^3He pressure in all sections is zero.* The coefficient of nonuniformity is 1.24 in this case. The asymmetry in curves 1 and 2 ("sag" on right-hand side of plot) is caused by control elements inserted to a depth of 200-220 mm.

The energy Q along the height of the channel with a seven-element assembly (Fig. 3) is of a similar nature, from which it is seen that the attenuation of the energy release at these values of $\Sigma_a d$ is less than the attenuation of Φ. The energy distribution along the height of the assembly (see Figs. 2 and 3) and the various fuel elements can be controlled continuously within wide limits; in particular, it is possible to shape an almost even profile of energy distribution over the height of the assembly (curves 5 and 6). With the chamber a maximum change of 2.4 times was obtained in the energy released in section 5, the mean energy release in the assembly decreasing by a factor of two in the process.

The variation of the uranium fission density (μ^{235}) in the cross section of the central fuel element is shown in Fig. 3b. The solid curves were obtained by calculation in the S_4 approximation of the Carlson method [5], whereas the empty circles denote experimental points. The large experimental errors at the ends of the curves are explained by the difficulty encountered in determining the detailed shape of the microdistribution of the energy at the boundary of the fuel element.

Calculations of the distributions of the thermal-neutron flux along the radius of the reactor in the S_4 approximation for various values of $\Sigma_a d$ showed that there is good agreement with experiment within the limits of the active zone. In the empty experimental channel the calculation underestimates the value of the neutron flux by 5-6%; this can be obviously considered a drawback of the S_4 approximation in calculations of large air cavities. The calculations were carried out by a one-dimensional kinetic program [6] with a system of 26-group constants. The program permitted us to take account of a neutron leakage from the end planes of the active zone. The leakage from the experimental channel was taken to be zero.

The reactivity measurements showed that the chamber without ^3He introduces a negative reactivity (−0.3%), whereas the experimental channel introduces a positive reactivity (+1.7%). The reactivity of some sections of the chamber is plotted in Fig. 4 as a function of the ^3He pressure. The difference between curves 1, 2 and 3, 4 is due to interference between the sections. The total contribution to the reactivity from all sections for P = 1114.6 kPa is −2.4%.

In conclusion, the authors would like to thank the personnel of the critical test stand at the Institute of High-Energy Physics, Academy of Sciences of the Kazakh SSR, as well as V. P. Kiselev and Sh. Kh. Gizatulin for their assistance in performing the experiments.

LITERATURE CITED

1. Zh. S. Takibaev et al., IFVÉ, Preprint PP-3 [in Russian], Inst. Fiz. Vys. Énerg., Akad. Nauk Kaz. SSR, Alma-Ata (1973).
2. Yu. L. Tsoglin et al., in: High-Dosage Dosimetry [in Russian], Fan, Tashkent (1966), p. 136.
3. V. B. Klimentov, G. A. Kopchinskii, and V. G. Bobkov, At. Energ., 29, No. 4, 283 (1970).
4. A. Ertaud and P. Zaleske, J. Phys. Radium, 14, 191 (1953).
5. B. Carlson and J. Bell, in: Proceedings of the Second International Conference on Peaceful Uses of Atomic Energy. Reactor Physics [Russian translation], Vol. 3, Atomizdat, Moscow (1959), p. 408.
6. L. N. Yaroslavtseva, NIIAR Preprint P-9, Melekess (1968).

*For the other curves, $\Sigma_a d$ is given only for those sections which contain helium.

LUMINOUS EMITTANCE OF NEUTRON BEAM IN AIR

A. V. Zhemerev, Yu. A. Medvedev,
and B. M. Stepanov

UDC 551.594.5

The paper considers a method of visualizing neutron fields in air in the optical region of the spectrum. Luminescence stimulated in air by neutrons with an energy of ∿10 MeV or less, in principle, occurs under the action of charged particles (electrons, protons, and α particles) with an energy of ∿1 MeV formed during the propagation of neutrons in air. It has been experimentally shown [1-3] that the character of the excitation of luminescence in air by protons and α particles with an energy of ∿1 MeV is roughly the same as in excitation with electrons and the luminous efficiency η (ratio of luminous energy in the optical range to the absorbed energy of fast charged particles) does not depend on the type and energy of the ionizing particle. Thus, the intensity of neutron-stimulated luminescence in air is determined by the absorbed neutron energy.

Production of heavy charged particles (protons, α particles) and γ rays is possible right during the interaction of neutrons with the nuclei of atoms in the make-up of atmospheric air, the ratio of γ-ray yield to charged-particle yield being determined by the energy dependence of the nuclear reactions. Since their paths in air are ∿1 cm, we can assume that protons and α particles are absorbed right where they are produced. However, the path of γ rays runs into hundreds of meters so that the absorbed γ-ray energy is distributed over some volume. The absorbed energy of a neutron consists of the absorbed energies of short-range radiation (protons, α particles) $I_p(\mathbf{r}, t)$ and long-range radiation (γ rays) $I_\gamma(\mathbf{r}, t)$. These quantities are related to the neutron field $N(\mathbf{r}, \varepsilon, t)$ by

$$I_p(\mathbf{r}, t) = \eta \int d\varepsilon v N(\mathbf{r}, \varepsilon, t) \sum_i \sigma_i(\varepsilon) E_i(\varepsilon); \quad (1)$$

$$I_\gamma(\mathbf{r}, t) = \eta \int d\varepsilon v \sum_i \int d\mathbf{r}' N(\mathbf{r}', \varepsilon, t) \sigma_i(\varepsilon) \times I_a[E_i(\varepsilon), \mathbf{r}-\mathbf{r}', t-t'], \quad t-t' = r'/c, \quad (2)$$

where v and ε are, respectively, the neutron velocity and energy; $\sigma_i(E)$ is the macroscopic cross section of the i-th reaction leading to the production of a charged particle or a γ ray with an energy of $E_i(\varepsilon)$; $I_a(E_i, r, t) = I_a(E_i, r)\delta(t)$; $I_a(E_i, r) = A \exp(-\mu r)[1 + C\mu r \cdot \exp(D\mu r)]/4\pi r^2$ is the absorbed energy from a stationary, isotropic point source of γ rays with an energy of E_i [4]; and t' is the time at which the γ ray is produced. The delay of γ rays is taken into account in Eq. (2). The summation over i in Eqs. (1) and (2) is performed for all possible reactions. The neutron field $N(\mathbf{r}, \varepsilon, t)$ can be calculated, e.g., by the Monte Carlo method.

Note that luminescence in air can also be stimulated by recoil nuclei which arise in the elastic scattering of neutrons with an energy of ∿2 MeV or more.

Neutrons with $\varepsilon \leqslant 0.45$ MeV may be absorbed as a result of the radiative capture reaction $^{14}N(n, \gamma)^{15}N$ and the $^{14}N(n, p)^{14}C$ reaction with the emission of a proton [5]. The energy release of these reactions are

$$E_{pr} = Q_p \Sigma^0_{pr}/\Sigma^0_a; \quad E_{n\gamma} = n_\gamma E_\gamma \Sigma^0_{n\gamma}/\Sigma^0_a,$$

where $\Sigma^0_{n\gamma}$, Σ^0_a, and Σ^0_{pr} are, respectively, the coefficients of radiative capture, total capture, and neutron capture with emission of a proton [6] ($\Sigma^0_{pr}/\Sigma^0_{n\gamma} = 25$ [5]); $Q_p = 0.62$ MeV is the energy of the reaction with emission of a proton [5]; $n_\gamma = 2.25$ is the average number of γ

Translated from Atomnaya Énergiya, Vol. 42, No. 5, pp. 407-408, May, 1977. Original article submitted May 14, 1976.

rays and E_γ= 4.96 MeV is the mean energy of γ rays produced in the radiative capture of a neutron [7]. On substitution of the numerical values, we get E_{pr} = 0.6 MeV and $E_{n\gamma}$ = 0.43 MeV.

We determine the luminous intensity of an elementary volume of air at the outlet of a thermal-neutron reactor. Taking $f = 10^{12}$ cm^{-2}·sec^{-1} as a typical value of the thermal-neutron flux, we obtain

$$I \approx \eta E_{pr} f / l_a \approx 10^{-9} \text{ W/cm}^3,$$

where $\eta \approx 10^{-4}$ [1-3]; and $l_a \approx 100$ m is the path of thermal neutrons to absorption. Such an intensity can be recorded easily.

Let us consider the luminescence stimulated in air by a point isotropic source of neutrons with an initial energy of $\varepsilon_0 \leq 0.45$ MeV. Let us calculate the luminous intensity (we call it the intensity of luminescence over a disk) recorded by a radiation detector whose angle of collimation is formed by two conic surfaces with slightly different apex angles; the line joining the center of the source and the detector is the axis of symmetry. Suppose that the light detector is at a large distance ($R_0 \gg \mu^{-1}$) from the neutron source; then the luminous intensity over a disk is determined by a light quanta emitted by a volume formed by two infinite cylindrical surfaces of radii ρ and ρ + Δρ with the source–detector line as the axis of symmetry. The intensity of the luminescence over a disk, stimulated by protons, is given by

$$D_p(\rho, t) = \eta [E_{pr} N_0 \rho \Delta\rho \Sigma^0_{pr} / 8\pi R_0^2 \tau(t)] \exp\{-\Sigma^0_a t - r^2/4\tau(t)\}; \quad (3)$$

the intensity of luminescence over a disk, stimulated by γ rays, is given by

$$D_\gamma(\rho, t) = \alpha f(\rho, t) D_p(\rho, t), \quad (4)$$

where

$$f(\rho, t) = \frac{\beta^2}{\sqrt{\pi}} \int_0^\infty \frac{dy \exp(-y^2/4)}{\sqrt{x^2+\beta^2+y^2}} \int_0^\infty \frac{dz}{z} \exp\{-\beta z - z^2/4\} \left[1 + C\mu z \exp(D\mu z)\right] \operatorname{sh} \frac{z}{2\beta} \sqrt{x^2+\beta^2 y^2};$$

$\alpha = 2n_\gamma \Sigma^0_{n\gamma} A / E_{pr} \Sigma^0_{pr}$; $\mu \approx 1$; $\beta = \mu\sqrt{\tau}$; $x = \mu\rho$; τ(t) is the size of the delayed neutrons [6]; N_0 is the total number of neutrons emitted by the source. In writing Eqs. (3) and (4) we used an analytic expression for the captured-neutron field which is proportional to $\exp\{-\Sigma^0_a t - r^2/4\tau(t)\}/[4\pi\tau(t)]^{3/2}$.

Next, we study Eq. (4). Let C = 0, i.e., we take no account of γ-ray scattering. For small x ($x \ll 2\beta$) we expand the hyperbolic sine of Eq. (4) in a series, retaining the first two terms. Upon integrating, we have

$$f(\rho, t) = [7I + 2\beta^2 (I - 1)]/12,$$

where

$$I = \sqrt{\pi}\beta \exp(\beta^2) [1 - \operatorname{erf}(\beta)];$$

erf(β) is the error function. When $\beta \ll 1$, $f(\rho, t) \approx \sqrt{\pi}\beta/2$.

For large values of x ($x \gg 2\beta$), the hyperbolic sine of Eq. (4) can be replaced by exp(x)/2. Using the saddle-point method to evaluate the integrals with respect to z [saddle point $z = (\sqrt{x^2 + \beta^2 y^2} - 2\beta^2)/\beta$] and with respect to y [saddle point y = 0], we have

$$f(\rho, t) = \sqrt{\pi x/2} [\beta^2/x (x - 2\beta^2)] \exp\{(x^2/4\beta^2) + \beta^2 - x\}.$$

Thus, visualization of the luminous field yields information about the absorbed energy and, for small x, also gives us an idea of the field of captured neutrons.

Let us evaluate the luminous flux by Eq. (3): $(\Sigma^0_{pr})^{-1} \approx 0.06$ sec [5] and $N_0 \approx 10^{23}$ [8]. Let ρ = 300 m, Δρ = 10 m, $\tau = 2 \cdot 10^4$ m^2, R_0 = 30 ρ, and t = 0.06 sec; then $D_p \approx 10^{-8}$ W/cm^2, which is perfectly measurable by present-day optical means.

LITERATURE CITED

1. C. Fan, Phys. Rev., 103, No. 6, 1740 (1956).
2. W. Borst and E. Zipf, Phys. Rev., 1A, No. 3, 834 (1970).
3. M. Hirsh, E. Poss, and P. Eisner, Phys. Rev., 1A, No. 6, 1615 (1970).

4. M. N. Wrobel (Vrubel'), S. N. Sidneva, and A. S. Strelkov, At. Energ., 34, No. 1, 47 (1973).
5. V. M. Kuvshinnikov et al., in: Nuclear Constants [in Russian], No. 16, Atomizdat, Moscow (1974), p. 53.
6. A. V. Zhemerev et al., At. Energ., 38, No. 3, 174 (1975).
7. Nuclear Data [in Russian], Atomizdat, Moscow (1969), p. 391.
8. H. Sandmeier, S. Dupree, and G. Hansen, Nucl. Sci. Eng., 48, 343.

EFFECT OF PRE-IRRADIATION ON OXIDATION OF ALLOY Zr + 2.5% Nb

M. G. Golovachev, V. I. Perekhozhev, V. E. Kalachikov, and O. A. Golosov

UDC 621.039.531:669.296'293

Oxidation of the Zr + 2.5% Nb alloy is usually intensified by the action of radiation from a nuclear reactor [1]. To understand the nature of this effect it is desirable to consider the influence of pre-irradiation on subsequent oxidation of Zr + 2.5% Nb.

The studies were carried out with specimens which had undergone quenching from 840°C with subsequent 40% deformation and annealing at 550°C for 5 h in a vaccum no worse than $5 \cdot 10^{-5}$ mm Hg. Before oxidation, some of the specimens were irradiated in the active zone of a reactor at 80°C with a fluence of $2.6 \cdot 10^{19}$ neutrons/cm^2 ($E \geq 1.1$ MeV). The effect of the irradiation on the properties of the alloy was evaluated by the changes in the electrical resistivity, measured at room temperature on specimens with dimensions of 50 × 2 × 0.5 mm. Isochronal annealing of the irradiated and unirradiated specimens was carried out in a vacuum furnace over a range of 50°C. The holding time at each temperature was 2 h since it was established in preliminary experiments that even at a low temperature (170°C), annealing for 1.5 h was sufficient for practically complete restoration of the initial resistivity.

The variations in the electrical resistivity of the irradiated and unirradiated alloy during the process of isochronal annealing are plotted in Fig. 1. The error in determining the resistivity of the alloy was 0.5%. Each experimental point corresponds to the mean of measurements of two specimens.

On the basis of data concerning the variations in the electrical resistivity under isochronal annealing of the irradiated alloy, we chose three oxidation temperatures at which the resistivity of the irradiated alloy is greater than (250°C), almost equal to (330°C), and less than (400°C) that of the unirradiated alloy. Specimens measuring 30 × 5 × 1 mm were oxidized in a stream of moist (5-7 vol.% vapor) of commercially pure nitrogen with an overall gas flow rate of 5-10 liters/h. The specimens were weighed on VLAO-100 scales with a sensitivity of $5 \cdot 10^{-5}$ g. The increases given in Table 1 for each temperature are averages for 3 or 4 specimens.

TABLE 1. Increase in Weight of Zr + 2.5% Nb Alloy after 100 h of Oxidation, mg/dm^2

State of alloy	Testing temp., °C		
	250	330	400
Unirradiated	2,0±0,9	7,2±1,5	16,1±1,3
Irradiated with fluence of $2.6 \cdot 10^{19}$ neutrons/cm^2 ($E \geq 1.1$ MeV)	4,5±1,3	8,1±1,3	10,7±1,2

Translated from Atomnaya Énergiya, Vol. 42, No. 5, p. 409, May, 1977. Original article submitted July 13, 1976.

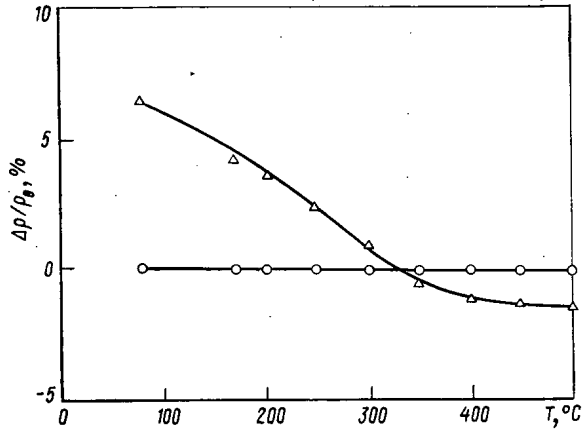

Fig. 1. Relative variation of resistivity of Zr + 2.5% Nb alloy during process of isochronal annealing: Δ) irradiated with a fluence of $2.6 \cdot 10^{19}$ neutrons/cm^2; O) unirradiated.

When the temperature is raised from 250 to 400°C the process of oxidation is intensified for both unirradiated and irradiated specimens. However, the effect of pre-irradiation on the oxidation of the alloy is not unique at each temperature investigated. At 250°C the irradiated specimens display a larger increase in weight than do the unirradiated. At 330°C this difference practically does not exist and at 400°C the pre-irradiated specimens are more resistant to oxidation than are the unirradiated.

A correlation can thus be observed between the variations in the resistivity and the resistance to oxidation for irradiated specimens of the Zr + 2.5% Nb alloy; a lower resistance of oxidation corresponds to a higher electrical resistivity.

A multitude of radiation-induced defects are formed in the crystal lattice of the alloy in the process of irradiation. During annealing, the defects either form complexes or migrate to dislocations, grain boundaries, etc. However, some radiation-induced defects are preserved up to a temperature of 300-350°C, as evidenced by the increased electrical resistivity. This increased concentration of defects (in comparison with the unirradiated materials) evidently leads to accelerated oxidation of the alloy.

Annealing of irradiated specimens at 400°C probably gives rise to a further stabilization of the alloy structure. This, as is known [2], enhances the oxidation stability, which proves to be higher than in unirradiated specimens.

LITERATURE CITED

1. Sueo Nomura, Nippon Genshiryoku Gakkaishi, 11, No. 6, 353 (1969).
2. J. Le Surf, in: Proc. Symp. ASTM (STP) Applications-Related Phenomena for Zirconium and Its Alloys, Philadelphia (1969), p. 286.

DETECTION OF START OF BOILING OF LIQUID METAL COOLANT

K. A. Aleksandrov, V. A. Afanas'ev,
N. G. Gataullin, and V. V. Golushko

UDC 621.039.534.6

One method of detecting when the coolant starts boiling in the core of fast reactors is an acoustic method [1], based on the recording of noise from forming and "collapsing" vapor bubbles. The principal difficulty in using this method in power reactors is attendant upon the presence of an intense noise background generated by the work of the pumps and the flow of the coolant. It is, therefore, necessary to make the proper choice of the frequency range of detection and the best signal-to-noise ratio while preserving an adequate intensity of the useful signal.

Detection of the start of boiling of sodium with various sensors was studied in a BOR-60 reactor. The assembly used incorporated a boiler and acoustical transducers: of the waveguide type (steel rod 10 mm in diameter and 7 m in length with a piezoelectric element of TsTS-19 ceramic attached to the upper end) and of the immersible type (with a piezoelectric element made of lithium niobate [2] and TsTS-19 ceramic). The diameter and thickness of the piezoelectric element of the first immersible transducer are 10 and 3 mm and those of the second are 12 and 1.5 mm. The assembly was installed above the core: the transducers were at the level of the packet heads at a distance of 250 mm from the boiler.

The operation of the boiler is based on the passage of an alternating current through a tube containing sodium; the volume of the sodium being heated is 3 cm^3. During boiling the vapor bubbles leaving the tube "collapse" in the volume of underheated sodium. The instant at which boiling begins is monitored by an abrupt drop in the supply current. Boiling was started 25 times at various coolant flow rates through the reactor.

Studies of the intrinsic noise of the BOR-60 reactor showed that the effective value of the noise amplitude is related only to the variations in the coolant flow rate; the shape of the spectrum remains practically unchanged. Temperature and power variations over a broad range do not appreciably affect either the amplitude or the spectrum of the noise, which is in agreement with the data of [1]. There is practically no reactor noise at frequencies above 100 kHz.

The experiments were carried out at zero reactor power and a temperature of 210°C. This made it possible to simplify the design of the assembly and to use a piezoceramic immersible transducer with a high sensitivity. In addition to the acoustic transducers mentioned above, in the experiments we also used a clamping transducer with a piezoelectric element of TsTS-19 ceramic; this transducer, measuring 10 mm in diameter and 1.5 mm in thickness, was set up on the reactor lid. This transducer recorded a higher level of noise background at all frequencies than any of the other transducers did.

The signals from the piezoelectric transducers were transmitted to a wideband preamplifier from which they went to the main amplifier via a high-frequency filter with a "cutoff" frequency of 50 kHz. Then the signals were fed into a random-process analyzer [2] for amplitude, time, and parallel frequency analysis in the frequency range 20-500 kHz.

In the case of all measured spectra of boiling noise, in order to prevent signals being recorded in the absence of boiling the discrimination level of the instrument was set slightly above the level of background noise recorded by the transducer on the lid at the maximum flow rate. Figure 1 shows the boiling noise spectra recorded by the various transducers at zero and maximum rate of coolant flow through the reactor. The coordinates of the individual

Translated from Atomnaya Énergiya, Vol. 42, No. 5, pp. 410-411, May, 1977. Original article submitted July 13, 1976.

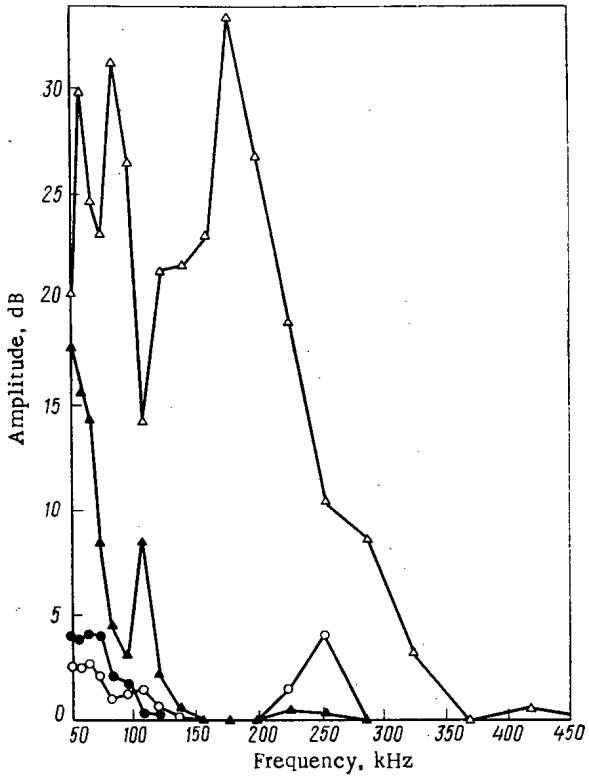

Fig. 1. Boiling noise spectra of sodium: ●) clamping transducer of lithium niobate (zero flow rate); O) waveguide-type transducer (flow rate 960 m^3/h); ▲) clamping transducer on reactor lid (zero flow rate); Δ) piezoceramic clamping transducer (flow rate 960 m^3/h).

points are determined by the mean frequency of the resonance filters of the analyzer and the time-averaged measurements of the signal amplitude, referred to the discrimination threshold which was the same in all experiments.

Signals of boiling are recorded most successfully by clamping transducers (with piezoelectric element of TsTS-19 ceramic). It should be noted that boiling can be recorded even by transducers set up on the reactor lid. For the immersible transducer the ratio of the effective value of the signal during boiling to the background noise in the frequency range above 50 kHz is no less than 30 dB at maximum coolant flow rate. This ratio grows as the frequency increases.

The measurements showed that to detect when sodium begins to boil in a reactor the most acceptable frequency range is 80-300 kHz, where the maximum signal-to-noise ratio is observed. The use of piezoelectric transducers with resonance at frequencies in this range makes it possible to isolate the useful signal more reliably. The boiler of simple design used in the experiments can be a convenient means of adjusting and monitoring acoustical systems for the diagnosis of the onset of boiling by sodium coolant in a fast reactor.

LITERATURE CITED

1. V. M. Baranov, Ultrasonic Measurements in Atomic Engineering [in Russian], Atomizdat, Moscow (1975).
2. K. A. Aleksandrov et al., NIIAR Preprint P-9(275), Dimitrovgrad, Bulgaria (1976).

DIRECT ENERGY CONVERSION OF MONOENERGETIC ION BEAMS WITH SPACE-CHARGE COMPENSATION

O. A. Vinogradova, S. K. Dimitrov,
A. S. Luts'ko, V. M. Smirnov,
and V. G. Tel'kovskii

UDC 621.039.6

The injection of fast atoms into a plasma can serve as one of the methods for plasma heating in tokamaks [1]. Estimates show [2] that a sufficiently high energy efficiency ($\gtrsim 0.7$) can be obtained if direct conversion of the energy of ions that are not neutralized in the neutralizer is employed.

This paper discusses a converter using compensation of the ion space charge by an electron flux in crossed magnetic and electric fields ($\mathbf{E} \times \mathbf{H}$) which makes it possible to convert the energy of comparatively dense ion beams. The device is more compact than those previously proposed. At the present time, several alternative locations of the converter in the injection system are under consideration. It was suggested [2] that the beam of unneutralized ions be deflected by about 90° by means of a bending magnet and the energy then converted. A beam can be deflected by means of the magnetic field of a tokamak. A system for conversion of ion energy along the flow channel was also proposed, i.e., the so-called in-flight conversion.

It is expedient to use the converter with $\mathbf{E} \times \mathbf{H}$ fields discussed here in an arrangement with a bending magnet. The instrument is placed immediately behind the magnet and makes it possible to convert the energy of a beam at the same density as that with which it emerged from the magnet. In this case, there is no necessity for expansion of the beam to a low density since the space charge is compensated by electron fluxes in the converter with $\mathbf{E} \times \mathbf{H}$ fields. The transverse dimensions of the flow are relatively small, and a lens, rather than a grid, can be used to remove electrons from the beam, which makes it possible to increase the energy flux density considerably.

The scheme for conversion with $\mathbf{E} \times \mathbf{H}$ fields is shown in Fig. 1. The ion flux is encompassed by loops, one side of which is an electron emitter (E) and the other side a collector (C). The potentials $\varphi_1, \varphi_2, \ldots, \varphi_N$ are applied to the loops; the potentials increase linearly with distance in proportion to the approach to the ion collector, which consists of jalousie louvres at the stopping potential φ_T.

Power losses during stopping of a dense beam of high-energy ions in such a system ($n_i = 10^9$–10^{11} cm^{-3} is the density of the ion beam and $W_i = 100$–200 keV is its energy) were estimated in this work. These values of density and energy are typical of ion fluxes in the

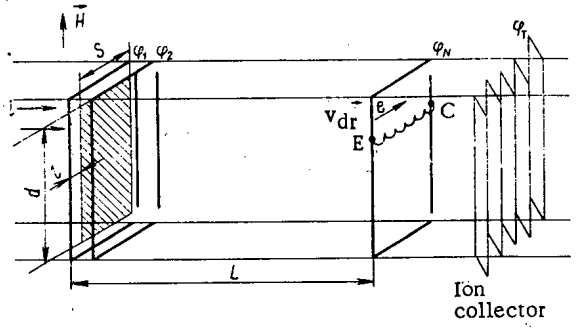

Fig. 1. Diagram of converter with $\mathbf{E} \times \mathbf{H}$ fields.

Translated from Atomnaya Énergiya, Vol. 42, No. 5, pp. 411-412, May, 1977. Original article submitted July 30, 1976.

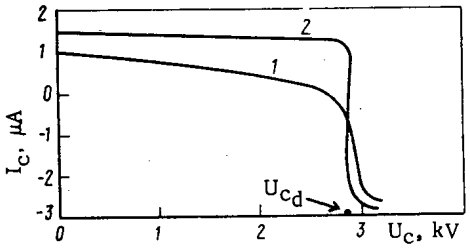

Fig. 2

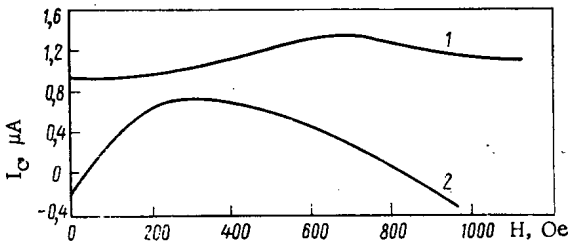

Fig. 3

Fig. 2. Dependence of collector current on collector potential for H = 0 (1) and H = 250 Oe (2).

Fig. 3. Dependence of collector current on magnetic field intensity for U_c = 0 (1) and U_c = 2.85 kV (2).

injector of thermonuclear reactors based on a tokamak or open trap. In the dependence on the energy and density of the ion beam, limitations are imposed on the parameters of the converter (H, external magnetic field; L, length of stopping space; S and d, transverse dimensions of the ion beam along the drift velocity v_{dr} and along H respectively; l, distance from the emitter loop to the ion beam) which are determined by the following conditions [3]: smallness of the stopping space in comparison with the ion Larmor radius, $\alpha_1 = rL/r_{Li} \ll 1$; smallness of the electron Larmor radius in comparison with the length of the stopping space, $\alpha_2 = rr_{Le}/L \ll 1$; smallness of the power P_e consumed in heating thermal electrons from the emitters in comparison with the power P_i in the ion beam, $\alpha_3 = P_e/P_i \ll 1$; smallness of the loss in acceleration of electrons pulled into the beam from an emitter with formation of a virtual anode in the emitter—beam region and with insufficient compensation of the beam by electrons, $\alpha_4 = P_e/P_i$, where P_e is the power of the accelerated electrons. Energy losses because of Coulomb collisions between electrons and ions, losses through radiation from electrons, and losses through ionization of residual gas molecules by the ions are several orders of magnitude less than the losses discussed above. Losses through acceleration of ionized residual gas molecules and in pumping out the device can be optimized and are no more than one percent.

The efficiency of a converter with E × H fields was calculated for the injectors of presently planned tokamaks. Given below are parameters for two versions of the injectors and the losses in the converter ($\alpha_1 - \alpha_4$):

W_i, keV	80, 160
P_i, MW	1.48, 6.81
S × d, cm^2	25 × 62.5
$n_i \times 10^9$, cm^{-3}	0.26, 0.43
α_1	$1.2 \cdot 10^{-7} \cdot H^2$, $0.6 \cdot 10^{-7} \cdot H^2$
α_2	$2.6 \cdot 10^6/H^3$, $7.3 \cdot 10^6/H^3$
α_3	45/H, 32/H
α_4 (l = 0.5 cm)	3.6/H, 3.8/H
Optimal magnetic field H, Oe	500-800, 700-1000
Minimal overall losses, %	15, 12

The values of the energy loss and of the magnetic field show that this converter can be used in modern large-scale tokamaks for improvement of the energy balance in injector circuits.

Conversion of ion energy in E × H fields was experimentally studied on a model intended for the analysis of methods for stopping charged particles in E × H fields. The experiments were performed in two ways: 1) stopping of the ion beam in a system with collection of secondary electrons (parasitic background) produced in the stopping space through interception of the ion beam by structural elements of the converter. The purpose of this experiment was to confirm the possibility of using parasitic electrons for compensation of the ion space charge; 2) stopping of the ions with compensation of the positive space charge by electron fluxes directed perpendicularly to the geometric axis of the beam and produced by special emitters.

The effect of a magnetic field is seen in Fig. 2, which shows the dependence of the collector current I_c on the collector potential U_c for an ion energy W_i = 3 keV at the entrance to the stopping space (with and without a magnetic field present). With a magnetic field present (H = 250 Oe), the secondary electrons drift across the converter and I_c rises since secondary electrons do not reach the collector. In a simple electrostatic field, the collector current falls with increasing U_c (and, consequently, with increasing stopping power eU_c/W_i) in such a way that $I_c = 0$ when $eU_c/W_i = 0.85$. With stopping in E × H fields, I_c decreases insignificantly up to the point $eU_c/W_i = 0.96$, where the collector current drops sharply to zero and becomes negative with further increase in stopping power since the flow of secondary electrons to the collector is intensified.

The relationship $I_c(U_c)$ for ions of other energies in the range studied has a similar form. The value H of the magnetic field at which the curves $I_c(U_c)$ were taken for different W_i was chosen from plots of the relation $I_c(H)$ made for the appropriate specified U_{cd} and W_i (Fig. 3). These curves have a maximum which is shifted in the direction of smaller H with increase in the stopping power eU_c/W_i for each fixed energy W_i. Values of H corresponding to these maxima were taken as optimal. It was found experimentally that the optimal values of H increased linearly with increasing energy, having a gradient of 60 Oe/kV.

The experiment employing an artificial electron screen demonstrated the possibility of compensating the ion space charge by electron fluxes produced by special emitters. However, a significant increase in converter efficiency was not observed since the effect of the repulsive forces of the space charge was relatively small in this experiment.

LITERATURE CITED

1. V. I. Pistunovich, Preprint IAÉ-2209, Moscow (1972).
2. J. Hovingh and R. Moir, Nuclear Fusion, 14, 629 (1974).
3. O. A. Vinogradova et al., Abstract 2179-76, Izd. VINITI, Moscow (1976).

SURFACE β-ACTIVITY OF SOIL AND VEGETATION CAUSED BY NUCLEAR-EXPLOSION PRODUCTS AND ITS DEPENDENCE ON THE VERTICAL MIGRATION OF ISOTOPES

K. P. Makhon'ko and A. S. Avramenko

UDC 550.378

The fallout of nuclear-explosion products from the atmosphere leads to an accumulation of radioactive isotopes on the soil and vegetation cover [1, 2]. At the same time, these isotopes migrate into the soil and decay radioactively [3, 4]. The surface β-activity of the soil increases or decreases, depending on whether the first or the second process predominates. Brendakov et al. [5] give data on the vertical distribution in the soil of fission products from explosions from 1963 to 1967. The activity of the soil was observed to have a maximum in 1963; since 1968 it has remained roughly constant, due to the natural radioactivity of the soil and vegetation. In Fig. 1 the variations of the surface activity of naturally occurring soils are plotted as a function of time; the plot was obtained by measuring hard β radiation (E_{max} > 0.35 MeV). The level of the natural background is indicated by a dashed line. The migration of nuclear-explosion products was measured. This effect in the surface layer of the soil vegetation cover can be calculated from the difference between the sum of the cumulative atmospheric fallout of the various isotopes formed during a nuclear explosion and the surface β-activity of the soil actually observed. The calculations (Table 1) were based on experimental data [1, 2] and the ratio of the activity of short-lived isotopes over a period of 1 year [6]. Table 2 gives the numerical values of the fraction A_{det}/A

Translated from Atomnaya Énergiya, Vol. 42, No. 5, pp. 413-414, May, 1977. Original article submitted November 29, 1976.

TABLE 1. Radioisotopic Composition of Soil Pollution in Summer of 1963

Radionuclide	A, μCi/km²	A_{deg}/A, %	Radionuclide	A, μCi/km²	A_{det}/A, %
^{54}Mn	45	0	^{125}Sb	107	4,2
^{89}Sr	36	51,5	^{127}Te	30	12,5
^{90}Sr	33	4,1	^{137}Cs	56	6,3
^{90}Y	33	67,4	^{141}Ce	7	3,0
^{91}Y	80	54,0	^{144}Ce	200	0
^{95}Zr	250	1,1	^{144}Pr	200	74,0
^{95}Nb	250	0	^{147}Pm	185	0
^{103}Ru	25	0,4	^{151}Sm	3	0
^{106}Ru	465	0	^{155}Eu	25	0
^{106}Ru	465	77,0			

TABLE 2. Weighted Mean Depth of Penetration of Nuclear-Explosion β Products into Soil, d mm

Yr	Calc.	Expt.	Yr	Calc.	Expt.
1963	3	4	1966	7	10
1964	5	7—8	1967	12	10—14
1965	4	9—10			

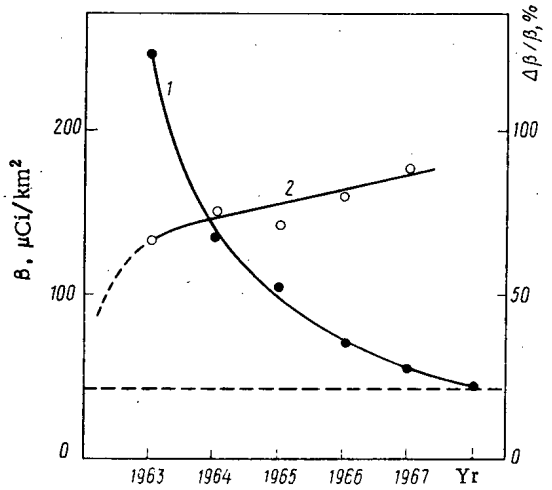

Fig. 1. Hard β radiation from soil surface: 1) variation with time; 2) attenuation Δβ/β due to vertical migration of isotopes.

of surface activity, where A_{det} is the β radiation detected and A is the excess of the isotope in the soil. The calculation of the accumulation of hard β-emitters on the soil surface for the middle of each year enables us to find the attenuation of the radiation owing to the penetration of isotopes into the soil with time. A large proportion of β-activity with $E_{max} > 0.35$ MeV is absorbed by the soil and the radiation drops by almost an order of magnitude in 5 years as a result of vertical migration (curve 2 in Fig. 1).

Let us find the depth to which nuclear-explosion products penetrate into the soil. The profile of their concentration is described by an incomplete γ function [4], but in a number of cases or in the surface layer of the soil it is quite close to the exponential function [4, 5] with exponent a. It is not difficult to show that in this case the weighted mean depth of penetration of nuclear-explosion products into the soil ("excess center") is given by

$$d = 1/a = \frac{A-\beta}{\beta\mu}, \quad (1)$$

where A and β are, respectively, the calculated and observed excess of nuclear-explosion products in the soil, the observed value being found from the β radiation; $\mu = 6 \cdot 10^{-3}$ cm²/mg is the coefficient of β-particle absorption by the soil, equivalent to the β-particle absorption by the real mixture of isotopes. Table 2 gives the values of d calculated by Eq. (1) and the experimental values [5]. They are seen to be in satisfactory agreement. Thus, the weighted mean depth of the penetration of β-emitters into the soil increases at the rate of several millimeters per year (without corrections for the decay of isotopes in the process of migration.

LITERATURE CITED

1. N. V. Vasil'eva et al., Tr. Inst. Élektromekh., No. 25, 166 (1972).
2. K. P. Makhon'ko et al., Tr. Inst. Électromekh., No. 6(64), 64 (1976).
3. F. I. Navlotskaya, Migration of Radioactive Products of Global Fallout in Soils [in Russian], Atomizdat, Moscow (1974).

4. K. P. Makhon'ko, in: Radioactive Isotopes in Soils and Plants [in Russian], Kolos, Moscow—Leningrad (1969), p. 48.
5. V. F. Brendakov et al., Tr. Inst. Élektromekh., No. 5, 143 (1970).
6. M. P. Grechushkina, Tables of Composition of Products of Instantaneous Fission of ^{235}U, ^{238}U, and ^{239}Pu [in Russian], Atomizdat, Moscow (1964).

ALLOWANCE FOR FLUCTUATIONS OF RADIATION FLUX IN ACTIVATION ANALYSIS

Pham Zui Hien

UDC 543.53

In activation analysis experiments the effect of radiation flux is usually eliminated by simultaneous irradiation of a specimen and a standard or by the use of an external standard [1]. Although these methods, in principle, ensure good accuracy, they do have shortcomings which limit the efficiency of the method of analysis and cannot always be used successfully, especially in cases when short-lived isotopes are formed. This paper gives a simple method of determining the induced activity with allowance for the fluctuations of the radiation flux during irradiation. The source of radiation used was a neutron generator with an integrated yield of the order of 10^{10} particles/sec. The neutron monitor consisted of a long counter with an SNM-11 detector. With the aid of scalers controlled by a timer (or time analyzer) the monitor also recorded the time distribution of the intensity of the neutron generator during irradiation. The activity was calculated by summing the activities induced by neutron irradiation in every channel of this time distribution. It is easily shown that the solution of the activation equation can be written as

$$A = A_1 (1 + \delta). \tag{1}$$

The quantity A_1 is the part of the activity associated with the mean value of the neutron flux:

$$A_1 = \alpha N f [1 - \exp(-\lambda t)], \tag{2}$$

where λ is an isotope decay constant; t is the irradiation time; N is the number of atoms of the element being determined; f is the average number of neutrons per channel; and α is a coefficient. The quantity δ in Eq. (1) is a correction associated with the neutron flux fluctuations during irradiation:

$$\delta = \frac{e^{-\lambda t}}{f(1-e^{-\lambda t})} [\delta f_1 (e^{\lambda t/n} - 1) + \delta f_2 (e^{2\lambda t/n} - e^{\lambda t/n} + \ldots + \delta f_n (e^{\lambda t} - e^{\frac{n-1}{n}\lambda t})]. \tag{3}$$

Here, n is the number of channels; f_i is the number of neutrons detected in the i-th channel; and $\delta f_i = f_i - f = f_i - (1/n)\sum_t f_i$ ($\sum_i \delta f_i = 0$). If neutron flux fluctuations are neglected ($\delta f_i = 0$) and if n = 1, we have $\delta = 0$. In the general case, the neutron flux fluctuations are taken into account by calculating the correction δ and using Eq. (1) and the experimental value of A to find A_1 which, according to Eq. (2), is proportional to the number of atoms of the element being determined. Clearly, the more channels, the more accurate the calculation of δ by Eq. (3). However, in practice it is always possible to calculate the correction by Eq. (3) with sufficient accuracy with a small number of channels.

By way of illustration we give the results of making allowance for neutron flux fluctuations during activation of silicon, aluminum, and iron in bauxites in the reactions $^{28}Si(n, p)^{28}Al$ ($T_{1/2}$ = 2.31 min), $^{25}Al(n, p)^{27}Mg$ ($T_{1/2}$ = 10 min), and $^{56}Fe(n, p)^{56}Mn$ ($T_{1/2}$ = 2.58 h) [2]. Each specimen and standard was irradiated for 8 min, the counter recording the number

Translated from Atomnaya Énergiya, Vol. 42, No. 5, pp. 414-415, May, 1976. Original article submitted June 11, 1976.

TABLE 1. Neutron Flux Fluctuations in an Irradiation

Channel	f_i ($\times 10^{-1}$)	$\delta f_i/f$, %	Channel	f_i, ($\times 10^{-1}$)	$\delta f_i/f$, %
0—1	10 935	2,88	4—5	10 715	0,08
1—2	10 980	3,28	5—6	10 428	—1,9
2—3	10 701	0,65	6—7	10 379	—2,35
3—4	10 525	—0,98	7—8	10 378	—2,35

TABLE 2. Calculated Corrections δ

n	^{28}Al	^{27}Mg	^{56}Mn
1	0	0	0
2	—0,0079	—0,0022	0
4	—0,011	—0,0031	0
8	—0,0115	—0,0035	0

of neutrons per minute. This permitted the correction to be calculated with n = 1, 2, 4, and 8. Table 1 gives the experimental data on neutron flux fluctuations in an irradiation. The "fluctuation amplitude" $(\delta f_i/f)_{max}$ is 3%. The results of calculations of δ are given in Table 2. As the half-life of the isotope decreases, the correction increases and becomes significant in comparison with the other experimental errors (1.2% for ^{28}Al). It is also seen from Table 2 that to obtain an accuracy of better than 0.1% for the isotopes ^{28}Al, ^{27}Mg, and ^{56}Mn it is sufficient to calculate the correction from Eq. (3) with n = 4-8.

LITERATURE CITED

1. D. De Soete, R. Gijbels, and J. Hoste, in: Chemical Analysis, Vol. 34, Wiley-Interscience, New York (1972), Chap. 10, p. 449.
2. B. S. Dzhelepov and L. K. Peker, Decay Schemes of Radioactive Nuclei. A < 100 [in Russian], Nauka, Moscow (1966).

ACTIVATION OF ELEMENTS IN (γ, γ') REACTION BY ^{16}N γ RAYS

U. Akbarov, U. Uzakova, and K. Umirbekov

UDC 639.144.7

Activation determination of elements by isomers formed in the (γ, γ') reaction has been the subject of a number of papers. In most of the papers the γ sources are electron accelerators [1, 2], which are expensive installations. Some of the papers discussed work in which γ quanta from ^{60}Co [3], ^{116m}In [4], and ^{24}Na [5], with a maximum energy of 1.33, 2.17, and 2.75 MeV, respectively, were used for the (γ, γ') reaction. However, because of the low values of these energies for obtaining isomers with a measurable activity, it is necessary to use high-intensity γ sources and large-volume specimens. Taking this circumstance into allowance, we used radioisotopes with more energetic γ rays to obtain isomers in the (γ, γ') reaction. Among artificial radioisotopes the highest γ-ray energy is possessed by ^{16}N which has a half-life of 7.4 sec and emits γ rays of 6.14 and 7.11 MeV (69 and 4.9%). This isotope can be formed from nitrogen, oxygen, and fluorine under the action of neutrons in ^{15}N(n, γ)^{16}N, ^{16}O(n, p)^{16}N, and ^{19}F(n, α)^{16}N reactions. The ^{19}F(n, α)^{16}N reaction was chosen as the most convenient for using reactor neutrons.

To do this, a fluorine compound (containing 100 g fluorine) was packed in a cylindrical vessel with a well and was irradiated for 20 sec in the channel of a VVR-SM water-moderated—water-cooled reactor. The ^{19}F(n, α)^{16}N reaction was observed under the action of the fast neutrons of the reactor. After irradiation the vessel containing the fluorine was removed from the neutron field of the reactor within 1-2 sec and placed on the element under analysis from which an isomer is formed in the (γ, γ') reaction. In view of the short half-life of ^{16}N the study was carried out mainly on elements whose isomers have a half-life of up to 1 min.

Translated from Atomnaya Énergiya, Vol. 42, No. 5, pp. 415-416, May, 1977. Original article submitted September 8, 1976.

TABLE 1. Nuclear Characteristics and Sensitivity of Determination of Elements

Element	Irradiation time, sec	Isomer	Half-life, sec	γ-ray energy, keV	Measuring time, sec	Sensitivity, g
Selenium	16	^{77m}Se	19	160	40	$2 \cdot 10^{-2}$
Yttrium	15	^{89m}Y	16	915	30	10^{-1}
Bromine	8	^{79m}Br	5	210	10	10^{-2}
Silver	22	^{107m}Ag	45	93	90	$2 \cdot 10^{-2}$
		^{109m}Ag	40	88		
Hafnium	16	^{179m}Hf	19	215	40	$2 \cdot 10^{-3}$
Tungsten	9	^{183m}W	5,5	105	10	$5 \cdot 10^{-2}$
Gold	11	^{197m}Au	7,4	279	15	10^{-2}

After irradiation with γ rays, the target element was delivered within 5 min to the measuring apparatus which consituted a scintillation γ spectrometer with NaI(Tl) crystal with well. The activity-measuring time was double the half-life of the isomer of the element under analysis. The nuclear characteristics of the isomers studied and the sensitivity obtained for each element, i.e., the minimum quantity of element for which a measurable isomer activity is produced, are listed in Table 1. The test of a measurable activity is the activity which corresponds to the number of counts in the photopeak of the analytical line of the isomer and is equal to $3\sqrt{N_b}$, where N_b is the number of background counts under the photopeak.

The studies point to the potentialities for achieving a high sensitivity in the analysis of elements by means of the (γ, γ') reaction by using the γ rays of ^{16}N formed from fluorine under the action of reactor neutrons.

The sensitivity values given in Table 1 were obtained at a neutron flux density of $1.8 \cdot 10^{13}$ neutrons/cm^2·sec, where the fraction of neutrons energetic enough to initiate the ^{19}F(n, α)^{16}N reaction does not exceed 10%. Consequently, the sensitivity of obtaining isomers rises significantly at a flux density with a high content of energetic neutrons. The sensitivity can be raised by using fluorine in large quantities by cycling irradiation of fluorine and the target element with subsequent cyclical measurement of the activity of the isomer formed, and by obtaining ^{16}N by irradiating fluorine circulating in a loop.

LITERATURE CITED

1. J. Otvos et al., Nucl. Inst. Methods, 11, 187 (1961).
2. S. Kodiri and L. P. Starchik, Zavod. Lab., No. 2, 191 (1970).
3. A. Veres, Acta Phys. Sci. Hung., 16, No. 3, 261 (1963).
4. I. A. Abrams and L. L. Pelekis, in: Methods and Application of Neutron-Activation Analysis [in Russian], Zinatne, Riga (1969), p. 71.
5. I. A. Abrams and L. Lakoshi, Izv. Akad. Nauk Latv. SSR, Ser. Fiz. Tekh. Nauk, No. 6, 3 (1969).

IMPACT TOUGHNESS OF STRUCTURAL GRAPHITE

Yu. S. Virgil'ev, V. V. Gundorov, and V. G. Makarchenko

UDC 621.039:532.21

Tensile strength cannot serve as a full-valued strength criterion in the design of structures in which cracks may form [1]. Therefore, to evaluate the work capacity of graphite prone to brittle fracture, it is advisable to use the characteristics of viscoelastic properties, especially impact toughness whose determination is one of the principal forms of mechanical testing [2]. This paper considers the impact toughness of domestic graphite structural materials and its relation with compressive strength.

The law of similarity is not satisfied in tests of brittle materials for impact toughness; therefore, the shape and absolute dimensions of specimens should remain unchanged [2, 3]. Moreover, the significant scatter of results necessitates a quite large number of tests. Some data [4] from tests of prismatic specimens indicated that the ratio a_n/σ_c is lower in stronger graphite than in graphite of lower strength. Irradiation of graphite resulted in an increase in the impact strength [5].

Variations in the impact toughness are related [6] to variations in other strength characteristics, the modulus of elasticity and bending strength, by

$$\partial a_n / a_n = -\partial E/E + 2\,\partial\sigma_b/\sigma_b.$$

In this study impact toughness was determined on an MK-0.2 pendulum impact testing machine with specimens measuring 8 mm in diameter and 10 mm in height. The specimens were mounted on the base of the machine with a holder which ensured that the pendulum would hit the specimen in the middle. The impact toughness was found from the formula

$$a_n = (Ql/0.785d^2)\cos\alpha,$$

where Q is the pendulum mass, equal to 1.136 kg; l is the pendulum length, 20 cm; d is the specimen diameter, 8 ± 0.1 mm; and α is the angle of deflection of the pendulum, in deg.

The average values of 15 determinations was taken for the results of measurements. The error of measurement did not exceed 10%. In the case of the strong materials KPG and VPG,

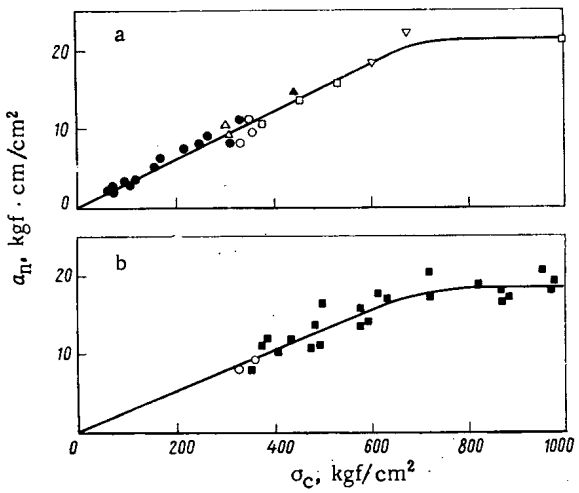

Fig. 1. Relation between impact toughness and compressive strength (a) before and (b) after irradiation in the range 70-300°C (the value given for ER specimens is the average for impact toughness for parallel and perpendicular specimens): ○) GMZ; ■) GMZ after irradiation; ▽, △) VPG; ▲) ZOPG; ●) ER; and □) MPG-6.

Translated from Atomnaya Énergiya, Vol. 42, No. 5, pp. 416-418, May, 1977. Original article submitted September 3, 1976.

TABLE 1. Properties of Materials Tested

Grade	Matrix	Method of shaping	No. of soakings with pitch	Temp. of treatment, °C	Density, g/cm³	Compressive strength, kgf/cm² *
ER and variants	Natural graphite	Pressing	Up to 3	2300	1,56—1,70	70—370 / 150—350
GMZ†	Calcinated petroleum coke	Extrusion	None	2300	1,65—1,70	350—450 / —
GMZ‡	The same	The same	None	2300	1,65—1,69	300—350 / 300—420
VPG	» »	» »	2	2800	1,80—1,85	600—700 / 400—500
KPG	Uncalcinated petroleum coke	Pressing	None	2400	1,75—1,85	600—800 **
MPG	The same	The same	None	2600	1,80	1000 **

* The numerator is the value for a specimen cut parallel to axis of blank and the denominator, perpendicular to the axis.

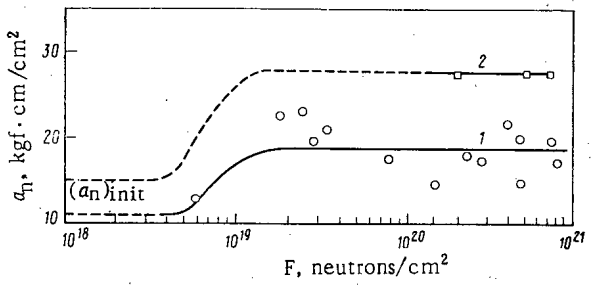

Fig. 2

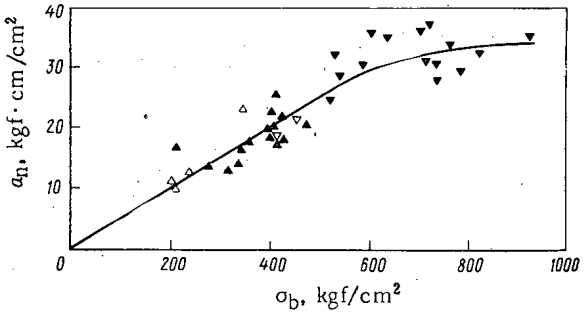

Fig. 3

Fig. 2. The dependence of the impact toughness of graphite on the fluence at temperatures of 70-300°C: O) VPG (perpendicular cut of specimens); □) KPG.

Fig. 3. Relation between impact toughness and bending strength of VPG graphite up to (▽, △) and after (▼, ▲) irradiation: △,▼ and △, ▲) parallel and perpendicular axes of shaping of blank for cutting specimens.

we determined the bending strength instead of the compressive strength. Graphite materials that differed substantially as to strength were tested (see Table 1).

To determine the effect of neutron irradiation on impact toughness, specimens of GMZ, VPG, and KPG graphite 8 mm in diameter and 50 mm in length were irradiated in the temperature range from 70 to 500-550°C with a fluence of 10^{19} to 10^{21} neutrons/cm² with $E \geqslant 0.18$ MeV. The irradiated specimens were tested together with unirradiated control specimens. The bending strength was first determined and then specimens of the dimensions given above were prepared from the fractured specimens. Half were tested under compression while the other half were tested for impact toughness. In view of the considerable radiation hardening only the bending limit was found for graphite VPG and KPG.

A tentative comparison was made of the results of parallel determination of the impact toughness of prismatic specimens on an MK-0.5 tester and cylindrical specimens on an MK-0.2 tester. It was found that with an error not exceeding ±40% there is a direct proportionality (with a coefficient of 0.2) between the values obtained for the impact toughness by the two methods. The difference was due to the fact that when more massive specimens were used, a large proportion of the pendulum energy was carried off by flying fragments.

The impact toughness is anisotropic, being higher in the direction of the pendulum blow, which is perpendicular to the preferentially oriented (00l) plane. This can be seen from the results of tests of anisotropic ER graphite whose strength was changed by impregnations with pitch alternating with annealings.

For all specimens tested the impact toughness and the compressive strength were found to be directly proportional, with a proportionality factor of $\sim 3 \cdot 10^{-2}$. However, as the strength grows above roughly 600 kgf/cm^2 the direct proportionality is not conserved and the increase in the impact toughness ceases (Fig. 1a). Some data give reason to suppose that a deterioration in the perfection of the crystal structure leads to a decrease in the factor of proportionality between a_n and σ_c.

Under the effect of neutron irradiation, the impact toughness increases, beginning from a fluence of $\sim 10^{19}$ neutrons/cm^2. After a fluence of $\sim 2 \cdot 10^{19}$ neutrons/cm^2 the change in the impact toughness because of the effect of radiation, which is more pronounced in high-strength graphite (Fig. 2), practically levels off. Since other strength characteristics, including compressive strength [5], also increase under neutron irradiation, the ratio between the impact toughness and these strengths is not affected (see Fig. 1b) up to $\sigma_c \leqslant 700$ kgf/cm^2.

A direct proportionality also exists between the impact toughness and the bending strength, although in a limited interval (Fig. 3). Comparison of the straight lines in Figs. 1 and 3 reveals that the slope tends to decrease for irradiated graphite.

LITERATURE CITED

1. J. Amesz and G. Volta, in: Proceedings of the Eleventh Biennial Conference on Carbon, Galtinburg, June 4-8 (1973), MP-5.
2. V. N. Barabanov, S. E. Vyatkin, and N. A. Lobastov, in: Structural Materials Based on Graphite [in Russian], No. II, Metallurgiya (1966), p. 135.
3. N. A. Shaposhnikov, Mechanical Testing of Metals [in Russian], Mashgiz, Moscow—Leningrad (1954).
4. V. P. Sosedov (editor), Properties of Structural Materials Based on Carbon [in Russian], Metallurgiya, Moscow (1975).
5. Yu. S. Virgil'ev, At. Energ., 36, No. 6, 479 (1974).
6. R. E. Nightingale (editor), Nuclear Graphite, Academic Press, New York (1962).

CsI(Tl) WELL-DETECTORS FOR LOW-BACKGROUND γ SPECTROMETRY

O. P. Sobornov

UDC 539.1.074

Well-detectors are of interest in the analysis of small amounts of radionuclides in samples of small volume (5-30 cm^3).

This paper compares spectrometric parameters, intrinsic background, and photoefficiency of CsI(Tl) and NaI(Tl) detectors 100 × 100, 80 × 80, and 60 × 60 mm in size (diameter × height) with wells 33 (35) mm in diameter and 60, 50, and 47 mm in depth, respectively. Measurements were made under identical conditions using a single FÉU-110 photomultiplier and the equipment described in [1]. The detectors 100 × 100 mm in size had conical quartz light-pipe—window combinations 20 mm thick and the other windows were of quartz or sodium glass. The outer diameter of samples in the wells of all detectors was 30 mm. A point source (^{135}Cs) and distributed γ sources [^{40}K (crystalline KCl), ^{137}Cs, ^{232}Th, and ^{238}U (with decay products)] were used. The latter were distributed in a Na_3PO_4 medium (analytic grade) and had a density of 1.3-1.4 g/cm^3 for a source size of 27 × 50 mm. Resolution was determined with distributed γ sources of ^{137}Cs and ^{40}K (R_{Cs}, R_K, %) and also with a point source of ^{137}Cs (R, %) at a distance equal to the diameter of the detector using standard techniques. In this paper, "resolution" is understood to mean the resolution of the spectrometer, which is determined by the equation

$$R = (r_s^2 + r_p^2 + r_a^2)^{1/2},$$

Translated from Atomnaya Énergiya, Vol. 42, No. 5, pp. 418-421, May, 1977. Original article submitted September 14, 1976.

TABLE 1. Parameters of CsI(Tl) and NaI(Tl) Well-Detectors

Detector		Resolution, %			Background count. rate (counts/min) in interval ΔE_γ, MeV					ε_p, %	ε and M (rel. units) in interval ΔE_γ, MeV							
											0,55—0,75		1,35—1,55		1,70—2,00		2,50—3,40	
Size, mm	Type	R	R_{Cs}	R_K	0,40—3,40	0,55—0,75	1,35—1,55	1,70—2,00	2,50—3,40		ε	M	ε	M	ε	M	ε	M
100 × 100; well 33 × 60	CsI (Tl)	11,0	10,7	8,1	304,0 (155,8) *	163,2 (45,6)	8,00 (7,30)	5,35 (5,52)	5,64 (5,76)	19,14	4,62	0,95 (1,79)	6,17	2,66	7,80	3,40	7,38	3,89
	NaI (Tl)	9,4	9,4	7,1	108,2	25,5	5,76	4,44	4,80	14,20	3,18	1,66	4,94	2,51	5,52	2,63	5,60	3,20
80 × 80; well 35 × 50	CsI (Tl)	10,6	10,1	7,8	89,3	24,9	4,42	3,28	3,61	10,00	2,60	1,37	3,33	1,94	3,67	2,04	3,80	2,50
	NaI (Tl)	8,8	8,4	6,5	71,4	16,6	3,78	2,64	2,88	7,62	2,08	1,34	2,54	1,60	2,65	1,64	2,82	2,08
60 × 60; well 35 × 47	CsI (Tl)	10,5	10,6	8,2	39,3	10,0	2,28	1,27	1,80	4,96	1,60	1,34	1,65	1,33	1,70	1,51	1,74	1,63
	NaI (Tl)	7,7	8,0	6,0	29,5	7,04	1,50	1,01	1,56	3,00	1,0	1,0	1,0	1,0	1,0	1,0	1,0	1,0

*Second detector of similar size.

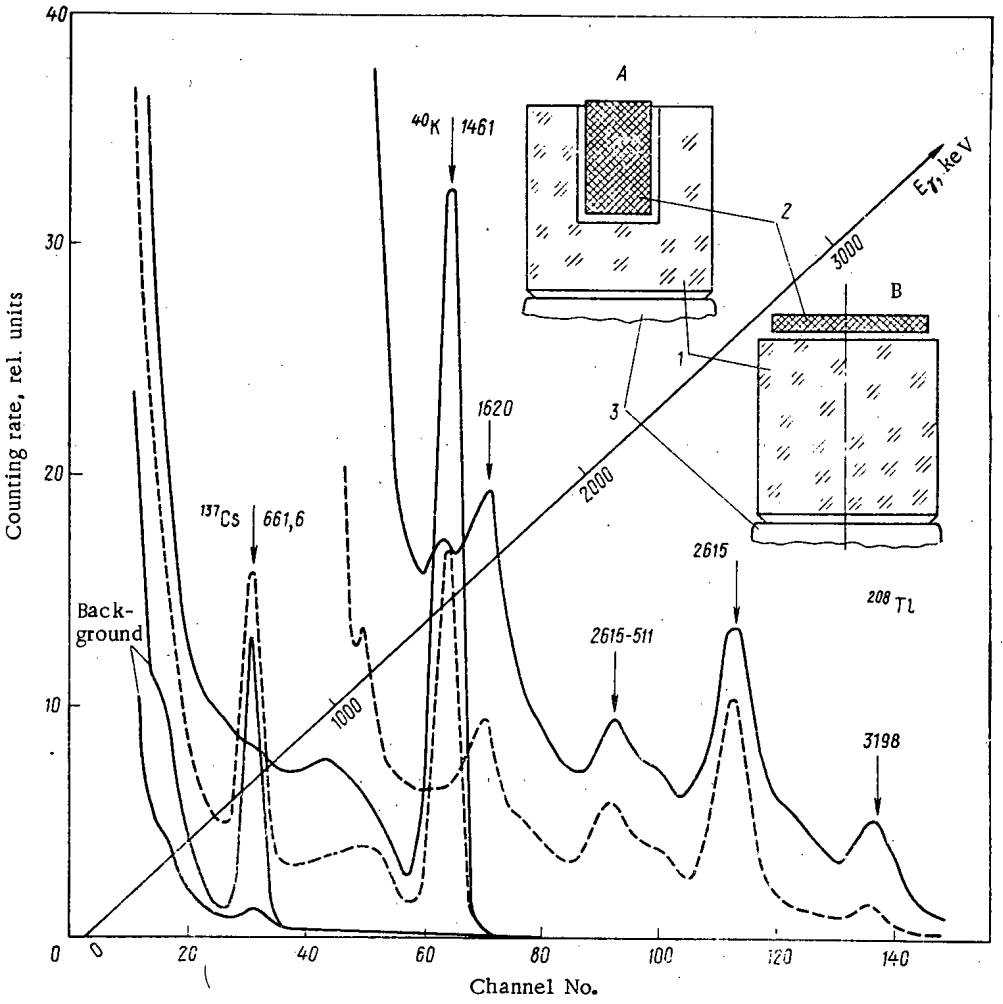

Fig. 1. Spectra from background and from distributed γ emitters ^{232}Th (with decay products) and ^{40}K (KCl). Measurement geometry A and B: ---) 76 × 76 mm CsI(Tl) scintillation unit; ——) 80 × 80 mm CsI(Tl) detector with 35 × 50 mm well; 1) detector; 2) sample; 3) photomultiplier.

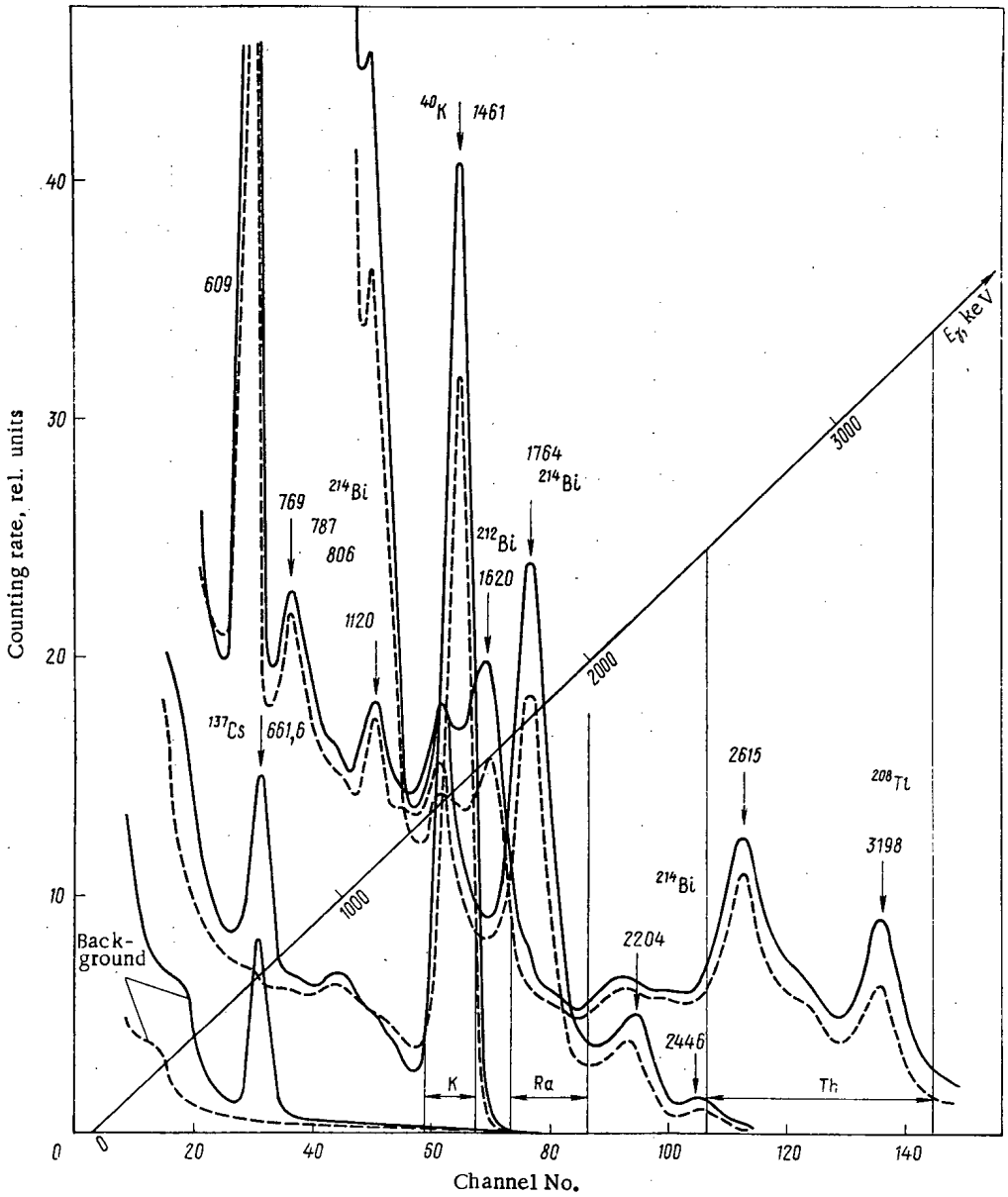

Fig. 2. Spectra from background and from the natural γ emitters ^{40}K, U—Ra, and Th (with decay products). 100 × 100 mm detectors with 33 × 60 mm well: ---) NaI(Tl); ——) CsI(Tl).

where r_s, r_p, and r_a are, respectively, the intrinsic resolution of the scintillator, photomultiplier, and analyzer. Since r_p and r_a are constants, R is arbitrarily considered to be the resolution of the detector. Furthermore, the correct resolution is considered to be that which is determined under the actual measurement conditions, i.e., in a detector well with a distributed source. It was found that $R_{Cs} = 1.32\ R_K$ in such a system.

A comparison of photoefficiency and intrinsic background was made in energy intervals (ΔE_γ, MeV) which contained the total absorption peaks (TAP) of the γ sources as well as the TAP and sum peaks for the cascades 1.120 + 0.609 in ^{214}Bi and 2.616 + 0.583 in ^{208}Tl, which were selected for application to the problem of individual determination of these radionuclides in mixtures. The photoefficiency ε_p of the detectors was determined from the TAP of ^{40}K (1.461 MeV) assuming that 1 g of potassium emits 3.25 γ quanta per second [2]. For detectors 100 × 100 mm in size, the efficiency for ^{40}K was 58.9 and 65.6% for NaI(Tl) and CsI(Tl) for well measurements; the photofractions were 23.3 and 29.2%, respectively. Differences in the spectral shape and in the efficiency of detectors of equal sensitive volume but different shape are shown in Fig. 1, where γ spectra from identical sources are presented which were obtained with a scintillation unit having a 76 × 76 mm CsI(Tl) crystal and with an 80 × 80 mm CsI(Tl) detector having a 35 × 50 mm well. Sources of ^{40}K (51.5 g KCl) and Th

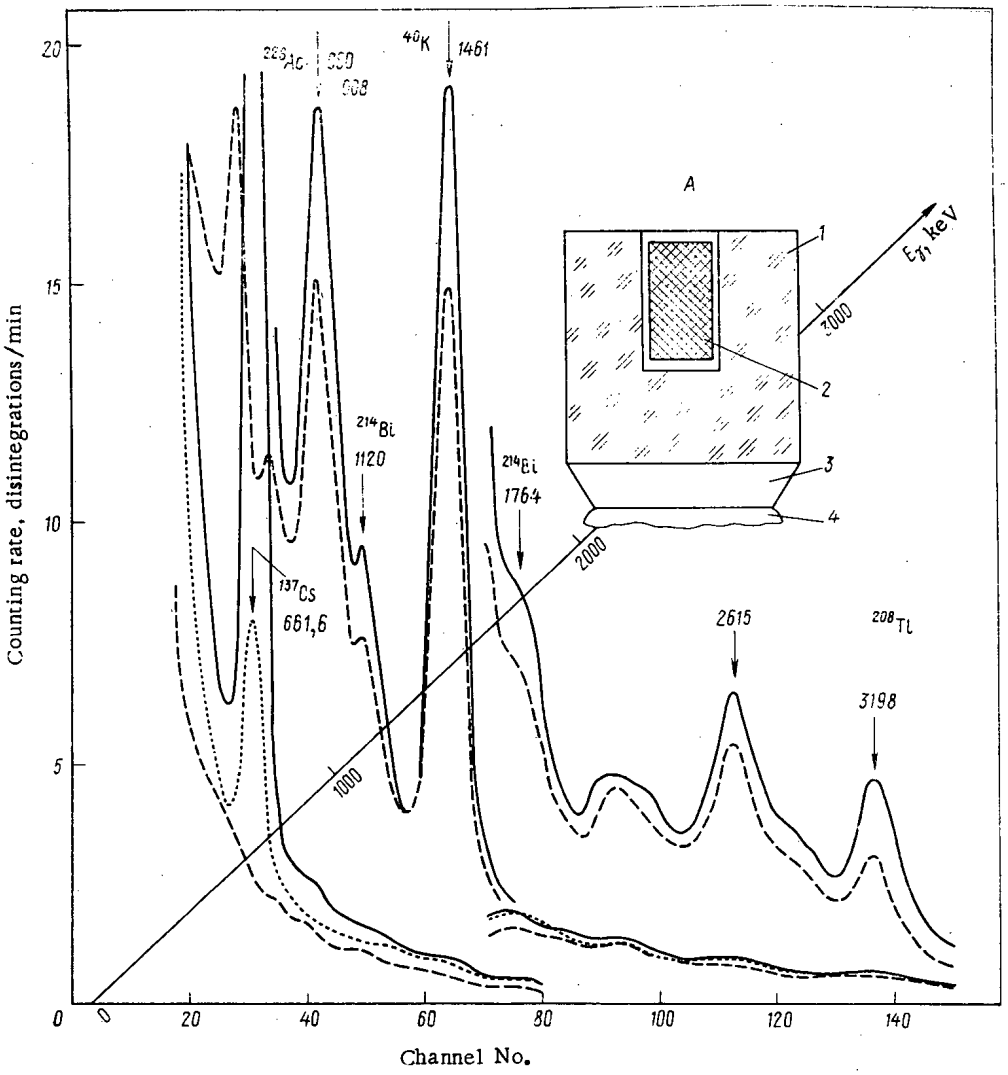

Fig. 3. Spectra from background and from rock (40 g of granite) in measurement geometry A: ---) NaI(Tl); ...) CsI(Tl); ——) CsI(Tl); 1) detector; 2) sample; 4) photomultiplier; 3) light-pipe—window.

(standard 55 g SVT-16A sample) were measured for the same time in a counting geometry optimal for the specified crystals (on the face and in the well, respectively). Measured results for the parameters of the detectors compared are given in Table 1. Because of the difficulty of producing distributed γ sources of optimal size for each detector, the experimental data have an error of $\sim$10%.

Figure 2 shows spectra from natural γ emitters and Fig. 3 shows the background spectra for one NaI(Tl) and two CsI(Tl) detectors 100 × 100 mm in size with 33 × 60 mm wells along with spectra from rock (granite) obtained with both types of detectors. The intrinsic background N_b of a γ spectrometer can be considered to be made up of two components recorded by the detector: environmental radiation n_0 and the intrinsic radiation n_s of the scintillator, i.e., $N_b = n_0 + n_s$. Since the first component (for specific shielding) depends on the relation of the cross sections for γ-ray interactions with the scintillator material and the second, in addition, on the content of ^{137}Cs, ^{40}K, ^{87}Rb, and other radionuclides in the detector, the data presented in Table 1 for the background is in terms of relative values. The content of the ^{135}Cs fragment in CsI(Tl) detectors [3] limits the possibility of their use at energies below 0.8 MeV. In some detectors, however, the ^{137}Cs content is beyond the limits of detection. This situation gives rise to the need for special purification of raw material for CsI(Tl) crystals.

To compare the "quality" of the detectors, the criterion $M = \varepsilon/\sqrt{N_b}$ was used where ε is the counting efficiency in a given interval. Table 1 gives values of ε and M for all detectors relative to the 60 × 60 mm NaI(Tl) detector with a 35 × 47 mm well. These data indicate

that the use of CsI(Tl) with a well makes it possible to increase the productivity of analyses significantly or (for the same exposures) to increase the sensitivity and reduce the error. This is facilitated by the great stability of spectrometric parameters in time which reduces the number of measurements made for monitoring metrologic parameters and for calibration of gamma spectrometers. Notice also that the 60 × 60 mm CsI(Tl) detector with a well is of better "quality" than the 76 × 76 mm CsI(Tl) detector (without a well), the sensitive volume of which is about 2.8 times greater.

The author is grateful to L. L. Nagorna and Ya. A. Zakharin for the preparation of high-quality CsI(Tl) detectors 100 × 100 mm in size.

LITERATURE CITED

1. Yu. A. Surkov and O. P. Sobornov, At. Energ., 34, No. 2, 125 (1973).
2. J. Adams and P. Gasparini, Gamma-Ray Spectrometry of Rocks, Elsevier Publ. Co., Amsterdam—London—New York (1970).
3. O. P. Sobornov and O. P. Shcheglov, At. Energ., 39, No. 1, 63 (1975).

THIRD SYMPOSIUM OF COMECON MEMBER-NATIONS ON "WATER REGIMES, WATER TREATMENT, AND LEAK-TESTING OF FUEL ELEMENTS IN ATOMIC POWER PLANTS"

Yu. A. Egorov and A. V. Nikolaev

In accordance with the plan of operation of the COMECON Standing Committee on Atomic Energy, a regular scheduled symposium was held in Neubrandenburg (German Democratic Republic) to sum up work done on water regimes, water treatment, and leak-testing of the jackets of fuel elements in atomic power plants with water-moderated—water-cooled reactors in COMECON member-nations. Participating in the symposium were specialists from Bulgaria, Czechoslovakia, the GDR, Hungary, Poland, and the USSR as well as representatives of the COMECON Secretariat and the IAEA. A total of 63 papers were read in five sections at the symposium.

The section on "Water Regimes, Corrosion, and Water Treatment in the Primary Circuit" discussed papers on experience gained in operating water purification systems, ways of monitoring corrosion processes, and the behavior of active and inactive corrosion products in coolants. A number of papers in this section were devoted to the study of water-purification technology, especially the capabilities of electromagnetic filters, purification of coolants by ion-exchange filters, the study of the sorption kinetics of some corrosion and fission products, the effect of continuous purification on the concentration of active products in a coolant, as well as the results of studies on the processes in a coolant with boron control and the properties of ion-exchange materials, including their radiation stability.

The papers discussed in this section showed that in recent years the COMECON member-nations have developed water-treatment systems and apparatus for atomic power plants with various sources of water supply and that they have also developed and tested designs of electromagnetic filters whose application significantly improves purification of water from corrosion products and, consequently, reduces the density of active and inactive deposits on the surfaces in technological circuits. Much work has been done on developing technological regimes for boron control with the aid of ion-exchange materials and on developing systems for the regeneration of boric acid from drain water. Studies of the properties of ion-exchange resins made it possible to select requirements for nuclear-grade ion-exchange materials and to propose methods for testing them. Recommendations have been formulated for optimization of the water regime in atomic power plants with VVÉR-1000 (water-moderated—water-cooled) reactors.

The section noted some major areas in which investigations should be pursued in coming years. These include analysis and generalization of experience from the operation of water-treatment installations, the study and evaluation of the corrosive state of equipment, development and testing of high-temperature systems for coolant purification, including systems with electromagnetic filters, improved ion-exchange materials, and the technology of regeneration of boric acid from effluents employing membrane processes, etc.

Papers presented to the section on "The Second-Circuit Water Regime" generalized the experience from the use of equipment at the Novovoronezhskaya, Koslodui, and Bruno Loishner atomic power plants with uncorrected water regime (e.g., the experience from the use of 0Kh18N10T steel evaporation surfaces in steam generators) discussed problems related to the organization of the water regime in some atomic power plants. Interesting material was considered in papers devoted to the study of purification by condensation, electromagnetic and ion-exchange filters, especially the use of electromagnetic filters in the high-temperature part of the secondary circuit (after the deaerators), and design studies on the hydrodynamics and lifetime of ion-exchange filters. The section took note of the need to standardize the

Translated from Atomnaya Énergiya, Vol. 42, No. 5, pp. 422-423, May, 1977.

secondary-circuit water regime, to study processes of corrosion of structural materials for secondary circuits under various water regimes, technological schemes of the circuit, and structural materials and systems for coolant purification, and to study the capabilities of electromagnetic filters for purifying secondary-circuit water as well as drain water.

The papers heard by the section on "Radioactive Deposits in the Primary Circuit" considered the results of studies on the effect of transient processes on the behavior of some radionuclides produced by corrosion in the Rheinsburg Atomic Power Plant and observations of the transport of radionuclides in a repeated-circulation circuit in the course of the operation of the Leningrad Atomic Power Plant. The section also discussed the results of laboratory research on the sorption and solubility of corrosion products, and particularly on the effect of the pH on the sorption of ^{60}Co by austenitic steel surfaces. An interesting paper among the materials of this section was one which considered a mathematical model of the sorption of active products on the surfaces of primary-circuit equipment, based on microscopic constants. The section noted the necessity of extending the research on the formation and transport of active corrosion products in the primary circuit, and especially the need to extend such studies in operating atomic power plants. Moreover, the section felt it would be useful to study the behavior of corrosion radionuclides on reactor and in-pile loops.

The section on "Leak-Testing Fuel-Element Jackets" discussed a number of papers on various aspects of leak-testing of fuel-element jackets in atomic power plants with water-moderated—water-cooled reactors, the method of appraising the state of the active zone according to the results of radiation monitoring of the primary-loop coolant, as well as various methods of detecting nonhermetic elements (by iodine radionuclides, by delayed neutrons, etc.), a method of detecting defective fuel assemblies by overcompensation of the field of energy liberation in the active zone. The section heard two reports on an experimental loop in the Eva reactor and the possibilities of using it to simulate leaks and to detect fission products in the coolant.

At the present time a working approach has been developed to the monitoring of leaks of fuel elements in atomic power plants with water-moderated—water-cooled reactors. This approach has three successive stages: continuous monitoring of the concentration of fission fragments in the coolant, periodic monitoring of the nuclide composition of fission fragments in samples of the coolant, and local monitoring (of each fuel-element assembly) in the shut-down reactor. Demagnetization is detected in the first stage and its degree is estimated in the second, whereas the third stage permits the defective assemblies to be rejected.

Just as the other sections did, this section also noted that it will be necessary to focus on the study of the possibilities of determining the direct contact of the coolant with the fuel by measuring the ^{239}Np concentration in the coolant, on the study of the mechanisms of leakage of radionuclides from fuel elements, particularly on fuel elements with artificial defects, on the development of a method of localizing defective fuel-element assemblies by overcompensation of the neutron field in the active zone, as well as on the unification of the criteria for rejection of defective fuel-element assemblies, and the methods and instruments of leak-testing of fuel elements.

The section on "Chemical-Analytic Control Monitoring" had papers on the development and use of automatic systems for the chemical monitoring and control of the water regime of the primary and secondary circuits of the atomic power plant. It was noted that such a system is in successful use in the Beloyarsk Atomic Power Plant. A considerable number of papers presented in this section were devoted to the development of techniques and instruments for the chemical monitoring of various coolant properties: to determine the concentrations of chlorine, boric acid, various corrosion-product and fission-fragment radionuclides, etc. At the present time, borometers are being developed and tested at the Kozlodui, Novovoronezhskaya, and Rheinsburg atomic power plants. A number of COMECON member-nations are commercially manufacturing instruments required for the water-chemical regime, e.g., for the automatic measurement of the pH of the coolant.

Chemical and radiochemical monitoring constitute the basis of reliable and safe operation of atomic power plants and problems should be solved comprehensively. Therefore, in coming years it is necessary to carry out work on the unification of ways and means of monitoring the water-chemical regime in atomic power plants and on putting together unified monitoring schemes, this being preceded by comparative tests of existing and newly developed instruments and methods in existing atomic power plants.

The discussion at the symposium on the problem under consideration was extremely useful and showed that problems of the water-chemical regime of atomic power plants are being successfully resolved. The symposium was held in a warm, businesslike setting.

INFORMATION

"RESPIRATION" OF THE SUN

N. A. Vlasov

Academician A. B. Severnyi and his co-workers of the Crimean Astrophysical Observatory have made an extremely interesting discovery: the sun's surface oscillates with a period of 160 ± 0.5 min [1]. A wide spot observed in the central region of the solar disk rises and falls. The surface moves at speeds of up to 2 m/sec and the amplitude of the displacement is about 10 km. It was possible to detect and measure such small oscillations by sensitive methods developed for measuring very small shifts of spectral lines. A large portion of the solar surface (perhaps even the entire surface) undergoes periodic radial oscillation, compressing and expanding. The sun "breathes." Elastic waves propagate inside the sun and one of them causes the respiration with a period of 160 min. For solar physics this discovery gives approximately the same possibilities as seismometry does for terrestrial physics.

The elastic waves may "show" the interior of the sun. Up to the present time this was expected only of the neutrino but tracking neutrinos has hitherto given an incomprehensible, almost negative result [2].

The period of 160 min refers to the most pronounced oscillation of the surface, but oscillations with other periods are also possible, although with a smaller amplitude. The standard theoretical models of the sun predict radial oscillations with a period of less than 1 h. The observed period is in agreement with the theoretical period of quadrupole oscillations. Quadrupole oscillations of large amplitude would be quite surprising. But if the observations confirm the global-radial character of the oscillations, then the discrepancy between the period and the theoretical value is all the more surprising. The study of "sunquakes" today is one of the most interesting, new areas of solar physics and has caught the attention of many astrophysicists [3].

LITERATURE CITED

1. A. Severny et al., Nature, 259, 87 (1976).
2. N. A. Vlasov, At. Energ., 41, No. 4, 251 (1976).
3. J. Christensen-Dalsgaard and D. Gongh, Nature, 259, 89 (1976).

Translated from Atomnaya Énergiya, Vol. 42, No. 5, p. 424, May, 1977.

FRANCO—SOVIET SEMINAR ON "CONCEPTION OF ATOMIC POWER PLANTS, TECHNOLOGY, AND OPERATION OF WATER-MODERATED—WATER-COOLED REACTORS"

V. A. Voznesenskii

The seminar was held at the Nuclear Research Center in Saclay from Dec. 8 to 10, 1976. The 15 papers read at the seminar dealt with general conceptions and prospects for the development of water-moderated—water-cooled power reactors, the experience from the operation of such reactors in the USSR, the fabrication of equipment for atomic power plants, standards and techniques for strength calculations, monitoring the state of the equipment prior to start-up and during operation, and purification of primary-circuit coolant from corrosion products.

The French program of construction of atomic power plants with water-moderated—water-cooled reactors and the characteristics of these power plants were the subject of a paper by M. Komez.

Notwithstanding the favorable experience from the operation of gas-cooled–graphite-moderated reactors, it has been found economically inadvisable to build any more such reactors for the production of electricity. The Soviet program provides for the construction by 1984 of 30 water-moderated—water-cooled reactor facilities with a power of up to 900 MW(E) and four with a power of up to 1300 MW(E). As a result, by the beginning of the 1980s a large proportion of electricity will be produced by atomic power plants, as shown by the data in Table 1.

The primary circuit of the 900-MW atomic power plant has three circulating loops without valves, as well as main circulating pumps, and vertical steam generators. To ensure the safety of the population and to protect the environment, the equipment is installed in a cylindrical protective shell (height 56 m, diameter 37 m), designed to withstand a pressure of 5 bars, which could arise during maximum design failure related to the loss of coolant. For emergency flooding of the active zone, there are three water tanks connected to the cold branches of the loop, three high-pressure pumps for emergency introduction of boric acid, and two low-pressure pumps, connected to the cold and hot branches of the loops. The active safety system and reliable power supply system have a double back-up.

Atomic power plants are protected against flooding, earthquakes, and other natural disasters and premises containing radioactive substances are protected from flying objects, both external (falling aircraft, parts of turbines) and internal, arising during leaks from the primary-circuit tubing. Special measures are undertaken against radioactive and chemical substances getting into the groundwater.

A paper by L. Gendry and B. Moreau reported on construction plans, technology, and characteristics of primary-circuit equipment for atomic power plants with water-moderated—water-cooled reactors. The first reactor vessel for the atomic power plant in Chooze was built in 1964. Nineteen reactor vessels had been fabricated for France, the USA, Switzerland, and Belgium by the end of 1976. The Framatom works (10,000 employees) can turn out eight reactor vessels and volume compensators as well as 18-24 steam generators per year. Water-moderated—water-cooled reactors can be constructed with a power of up to 2000 MW. The main stages in reactor-vessel fabrication are: fabrication of the individual parts of the vessel and cover (flanges, cowlings, bottoms, branch pipes), welding of the stainless facing onto the various parts, and subsequently welding the parts together. The bottom is pressed and

Translated from Atomnaya Énergiya, Vol. 42, No. 5, pp. 424-426, May, 1977.

TABLE 1. Generation of Electricity in France, %

Year	Thermal	Hydro	Atomic
1975	56,5	33,5	10
1985	12,0	18,0	70
2000	10,0	9,0	81

the other parts are forged. The vessel material is carbon steel, alloyed with molybdenum, manganese, and nickel. The facing is applied in two layers, each 4 mm thick; the first is Kh24N12 steel and the second is Kh20N10 steel. Much attention is paid to quality control.

The problems of making provision for seismic activity in designs for atomic power plants were discussed in a paper by M. Livoland. Atomic power plants are constructed in the country in regions with a seismicity of up to seven on the Richter scale. The increased force of the underground shock is taken into account when designing the systems and premises containing radioactive substances. The spectrum of earth tremors is placed in correspondence with the intensity of the earthquake. Various methods of calculation were considered for finding the displacements and stresses in the structures of atomic power plants with a known soil spectrum. In cases when the seismic-resistance of a structure is difficult to determine, studies are carried out on a vibrations stand. Of some interest is a way of reducing the seismic effects on the entire complex of premises of the reactor section by setting their common foundation on special sliding plates of bronze or lead, resting on a layer of synthetic rubber on top of the foundation. In this case, equipment designed for ordinary atomic power plants can be used in regions of high seismicity.

Special regulations worked out in France cover the design, fabrication, and use of pressure vessels for atomic power plants (paper by R. Roche). The main emphasis here was on the definition of the equipment to which the regulations apply; the responsibility of the fabricator and the operating organization; the choice of materials; and the quality program as well as documents to be presented to inspection agencies. The strength is evaluated with reference to excessive strain, plastic and elastoplastic instabilities, progressive deformation, and low-cycle fatigue.

Normal and emergency operating conditions of atomic power plants are divided into four categories with a different safety factor for each and the strength based on different limiting states. The strength is analyzed by various methods; in particular, the method of finite elements is used to design one of the most complex parts of the primary circuit as far as configuration is concerned, i.e., the spiral of the main circulating pump (paper by J. Beylac).

Various aspects of the quality control of the fabrication and the state of the primary-circuit equipment during assembly, start-up, and operation of the atomic power plant were considered in papers by R. Saglio and P. Bernard. Thus, to detect defects and to keep track of their development the French Atomic Energy Commission developed new nondestructive methods: inspection of the reactor-vessel metal by focused ultrasound during periodic checks, recording of acoustic emissions during hydraulic tests, and inspection of the connecting pipes of the steam generator by means of Foucault or eddy currents. A special machine has been built for setting up on the flange of the vessel for ultrasound and TV inspection of the vessel from the inside. In 1976 the machine was used successfully on the reactors of the Fressenheim and Chooze atomic power plants. During inspection of the steam-generator tubing with Foucault currents, a pickup travels over the entire length of the tubing. The characteristics of the signals corresponding to various types of damage are determined with the aid of standards with predetermined defects.

As a result of theoretical investigations, it is considered possible to construct efficient systems for monitoring the state of equipment on the basis of analysis of the noise in various parameters. For example, it is proposed to determine the displacements of devices inside the vessel by analyzing the signals from ionization chambers.

High-temperature filters have been developed for purifying the primary coolant from radioactive corrosion products (paper by L. Dollé). Two prototypes of such filters (electromagnetic and graphite) have been tested in use in loops. In the long term it is planned to construct filters for a coolant flow rate of up to 100 tons/h.

As a result of visits to the nuclear research centers at Grenoble and Cadarache, the Soviet specialists became acquainted with equipment and programs for research on the safety of water-moderated-water-cooled reactors.

Experimental thermotechnical test beds in Grenoble make it possible to study both steady-state heat exchange and the hydrodynamics in bundles of electrically heated rods as well as the processes associated with the formation of large leaks. The program of work with the Omega loop (pressure 170 bar, power up to 9 MW) envisages studies on the heat-exchange crisis under steady-state conditions for bundles of 25 rods with a diameter of 9.5 mm, with a pitch of 12.6 mm in a square array, and lengths of 2.12, 3.65, and 4.2 m (with uniform and cosinusoidal power distribution), as well as experiments on coolant loss. In the latter case, the tubing used in the first stage had an internal diameter of 12 mm and a heated segment 3.65 m long. An assembly of 36 rods of 3.65 m length is planned. In other loops (water and Freon), in addition to the heat-exchange crisis, a study is made of the distribution of the flow rate and the mixing between particular cells of bundles and there are plans to study the heat transfer in the post-crisis region. Special facilities have been provided for studying the heat transfer when the active zone is refilled following a big leak, as well as for studying critical flow rates, vapor condensation under the protective shell, and reactive forces during leaks.

In Cadarache, the Soviet specialists saw the Aquitaine-2 test beds and the Phébus loop, which were in the final stages of assembly. The test bed (pressure 170 bar, temperature 340°C) consists of two tanks connected by tubing of various diameters, lengths, configuration, support designs, etc. It is intended for studying the stresses and strains that arise in tubing elements during various types of rupture and the effects of the action of jets on concrete and other parts of the installation. The test bed is to be reconstructed later for studying the stresses in devices inside the vessel.

At the center of the active zone of a 50-MW(E) reactor is a high-pressure loop for studying the behavior of fuel elements under the conditions of large leaks. The leaks are organized in a special tank. Among the parameters whose role is to be elucidated are: the size and location of the leak; the linear power and the internal pressure of fuel elements; and the pressure, temperature, and the inlet of the injected coolant. Two types of assemblies will be used: one consisting of a single fuel element and one consisting of 25 fuel elements with an active-length diameter of 800 mm and pitch corresponding to the fuel assemblies used in atomic power plants. Present plans call for about ten experiments with one fuel element and 40 experiments with 25 fuel elements. To check the applicability of the results obtained with fresh fuel elements, some tests will be carried out with irradiated fuel elements. Provision has been made for on-site inspection of assemblies by optical means and by n and γ scanning, after which they will be sent to the hot laboratory.

The Franco—Soviet seminar permitted a quite broad exchange of information on many aspects of the construction and operation of water-moderated reactors and promoted the further strengthening of the scientific—technical ties between the USSR and France.

SOVIET–FRENCH SYMPOSIUM ON THE PRODUCTION AND APPLICATION OF STEEL PIPING IN INDUSTRY

G. V. Kiselev

The symposium was held in Moscow from Jan. 11 to 13, 1977. Papers on behalf of the French side were presented by the Vallurec company which specializes in the manufacture of a wide range of piping for various purposes, including for thermal and atomic power plants. The company has divisions which produce piping designed for work with corroding agents at low and high temperatures, under irradiation, etc. The materials used for the piping are stainless and pearlitic steels and nickel, titanium, and zirconium alloys.

It should be noted that it is possible to make long seamless tubes (up to 36 m) for the heat-exchange equipment of atomic power plants. For this purpose, use is made of two presses, of 1500 and 3000 tons, with vitreous lubricant. Cold-drawn tubes of small and medium sizes are produced of Soviet-made two-high and three-high mills. Weld seams on the tubes are made by plasma-arc welding.

The Vallurec company produces a wide range of tubing for "nuclear" applications, such as for fuel-element cans, heat exchangers, and steam generator of atomic power plants (see Table 1).

The characteristic features of the production are of interest. Thus, a shop in the town of Montbard making tubing for steam generators of atomic power plants measures 340 m long by 25 m wide, has been fitted with equipment for supplying cleaned and conditioned air so that the temperature and humidity can be controlled, and has specially insulated walls and a special floor, thus ensuring exceptional cleanliness during the process of fabrication. The shop has an annual capacity of ∿1 million m of tubing, which can be increased to 1.5 million. It makes straight and bent tubes with diameter of 12-25 mm, wall thickness 0.8-3 mm, and a bend radius of 2 tube diameters to 1.5 m. The tolerance of the wall thickness of the cold-drawn tubes is ±8%.

The tube move without turning on a special-purpose automatic line and then pass three measuring heads in succession. These devices permit the tubes to be inspected with the aid

TABLE 1. Chemical Composition of Steels

Grade			C	Cr	Ni	Mo	Ti	Nb
AFNOR	AISI	DIN						
Z6CN18.10	304	1.4301	⩽0,07	17/20	8/11	—	—	—
Z2CN18.10	304L	1.4306	⩽0,035	17/20	8/13 9/12	—	—	—
Z6CNT18.10	321	1.4541	⩽0,08	17/19	10/12	—	⩾5C ⩽0,6⩾5C	—
Z6CNNb18.10	347	1.4550	⩽0,08	17/19	10/13	—	—	⩾10C
Z6CND17.11	316	1.4401	⩽0,08	16/18	11/13	2,0/3,0	—	—
Z2CND17.12	316L	1.4404	⩽0,035	16/18	11/14	2,0/3,0	—	—
Z6CNDT17.12	316Ti	1.4571	⩽0,10	16/18 16/19,5	12/14 10,5/14	2,0/3,0 2,0/2,5	⩾4C ⩽0,6 ⩾5C	—
	Inconel 600*		⩽0,10	14/17	72/79	—	—	—
	Incoloy 800†		⩽0,10	19/22	30/35	—	—	—

*Fe 6/9.
†Fe the remainder.

Translated from Atomnaya Énergiya, Vol. 42, No. 5, pp. 426-427, May, 1977.

of eddy currents, and to find any flaws in the tube walls and measure the wall thickness by ultrasound. The ultrasonic monitoring transducers were tuned for 0.1-mm flaws; a flaw larger than 0.7 mm on the inside or outside surface is a criterion for rejection. Thickness measurement yields 50 results per turn of the head, i.e., about 250,000 measurements for one tube. The data are recorded on recorder tape as well as with the aid of a computer which controls devices that automatically mark zones where deviations are observed, thus separating acceptable from rejected tubes. The results of measurements and inspection are stored so that the history can be checked at any time. The number of tubes rejected in the process of fabrication and inspection does not exceed 8%.

Vallurec produces tubes of grade 304 and 316 austenitic steel, zirconium alloys (zircalloy-2, 4) for the cans of fuel elements for water-moderated—water-cooled and fast reactors; these tubes have a diameter of 5-28 mm, length 500-4500 mm (up to a maximum of up to 6000 mm) and wall thickness of 0.25-1 mm. Tubes are also made for sheathing fuel assemblies. For spacing the fuel elements in a package, wire is wound under a particular tension around the surface of a tube and welded to both ends of the tube. To reduce the swelling of the canning materials under the effect of the neutron flux in fast reactors, the tubes are cold-worked with a 10-20% strain. In view of the limitations arising out of the swelling of canning materials, a burn-up of 70,000 MW•day/ton has been adopted for the Superphénix reactor. The company has now started production of a range of tubes for the Superphénix.

The symposium was a useful meeting since it provided information about the manufacturing capabilities of one of the leading French companies engaged in the production of tubing for atomic power plants.

ELEVENTH CONFERENCE ON ENERGY CONVERSION AND RESEARCH ON THERMOELECTRONIC EMISSION IN THE USA

V. A. Kuznetsov

Under the terms of an agreement between the State Committee of the Council of Ministers of the USSR for Atomic Energy (GKAÉ) and the U.S. Energy Research and Development Administration (ERDA) a group of Soviet specialists participated in the work of the Eleventh Interdepartmental Conference on the Engineering Problems of Energy Conversion which took place in State Line, Nevada, from Sept. 13 to 16. After the conference, the Soviet specialists visited a number of scientific-research centers and companies engaged in the work on thermionic methods of energy conversion.

Eleventh Conference on Energy Conversion. In addition to the American specialists, scientists from 18 countries took part in the work of the conference. The more than 800 participants heard some 250 papers in 48 sessions. In 22 out of the 48 sessions the conference discussed primary sources of energy and ways of generating energy, in seven it dealt with the problems of accumulation and storage of energy, in ten it considered the demand for energy in transport, and in six it discussed the use of energy in outer space and in military and related technologies. A special session was devoted to papers by Soviet specialists: "The state of the art and directions of research on thermionic converters in the USSR" (V. A. Kuznetsov) and "Some results of research on fissile gas reactors" (V. M. Ievlev). The main attention at the conference was focused on the most effective use of energy from coal and solar energy in various areas of human activity. Methods of underground gasification of coal and production of synthetic gaseous and liquid fuels were discussed. It is interesting to note that such traditional nuclear centers as the Oak Ridge National Laboratory have become involved in work on this problem. On the other hand, much attention was devoted to ways of making more efficient use of the high-temperature potential obtained by burning coal or

Translated from Atomnaya Énergiya, Vol. 42, No. 5, pp. 427-429, May, 1977.

concentrating solar energy. In particular, the USA is doing extensive work on so-called high-temperature thermodyanmic "adapters" for electric power plants operating in a steam-turbine cycle. The adapters under consideration in the main are cycles of direct conversion of thermal energy into electrical energy by means of magnetohydrodynamic (MHD) generators or thermionic converters. It was reported at the conference that U.S. specialists intend to have a coal-operated combined MHD—steam-turbine power plant in service by 1989.

The conference attached equal importance to methods of converting solar energy into heat and electricity not only on spacecraft but also for satisfying such needs on the ground as residential heating and illumination, air-conditioning systems, irrigation systems, etc. Consideration is being given to the construction of comparatively small (low-power) solar energy units for supplying energy primarily to individual buildings or microregions. Along with this a project has been advanced for a 100-MW(E) power plant with a concentrator on top of a 275-m tower. A sodium loop would carry heat from the concentrator and surrender it to steam generators in the lower part of the tower. Concentrators in combination with thermionic converters are envisaged for small solar power plants [seven hundred KW(E)].

Of the other scientific—technical topics discussed at the conference, note should be taken of methods of obtaining, storing, and using hydrogen — a promising energy carrier.

Interest has been aroused in the accumulation of energy contained in hydrogen and metal hydrides, especially in calcium hydride. In the opinion of the authors of the papers, most promise is held out by the application of hydrogen in aviation, in industry, and in homes, for the generation and storage of energy, in agriculture (fertilizer production), and municipal transport.

Considerable attention was paid at the conference to the use of geothermal heat. Many papers were concerned with the optimization of binary cycles for geothermal systems.

The conference also heard papers on electrochemical, wind, nuclear, and thermonuclear generation of electricity, heat pipes, etc. Some meetings were devoted to power generation in space.

On the whole, the conference (in its selection of papers and make-up of the participants) reflected the trend that exists at present in U.S. power engineering: the use of coal and nuclear energy in the near future and the use of solar, geothermal, and thermonuclear energy in the long run.

Thermionic Research. As is well known, the U.S.A. had a national program of research on thermionic conversion of energy, the goal being to construct a reactor-converter with electricity-generating channels (EGC) built into the reactor core. This program was taken to the stage of group testing of full-size five-element electricity-generating channels, built by the Gulf General Atomic Company. The tests showed that the channels could operate under reactor conditions for 9000 h at an energy intensity of 2.5-3 W/cm^2. Outside the reactor, the various elements operated for 46,000 h with 15% efficiency.

On the basis of the EGC, designs were worked out for a reactor-converter with a power of 5 to 120 kW(E) for various applications in space. About 80 million dollars were spent on the program. In 1972, the work on a thermionic reactor-converter for space applications was halted when the space program was altered. In 1975 the research was resumed under a joint ERDA—NASA program with the following objectives: 1. Construction in the 1980s of a thermionic nuclear power plant with a high specific power for spacecraft with electrical jet engines, tentative rating $\sim$500 kW(E) with a lifetime of 75,000 h. 2. Development of high-temperature additions, mainly for conventional power plants with a steam-turbine cycle in order to raise the efficiency from 40 to 50% and higher without any significant increase in the capital expenditure and cost of the electrical energy. The first stage of the program calls for the development of the scientific—engineering prerequisites for constructing improved thermionic converters. The first stage is to be carried out in 1980-1982 and is expected to cost about 20 million dollars. The principal scientific—engineering problems to be solved are those of fabrication of about 1 eV with a lifetime of tens of thousands of hours and cutting the energy losses in the interelectrode gap; as a result of the solution of these two problems the barrier index should be reduced to $\sim$1.5 eV, as compared to $\sim$2 eV in the first-generation thermionic converters. Consequently, it is proposed to build a high-efficiency thermionic converter with an efficiency of 20 and 30%, respectively, at 1400 and 1700°K. The best barrier index attained at present is $\sim$1.9 eV, which ensures an efficiency of 9-16.5% at 1400-1700°K.

More than 15 organizations have been involved in the execution of this program. The main work is being done in the laboratories of the Thermo Electron Engineering Corp. and Rezor Associates as well as the Jet Propulsion Laboratory. According to estimates, more than 70 scientific workers are now engaged in the U.S. program of research on the physics of thermionic converters. The 1976 expenditure on this work was 2.5 million dollars and the planned expenditures for 1977 are 3.5 million dollars.

Since the thermionic nuclear power plant for space applications is required to have a lifetime of 75,000 h and since it is proposed to construct thermionic converters with a significantly reduced emitter temperature, the main variant considered is that of a reactor power plant with a remote thermionic converter to which heat is transported from the reactor by heat pipes. According to estimates by American specialists, with the parameters attained it is possible to have a specific weight of 23-26 kg/kW(E) for the thermionic converters; with the parameters predicted for 1980 (thermionic converter efficiency $\sim$19%) it is expected that the specific weight will be reduced to $\sim$17 kg/kW(E).

The thermionic addition to the steam-turbine cycle is being considered in two variants: 1) installation of a thermionic converter right in the furnace chamber of the steam boiler (Thermo Electro Engineering Corp.); 2) construction of modules containing a thermionic converter and steam generator, so-called thermionic heat exchangers (Rezor Associates).

Much work is being done in the U.S.A. to assess the prospects of improved thermionic converters. The assessment is being made according to the following parameters: electron work function, thermal stability, electrical conductivity, production technology, and economy. Some 60 different materials have been tested in recent years; a large group of these materials have an electron work function of 1-1.2 eV at $\sim$450°K in cesium. At present, U.S. specialists find that the following are promising: lanthanum and cerium hexaborides; zinc oxide; a mixture of barium, strontium, and calcium oxides; and metallic rhenium, platinum, and tungsten. The electron work function of LaB_6 and CeB_6 in cesium vapor in the presence of oxygen is $\sim$1 eV at 600°K. A work function of $\sim$1.18 eV at 550°K and $\sim$1.38 eV at 700°K was obtained in ZnO specimens in cesium vapor ($p_{Cs} \sim 10^{-3}$ mm Hg) without the addition of oxygen. This is the lowest index obtained in cesium vapor without the addition of oxygen. Zinc oxide is stable in air and has a high thermal conductivity but begins to decompose in cesium vapor at 700°K.

To bring down the cost of thermionic converters with an emitter temperature of $\sim$1400°K, heat-resistant steels and high-temperature alloys of the type of Inconel and Hastelloy are being considered as materials for the electrodes (emitter and collector). Research has been started on a new class of compound, the diborides of the transition metals (Ta, Zn, Ti).

Mention should be made of the work done at New York University on thermionic converters operating in a pulsed mode with ionization of cesium by an electrical discharge, shf radiation, and excited nitrogen molecules. The pulsed mode of a triode thermionic converter was studied; 100-V electric pulses of 0.1-μsec duration ensured the passage of current through the converter in 300 μsec. Interesting research has been done on thermionic converters with electrodes with an extended surface. This research was initiated to a significant extent by work which Soviet scientists reported in 1975 at the Eindhoven conference of specialists on thermionic emission. Specialists are counting on obtaining thermionic converters with a barrier index of 1.7 eV by extending the electrode surfaces and using various coatings on projections and hollows of the thermionic converter. At present, a barrier index of 1.93 eV has been achieved. It is expected that the main effect will be obtained by reducing the energy losses in the plasma.

A radical way of cutting energy losses in the interelectrode space that is being looked at is that of going over to a vacuum-mode thermionic converter with flexible collector and very small interelectrode gap ($\sim$1 μ).

Research on thermionic emission has convinced U.S. specialists that the second-generation thermionic converters (with a barrier index of 1.5 eV) can be constructed in a quite short time. The prospects for attaining the parameters of third-generation thermionic converters (with a barrier index of $\sim$1 eV) are not clear because there is no major way of combatting transport energy losses in the interelectrode gap (apart from reducing its size).

INTERNATIONAL MEETING ON SYNTHESIS OF AND SEARCH FOR TRANSURANIUM ELEMENTS

B. I. Pustyl'nik

The ever-increasing interest in the physics of heavy ions is determined by their unique possibilities for the synthesis of, and search for, nuclei in unusual, extremal states with respect to nucleonic composition, excitation energy, and angular momentum. Extensive consideration has recently been given to the possibility of synthesizing nuclei with an anomalous density in reactions with heavy ions.

The prospects of the development of heavy-ion physics were the subject of the introductory paper by G. N. Flerov at the international meeting which was held in Dubna from Dec. 9 to 13, 1976. The purpose of the meeting was to discuss the situation extant in regard to one of the fundamental problems of nuclear physics, viz., the possible existence of islands of stability for superheavy (SH) elements with $Z \geq 110$ and $N \sim 184$.

The search for SH elements in nature has been pursued for a number of years now in Dubna. Extremely sensitive and selective methods developed in Dubna make it possible to conduct the search in natural materials if their concentration is $\sim 10^{-14}$-10^{-16} g/g with half-lives $T_{1/2}$ of 10^{8}-10^{10} years. The most promising results have been obtained in the analysis of meteorites of the type of Allende and Efremovka carbonaceous chondrites (G. M. Ter-Akop'yan, Joint Institute of Nuclear Research). In measurements over a long time, some 50 spontaneous fission events which could not be explained by the fission of uranium (its content in the specimens was $3 \cdot 10^{-8}$ g/g) or by the background of cosmic radiation were observed. It is not ruled out that what has been observed in these experiments is a new natural spontaneously fissionable emitter, the second after uranium.

Sensational work by a group of American scientists, who in 1976 reported the simultaneous discovery of three natural superheavy elements with Z = 116, 124, and over 126, was not confirmed in experimental verification on the proton accelerator of the Technical University of Zurich (paper by W. Wolfli, Switzerland) nor by a method employed by a joint Franco–Polish group (M. Efer, France): superheavy nuclei were not detected. Experiments performed at Darmstadt (GFR) and Oak Ridge and Berkeley (USA) also gave negative results. Along with this the interest in the search for superheavy elements in nature grew substantially. Highly sensitive and efficient methods of analysis have been created in various centers in the world.

The chemical properties of superheavy elements were the subject of a paper by I. Zvar (JINR). The indeterminacy that exists in their determination hinders the choice of an optimal method of concentration. A method of chemical separation of superheavy elements from natural materials or from targets irradiated in an accelerator has been developed in Dubna and Rossendorf and has been used in experiments on the synthesis of superheavy elements (B. Eichler, GDR).

Artificial Synthesis of New Transuranium and Superheavy Nuclei. Expected Properties of New Nuclei. This major section of the conference comprised seven papers. A wealth of experimental material was presented in a review paper by Yu. Ts. Oganesyan (JINR) who gave the newest results concerning the synthesis of new elements in Dubna.

A series of experiments were carried out on the synthesis of superheavy elements with Z of 110-116 and N of 163-178 in reactions with ^{48}Ca ions. The isotopes ^{232}Ta, ^{231}Pa, $^{233-238}$U, ^{243}Am, and ^{244,246,248}Cm were used as targets. Because of the absence of a background of spontaneous fission of target nuclei and nuclear-reaction products (with neighboring Z and N), a method with a response speed of ≥ 0.01 sec was used for light isotopes of

Translated from Atomnaya Énergiya, Vol. 42, No. 5, pp. 429-430, May, 1977.

superheavy elements. In reactions with a curium target, a special method was developed for chemically separating superheavy elements from the huge background of spontaneous fission of curium and fermium; the method took several hours. In both cases, the spontaneous-fission sensitivity limit was attained at a level of $5 \cdot 10^{-35}$ cm^2. Moreover, phenomenological estimates of the binding energy of nucleons and α particles in heavy nuclei yield a comparatively long α-decay lifetime for the isotopes of superheavy elements with $N > 170$ (N. N. Kolesnikov, Moscow State University). Therefore, α decay was studied along with spontaneous fission for a number of reactions. The upper limit corresponded to $\sigma \leq 10^{-34}$ cm^2. Upon comparing the data with the results of control experiments on obtaining element 102, in which the cross section in the reaction $^{208}Pb + {}^{48}Ca$ was $\sim 5 \cdot 10^{-30}$ cm^2, one can assume that such an abrupt drop is due to the fact that the half-life of the superheavy element is shorter than the accessible interval of time: less than 0.01 sec for Z = 110-115 and N = 163-173 and less than 10^4 sec for the isotopes of element 116 with $N \sim 174$-178. A much faster method is being developed for further experiments to permit measurement of the lifetimes of superheavy elements as short as 10^{-6} sec.

Analysis of the results enabled a number of parameters used in calculations to be refined and, in the opinion of the speaker, indicated a sharper drop in the lifetime of superheavy elements further from N = 184.

The second part of the paper by Yu. Ts. Oganesyan was devoted to the properties of new spontaneously fissionable isotopes with Z from 104 to 107, first synthesized in Dubna.

A new method developed at the JINR Laboratory of Nuclear Reactions for synthesizing transuranium elements served as the basis for a cycle of experiments which led to the discovery of the heaviest element with atomic number 107. Its isotope of mass A = 261 has $T_{1/2} \sim 2$ msec. The properties of new spontaneously fissionable isotopes of elements from 104 to 107, inclusively, first synthesized in Dubna show that with Z = 104 the rapid decrease in the half-life ceases; this can be interpreted as an indication of higher stability of nuclei upon passing into the region of superheavy elements.

The spontaneously fissionable isotope ^{260}Ku occupies a special place among the already known nine isotopes of this element with A = 253-261 (paper by V. A. Druina, JINR). Firstly, the element was discovered precisely with this isotope and, secondly, this was the first nucleus whose stability proved to be higher than the theoretical prediction by a factor of hundreds of thousands ($T_{1/2}$ = 0.1 sec instead of 10^{-6} sec). This circumstance triggered a long discussion with the Berkeley group of physicists about the reliability of the properties of the isotope. In 1976 the isotope ^{260}Ku was synthesized in one reaction, $^{249}Bk + {}^{15}N$. A half-life of 0.1 sec was obtained in all experiments ($^{242}Pu + {}^{22}Ne$, $^{246}Cm + {}^{18}O$, $^{249}Bk + {}^{15}N$) and the cycle can be considered completed. Final confirmation of the properties was thus obtained and, consequently, the priority of JINR in the discovery of element 104 was confirmed.

A paper presented by I. Kratz (GFR) gave a review of the chemical methods developed in Darmstadt for separating and identifying superheavy elements in reactions with ions heavier than argon. Beams of accelerated ions of krypton, xenon, and uranium have now been obtained in the UNILAC accelerator with an intensity of $\sim 10^{11}$-10^{10} particles/sec and a maximum energy of 7.5 MeV/nucleon. This enabled the authors of the paper to carry out U + Xe experiments (studied earlier in Dubna on the tandem cyclotron U-300 + U-200) as well as to obtain the first results on the irradiation of a uranium target with uranium ions. The irradiated targets were subjected to radiochemical separation. The major portion of the products are due to quasielastic and deeply inelastic transfer reactions. The experiments indicated that the threshold of deeply inelastic transfer reactions rises by a factor of roughly 1.2 when argon ions are replaced by uranium ions. Isotopes of elements from Bi to Au with cross sections of $(0.1\text{-}1) \cdot 10^{-27}$ cm^3 were identified at a maximum uranium ion energy of $\sim$1700 MeV. On assuming a two-particle mechanism of the formation of these nuclei, one could expect to obtain neutron-rich isotopes of transfermium elements up to Z = 105 in long U + U experiments.

A paper by V. Greiner (GFR) was devoted to a theoretical analysis of the possibility of synthesizing superheavy elements in reactions with xenon and uranium ions. It is predicted that there is a definite probability of nuclei of Z = 110-116 being synthesized in deeply inelastic multinucleon transfer reactions with the interaction of uranium ions. However, the experimentally discovered increase in the barrier to deeply inelastic interactions leads to a rise in the excitation energy of the products and may significantly reduce the yield of superheavy elements in such reactions.

Fission of Heavy Nuclei. The study of delayed fission of nuclei which are far from the line of β stability, i.e., fission from the excited state after β decay, was the subject of a paper by Yu. P. Gangrskii (JINR). The cross sections of the delayed fission of neutron-rich protactinium isotopes and neutron-deficient isotopes of berkelium, einsteinium, and mendelevium were measured. Analysis of the data yielded information about the character of the population of the levels of heavy nuclei in β decay and the form of the fission barriers. The results are in good agreement with the theoretical calculations and the magnitudes of the fission barriers of heavy neutron-deficient nuclei (V. V. Pashkevich, JINR).

In his paper, Yu. M. Tsipenyuk (Institute for Physical Problems, Academy of Sciences of the USSR, Moscow) presented data on the deeply inelastic photofission of $^{236,\ 238}$U nuclei. He reported on a study of a new effect, dubbed the isomeric shelf, consisting in the slope of the curve of the fission cross section changing abruptly as the photon energy decreases. Detailed evidence about the structure of the fission barrier may be obtained from investigation of this effect.

A paper by V. N. Okolovich (Institute of Nuclear Physics, Academy of Sciences of the Kazakh SSR, Alma-Ata) presented extensive experimental material about the fission of nuclei with Z = 56-90 by cyclotron-accelerated α particles with an energy E of up to 40 MeV. From the energy relations it follows that, for excited states of nuclei in the region of lead, shell effects appear in fission barriers up to E_{excit} ∿30-40 MeV. If the shell effects do not decrease very much at this energy, interesting information about the properties of superhigh elements can be obtained by studying the characteristics of induced fission. The results of the first investigations in this area were given in papers by Kh. Zodan and J. E. Pieniazkewicz (Penionzhkevich) (JINR). The kinetic energy of fission fragments of superheavy compound nuclei with Z = 112-115 were studied at E_{excit} ∿20-30 MeV; the nuclei were formed in the interaction of $^{40,\ 44,\ 48}$Ca ions with nuclei of lead, uranium, and americium.

The Study of the Mechanism of Interaction of Compound Nuclei. This topic was considered primarily with a view to discussing the optimal method of synthesizing superheavy elements in reactions with ions heavier than germanium. V. V. Volkov (JINR) analyzed experiments on the synthesis of superheavy elements in reactions with ions of germanium, krypton, xenon, and uranium and expressed the opinion that when ions heavier than krypton are used, the characteristic features of deeply inelastic multinucleon transfer reactions (mass, charge, and energy distribution) affords hope of synthesizing neutron-rich isotopes of heavy and superheavy elements in such reactions. The experimental situation in the study of deeply inelastic reactions with heavy ions was considered by I. Galant (France).

The possibilities of obtaining supercritical quasi-atoms in a collision with heavy ions were discussed in a paper by K. G. Kaunda (JINR).

The experimental program of research on the UNILAC accelerator was presented in a paper by R. Bock (GFR).

A paper by E. Reukel (GFR) analyzed the potentialities of a number of large experimental installations for doing work on the synthesis of superheavy elements and studying the mechanisms of reactions in the UNILAC accelerator. Among these, mention should be made of the SHITP separator of nuclear-reaction products (Wein velocity selector) and the mass separator for studying short-lived nuclei (>10 sec), set up on the heavy-ion beam of the accelerator. These are large installations for multiparameter analysis, employing a system of gas detectors for measuring the specific ionization, total energy, exit angles of the particles, and time of flight.

The closing session of the meeting was devoted to a general discussion.

SECOND IAEA MEETING ON LARGE TOKAMAKS

L. G. Golubchikov

The meeting, which was held in Princeton (USA) from Nov. 26 to Dec. 1, 1976, was attended by 100 specialists from the USA, France, Italy, Gt. Britain, Japan, the German Federal Republic, Holland, Sweden, and the USSR. The delegates heard papers on the TFTR, JT-60, JET, T-20, and T-10M tokamaks and became acquainted with the work done on controlled thermonuclear fusion in the PPL and how the equipment of the PDX and TFTR installations functions.

General Characterization of Projects. No significant changes were made in the philosophy of large tokamak reactor projects abroad after the Dubna meeting (June 1975). The principal physical and engineering parameters of the installations, apart from the T-20, remained practically unchanged. Since the T-10 has been reconstructed and used as the basis for the T-10M with superconducting magnetic coils and powerful heating system, the T-20 has been freed of work on solving part of the physical problems. In view of this, the deuterium—tritium experiment, obtaining extremely high neutron fluxes on the first wall, and finishing work on various engineering and technological problems of the thermonuclear reactor have taken on added importance. In the course of the development of foreign projects a significant stride has been made in recent years in the study of the practical realization of these projects; by contrast, in designing the T-20 more detailed consideration was given to new problems such as the blanket and increased radiation shielding as well as various technical and physical parameters.

Foreign projects are of interest from the point of view of detailed calculations of the development of the first stage of discharge in plasma, engineering and computational methods involved in designing various systems, concrete solution of the problems of assembly and dismantling, and development of power supply systems. All designs provide for the inductor to operate initially in the storage mode, with subsequent remagnetization of the core. Combined versions of power supply systems are based on mains supplies and electric generators.

The injector programs are linked with a general approach to the solution of engineering-design problems on the basis of the experience available from work done. The energy of particles and the power introduced into plasma by streams of fast neutral particles are chosen as follows: 80/160 keV and 25 MW for the JET, 120 and 20 for the TFTR, 65 and 15-20 for the JT-60, and 80/160 and 50 for the T-20.

The design of discharge chambers and tritium systems has not undergone any major changes.

The JET Facility (Euratom). Significant results have been obtained in the analysis of poloidal fields and on the basis of calculations corrections have been made to the parameters of windings, with allowance for the effect of the magnetic circuit and saturation of the central core. The cost has been calculated of both individual elements of the power supply system (two types) and the entire system with account for operating losses.

A variant under consideration involves coating the inner surface of the vacuum surface with low-Z materials, such as graphite. A new order of operations on the facility has been proposed. The essence of this new order is that a powerful injection of neutral particles of comparatively low energy is turned on in the initial stage of formation of the plasma filament, in the process of expansion of the filament. Since such beams of particles are trapped on the periphery of the plasma filament and the chamber is filled uniformly with hot plasma. Then begins the injection of high-energy neutral particles for further heating of the plasma. The temperature at the periphery is assumed to be 10-50 eV. This conclusion is based on new calculations of the radiation of iron atoms in a plasma.

Translated from Atomnaya Énergiya, Vol. 42, No. 5, pp. 431-432, May, 1977.

TABLE 1. Principal Characteristics of Large Tokamaks

Parameter	JET	TFTR	JT-60	T-20
Major radius, m	2,96	2,48	3	5
Minor radius, m	1,25	0,85	0,95	1,61
Plasma current, mA	3,1—4,8	2,5 (1,0) *	2,7	5
Stability margin at plasma edge	6	3,0 (7,5)	2,5	2,3
Ion temperature, keV	5	12,4 (6)	5—10	7—10
Ion density, cm^{-3}	$5 \cdot 10^{13}$	$11 \cdot 10^{13}$ ($8 \cdot 10^{13}$)	$(2—10)\ 10^{13}$	$(5—10)\ 10^{13}$
Energy lifetime τ_E, sec	1	0,2	0,2—1,0	2
Product $n \cdot \tau_E$, $cm^{-3} \cdot sec$	$5 \cdot 10^{13}$	$2,2 \cdot 10^{13}$ ($1,6 \cdot 10^{13}$)	$(2—6)\ 10^{13}$	10^{14}
No. of D–T neutrons per pulse	10^{20}	10^{18}	None	$10^{20}—10^{21}$
Cross section of plasma filament	Elliptical	Round	Oblate with external axially symmetric diverter	Round
Shape of coils	D-shaped	Round	Excited	D-shaped
Type of magnetic circuit	Iron	Excited		Iron

*Another variant is shown in parentheses.

A separate paper was devoted to the activation of the apparatus and design elements under the effect of neutron radiation. This paper described a method of calculation and presented a chart of the levels of activity in various parts of the facility.

The quantity of tritium used by the facility in one pulse is determined by the partial pressure of the hydrogen isotopes in the vacuum chamber at 10^{-5} to 10^{-3} mm Hg. To carry out 100 discharges in a deuterium–tritium mixture in the final stage of the experiment a total quantity of 10^5 Ci of tritium (to cover possible losses) is envisaged.

The design of the facility has been completed. About 13,000,000 dollars were spent to develop it and the equipment of the entire complex is valued at 250,000,000 dollars. The site for it has not yet been determined.

The TFTR Facility (USA). In contrast to other designs in which the magnetic field remained unchanged, in this case the possibility of increasing it from 5.2 to 6-7 T is being explored. In 1975 the design and technology of coils for 5.2 T were refined and the thermal and mechanical loads were calculated. This made it possible to draw nearer to their industrial fabrication.

The equipment of the facility is to get its power supply from two shock-excited generators with a total energy reserve of 4500 MJ and a power of 475 MVA. The power required from the supply network does not exceed 40-50 MW. It was decided to use slow, shock-excited generators of the vertical type. Space has been provided in the machine room for a third generator with the requisite equipment, thus making it possible to improve the reliability of the power supply system and to extend its capabilities.

Upon comparison of the opposing requirements, a resistance of 3.4 mΩ was chosen for the chamber circuit. A U-shaped sylphon bellows, shaped by hydraulic means, was selected on the basis of strength-of-materials analysis. The role of diaphragms is played by moving tungsten rails which confine the plasma filament vertically and by tungsten plates which are placed on the inner side of the liner.

It is proposed to preheat the chamber to 500°C and to condition it by frequent low-power discharges. To provide protection against penetration by tritium, the thin sylphon bellows are covered from the outside by an additional vacuum space with electrical insulation. The total quantity of tritium is to be limited to $5 \cdot 10^4$ Ci.

Four injectors are to be installed for additional heating of the plasma and space is to be reserved for two more. The 100-MW power supply system is being designed so as to permit the connection of six injectors with an efficiency of 28% and an injection-pulse duration of 0.5 sec.

The TFTR design has been completed and a model one-sixth of natural scale has been built. Princeton has been selected as the site for the facility and physical start-up is planned for 1981.

The JT-60 Facility (Japan). This is the only design which uses no iron and has the poloidal field coils placed internally. Its inventors believe that this design allows the apparatus to be assembled and dismantled repeatedly. Oxygen-free copper wire was chosen for the toroidal coils. The addition of 0.2% silver on the radially external portions increases the elastic limit by 40%. This wire has a remanent elongation of 0.2% with good electrical conductivity. Work is being completed on a full-scale model which is necessary for choosing the production technology. The geometry of the discharge chamber has been determined and the computational, experimental, and technological work has been done so that work on the detail design can begin. In contrast to other designs, the vacuum chamber has one wall and consists of eight bellow sections and eight rigid sections with an oval cross section.

The plasma is heated by 16 injectors, eight for injections from above and eight below at angles of +35° and −35°, respectively. Evacuation is effected at the rate of 10^7 liters/sec by means of cryopanels cooled with liquid helium.

The technicoeconomic basis for the project has been completely worked out. The cost of the facility has been put at 320,000,000 dollars. The construction site has not been determined, but priority is given to Tokyo. Physical start-up is to occur in 1980.

The design parameters of the facilities discussed above are given in Table 1.

The meeting also heard and discussed two projects for large superconducting tokamaks, the Soviet T-10M and the French Torus II with extremely close parameters ($R \sim 1.7$ m, $r \sim 0.65$ m, $H \sim 3$ T, $I_{pl} \sim 1.5$ MA). Torus II is to be built in Cadarache.

One section of the meeting discussed three different projects for the TNS (the generation of apparatuses following TFTR). These projects also propose using superconducting coils with total thermal insulation.

PROBLEMS OF THERMONUCLEAR EQUIPMENT AT THE WORLD ELECTROTECHNICAL CONGRESS

V. F. Grishin and S. M. Sokolovskii

With regard to breadth and topicality of scientific problems discussed and composition of participating countries and their representatives, the World Electrotechnical Congress, which is to meet in Moscow in June 1977, will be the largest scientific–technical forum in electrotechnical history.

The last electrotechnical congress, held in Paris in 1932, was attended by 1300 specialists. According to tentative data, the World Congress in Moscow will be attended by more than 2000 specialists from 30 countries. A total of 800 papers are to be read at 12 sections and subsections.

Many new problems to be discussed have cropped up in the time that has elapsed. The 1977 Congress will consider various aspects of powerful generators and power systems, thermonuclear installations and the electrotechnical equipment for them, new materials and electrical engineering technologies, energy conversion and electric drives, and microelectronics.

The Congress motto "The Present and Future of Electrical Technology" has been chosen to focus the attention of scientists and specialists on the discussion of the key problems in the development of electrical engineering to the end of the 20th century. One of the key problems is that of developing thermonuclear plants and the equipment for them. It is no accident, therefore, that at the first plenary session E. P. Velikhov (USSR) and E. Kintner (USA) will present a joint paper entitled "Problems and prospects of the construction of thermonuclear electric power plants." The report of R. Roberts (USA) entitled "The Future of Thermonuclear Reactors" dealt on the same subject.

Translated from Atomnaya Énergiya, Vol. 42, No. 5, p. 433, May, 1977.

Some papers discuss thermonuclear reactors proper: "Energy block with laser thermonuclear reactor" (N. G. Basov et al., USSR), "Experimental thermonuclear reactor of the tokamak type" (P. Reardon, USA), and "Electromagnetic problems of construction and power engineering aspects of thermonuclear reactors" (V. A. Glukhikh et al., USSR).

Electrotechnical devices for thermonuclear apparatuses will be taken up in the papers "Pulsed energy sources based on capacitive and inductive storage devices" (M. V. Kostenko et al., USSR), "High-speed pulsed high-voltage systems and elements for thermonuclear research" (M. Bielik [Belik], Poland), "Magnetic field systems for future toroidal reactors" (A. Knobloch, GFR), and "Problems of producing powerful pulses and three-phase generators of dense plasma and power sources for them" (I. A. Glebov et al., USSR). Also devoted to this subject are the papers "Asynchronous ironless shock-excited generators" (J. Rieu, France) and "The IEEE handbook on the reliability index of electrical equipment for atomic power stations" (J. Fragol, USA).

Considerable interest will be aroused by the paper "Ways of converting the energy of thermonuclear reactors into electricity" (G. A. Baranov et al., USSR). The paper by E. Bolginow "Problems of safety in nuclear facilities" (USA) will have an extended time limit.

Special-purpose electromechanical complexes for atomic power plants is the subject of papers by N. G. Basov et al. "Automation of a powerful laser apparatus for thermonuclear experiments" (USSR), A. Pearson "Computer-assisted control of nuclear facilities in Canada — present experience and prospects" (Canada), Yu. D. Proferansov et al. "Systems for monitoring and controlling technological processes of atomic power plants by means of control computers" (USSR), and V. Aleit "Problems of the development of control systems for atomic power plants" (GFR). These topics will also be discussed in papers by J. Saastomoinen "Computing systems at the Loviisa atomic power plant" (Finland) and E. Malaise and P. Gilsoule "Use of protective elements in automatic protective devices of nuclear reactors" (Belgium).

The Congress material can be used for long-range prediction in the domain of international standardization and for determining the most important areas to whose development attention will be paid in the immediate future.

The congress is organized by the Ministry of the Electrotechnical Industry of the USSR and the Academy of Sciences of the USSR in coordination with the International Electrotechnical Commission and is supported by the SIGRE of the IEEE (USA) and other international and national organizations.

During the congress in Moscow the international exhibition "Electro-77" will open and will present the newest Soviet and foreign electrotechnical equipment. At the same time the plenary session of the International Electrotechnical Commission will convene in Moscow.

These three very large undertakings will allow many of the rank and file to familarize themselves with the achievements and perspectives of development of electrotechniques, to participate in discussions, and to outline the perspectives and economic justifications for further research and construction of thermonuclear power plants.

USSR DISPLAY AT ELECTRO-77 EXHIBITION

N. P. Longinova

The International Electro-77 Exhibition "Electrotechnical Equipment and Electric Transmission Lines" will open in the Sokolniki Park in Moscow on June 9, 1977. Companies and organizations of more than 20 countries will show specialists and visitors samples of electrical engineering production in all of its variety from powerful complexes of electrical equipment for thermal, hydroelectrical, and atomic power plants to household appliances.

The Soviet Union will be the largest exhibition: its 4000 exhibits in two pavilions and outdoor areas will reflect the most economic methods of obtaining and converting electricity and present and future rational methods of transmitting and using electricity.

For the generation of electricity on the scales envisaged in the Tenth Five-Year Plan for the development of the national economy of the USSR, it is essential to further increase the unit rating of generators for the thermal, atomic, and hydroelectric power industry. Soviet generators are characterized by a high constructional and technological level and a high percentage of utilization of active and technological materials. In respect of technicoeconomic indicators, they rank among the best in the generator construction industry in the world. A model of the first cryo-turbogenerator with a 20,000-kW rating will be presented at the exhibition.

Electrical engineers are participating in the solution of the problem of the controlled thermonuclear reaction by constructing a large complex of semiconductor converters and control devices. The thermonuclear apparatus Tokamak-10 is being demonstrated at the exhibition.

The Soviet display will reflect the achievements in the development and creation of high-voltage technologies for open-wire transmission lines which operate at superhigh voltages and today are the most economical way of transmitting electricity over long distances. On show will be the main element in dc transmission, viz., a rectifier-inverter bridge built in modules based on semiconductor power converters.

The equipment for automation of the electricity generation on display at the exhibition will be based on extensive application of the latest advances in electrical engineering, electronics, and computer technique. A case in point is the V5/40 automated electrotechnical complex of the model-2400 hot-strip mill. It is intended for use in a control system for important technological processes or complex plant without allowing any interruptions in operation. However, its application is not limited to rolling mills. It can be used very efficiently in blast-furnace operation, as well as in atomic, thermal, and hydroelectric power plants, or superdeep drilling of oil and gas wells.

The Soviet Union will show a furnace for obtaining high-quality metal, a furnace for electroslag remelting. This is a unique plasma furnace constructed in collaboration with GDR scientists and opening up new prospects for commercial production of materials with special properties.

Recent achievements of the USSR in electric welding will be represented at the exhibition by plasmatrons for work in various atmospheres, permitting welding, cutting, and surfacing of almost all metals.

Much space in the Soviet exhibition is devoted to electrical engineering related to work in outer space. The central exhibit here will be the Meteor-2 earth satellite, constituting a sophisticated complex of electrotechnical, electromechanical, and radioelectronic devices

Translated from Atomnaya Énergiya, Vol. 42, No. 5, pp. 433-434, May, 1977.

which ensure that satellites function normally for a long time in orbit. Automated testing of the satellites is possible with the aid of the V5/40 automated computing complex.

The Soviet exhibition presents a wide range of diagnostic instruments and devices used in medicine. These include ultrasonic apparatus, therapeutical apparatus, semiconductor instruments for diagnostics, a standardized system of data collection from patients, as well as artificial heart, lung, and liver machines.

Many new exhibits are being shown in those sections of the exhibition which are devoted to transport, agriculture, and the gas and petroleum, extraction, and chemical industries.

A considerable portion of the exhibition is devoted to electrical machines, one of the important forms of electrical engineering production.

Conversion technology, cable technology, low-voltage apparatus, and electrical insulation materials will be well represented. The Soviet exhibit will be completed with a display of new highly economical sources of light lamps for various purposes, and a variety of electrical engineering products for the interiors of present-day homes and apartments and for different living styles.

F. A. Makhlis

THE RADIATION CHEMISTRY OF ELASTOMETERS*

Reviewed by E. D. Chistov

Research on the effect of radiation and high temperature on rubber is of scientific and practical interest in two ways. Firstly, rubber, which has been a traditional material in machine building, is used extensively in nuclear engineering. Secondly, notwithstanding the numerous experimental papers on radiation vulcanization and modification of elastomers, there are no books which give a quite detailed presentation of the "useful" application of radiation in order to obtain rubber materials with improved properties.

The book under review considers in detail those aspects of the radiation chemistry of elastomers that are most important from the scientific and practical points of view. The author has made a significant contribution to the study of the processes involved in the formation and transformation of the space lattices of a large range of elastomers under the effect of ionizing radiation, high temperature, and mechanical stress. The principal ideas presented by the author in the monograph "The Radiation Physics and Chemistry of Polymers," published by Atomizdat in 1972 and published in translation in the U.S.A. in 1975, have been developing successfully as applied to elastomers.

Chapter 1 analyzes the principal radiochemical transitions of a large number of rubbers at various temperatures and considers the radiation and radiation-oxidation processes that occur in them. First, the author describes the processes of change in the space lattice of elastomers under the simultaneous effect of ionizing radiation and mechanical stresses. It has been determined that in the case of most elastomers, the molecular chains of the rubber or lattice nodes are responsible for processes of radiation-induced destruction under various conditions. The radiation-induced destruction of the space lattice has been found to undergo an abrupt acceleration under mechanical stresses, this being due to the mechanical activation of the destruction process.

Chapter 2 gives detailed information about the process of radiation vulcanization of elastomers. The author considers the advantages and disadvantages of sources of γ rays and accelerated electrons, makes comparative technicoeconomic appraisals of the sources and the criteria for choosing them for radiation vulcanization of various rubber products. The distinctive features of radiation technology for the manufacture of rubber products are noted. Then the chapter deals with sensitizers for the process of radiation vulcanization of elastomers, the properties of radiation—cross-linked organosilicon, fluorine-containing, ethylene—propylene, and butadiene—nitrile rubbers, as well as general-purpose rubbers and latexes. Data are given on the thermal stability of rubber and the effect that the ingredients and production conditions of the rubber affect the stability. The processes of thermal and thermooxidation destruction in rubbers are discussed in detail.

Chapter 3 describes a promising new area of radiation modification of rubber with the aid of polyfunctional unsaturated compounds which, as a result of three-dimensional graft radiation polymerization in the rubber matrix, makes it possible to obtain materials with highly improved properties. A comparison is made of the effectiveness of various polyfunctional compounds as sensitizers to radiation cross-linking of elastomers. The mechanism of radiation cross-linking of a mixture of rubbers with polyfunctional unsaturated compounds is considered. The author also studies the processes by which the structures of these systems change under radiation and heat.

*Atomizdat, Moscow (1976), 200 pp., 1 ruble, 7 kopecks.

Translated from Atomnaya Énergiya, Vol. 42, No. 5, p. 435, May, 1977.

The radiation and thermoradiation stability of vulcanized rubbers based on fluorine-containing, organosilicon, ethylene—propylene, and butadiene—nitrile rubbers is taken up in Chap. 4. This chapter also presents the principal laws governing radiation aging of vulcanized rubber, depending on the type of rubber and the ingredients of the rubber composition, as well as the conditions of irradiation. A method is described for accelerated testing of the radiation stability of vulcanized rubbers at elevated temperatures.

The book has not reflected some aspects of radiation chemistry and technology. For instance, little information is provided about the elementary radiochemical processes in the first stages of radiolysis of elastomers, preceding processes of cross-linking and destruction (formation and transformation of intermediate active particles), and no examples are given of the use of vulcanized rubber products in nuclear engineering. In covering topics associated with the application of various radiation sources, the radiation safety of the process has been left out entirely. Nor is there any information about the effect of ionizing radiation on the dynamic, electrical, thermal, and optical properties of elastomers.

On the whole, the book is unquestionably of interest and useful to specialists in radiation chemistry and radiation technology as well as in the radiation materials science of polymer materials.

V. I. Vladimirov

PRACTICAL PROBLEMS OF THE OPERATION OF NUCLEAR REACTORS*

Reviewed by E. S. Glushkov

The book under review considers the practical problems which arise during the operation of nuclear reactors of various purposes. In many of the cases there is a discussion of the variable operating modes of the reactors, which are characteristic of energy plants used in transport as well as atomic power plants operating under variable loads.

Chapter 1 of the book deals with the nuclear reactor as a source of energy and radioactivity. In Chapter 2 the author describes processes which affect the operating mode of the reactor, its energy resources, and the possibility of executing various power adjustments with allowance for processes of poisoning due to fission products (xenon and samarium) that strongly absorb thermal neutrons. This chapter devotes particular attention to the poisoning that occurs during transition from one power level to another, to the reactor falling into the iodine pit, and to promethium dip. The reactor power, cooling, and nuclear safety are the subjects of Chapter 3.

The presentation of the material in the form of practical problems with subsequent analysis and solution of the problems makes for the rapid acquisition of the necessary knowledge for operating personnel to have an understanding of the physical processes and to make the correct decisions under various situations that arise during the operation of nuclear power plants. However, the author should have placed emphasis on the solution of many of the practical problems considered by using present-day small computers. This could have been done by shortening the description of the quite unwieldy graphicoanalytic method of solving problems pertaining to nuclear reactor poisoning during a power adjustment. In view of the sketchy presentation of the material in the first chapter the formulation and solution of some problems is not clear enough.

As a whole, however, the book is unquestionably a necessary and up-to-date text, especially for the operating personnel of nuclear power plants and designers in the area of ensuring reliable operation.

*Atomizdat, Moscow (1976), 184 pp., 1 ruble, 17 kopecks.

Translated from Atomnaya Énergiya, Vol. 42, No. 5, p. 436, May, 1977.

V. M. Gorbachev, Yu. S. Zamyatnin,

and A. A. Lbov

INTERACTION OF RADIATION WITH NUCLEI OF HEAVY ELEMENTS AND NUCLEAR FISSION*

Reviewed by N. A. Vlasov

The heavy nuclei of elements with atomic number $Z > 90$ are used in many areas of nuclear power engineering and related fields of science and engineering. Some of them constitute fuel for nuclear reactors while others are formed in reactors and then used in various devices, e.g., in energy sources for spacecraft or automatic meteorological stations. Skillful use of isotopes of heavy elements is impossible without knowledge of their properties which are quite manifold. The reference book under review has compiled data on the cross sections for the interaction of neutrons, γ rays, and charged particles with nuclei.

Neutron interactions have been studied the most thoroughly. The cross sections for elastic and inelastic scattering, radiative capture, and other reactions and fission are given for the entire energy range that has been explored and is of interest, i.e., from thermal energies to tens of megaelectron volts. The tables and graphs are accompanied by brief commentaries providing information about the state of research, about references that give more detailed information, and explanations concerning the table contents.

The second, large part of the handbook is devoted to the characteristics of the fission process. The book gives the yields and spectra of fission products, i.e., fragments of the entire mass range, instantaneous and delayed neutrons, γ rays, and x rays. The known characteristics of ternary fission are also given. The references from which the data have been taken are listed with the graphs and tables. It is true that there is no uniformity in the presentation of the references; sometimes they accompany individual tables and other times they refer to entire chapters. This somewhat complicates the use of the handbook.

The handbook is obviously very useful and a must for all workers in the field of heavy atoms and its publication is fully justified. Unfortunately, the book is reaching the reader with some delay and new data have already appeared; the authors are probably preparing an enlarged and improved edition. Since the use of heavy elements is expanding, a new edition can be welcomed in advance. It would seem sensible to combine into one volume entitled "Heavy Nuclei" the present handbook and the earlier one† by the same authors, treating them as separate volumes of one book.

*Atomizdat, Moscow (1976), 464 pp., 2 rubles, 57 kopecks.

†V. M. Gorbachev, Yu. S. Zamyatnin, and A. A. Lbov, The Principal Characteristics of Isotopes of Heavy Elements [in Russian], Atomizdat, Moscow (1975).

Translated from Atomnaya Énergiya, Vol. 42, No. 5, p. 436, May, 1977.

Yu. V. Kuznetsov

OCEAN RADIOCHRONOLOGY*

Reviewed by V. V. Gromov

This monograph by Yu. V. Kuznetsov, whose work on ocean radiochemistry is well known in our country and elsewhere, is the first attempt from the positions of radiochemistry to generalize and analyze widely used methods of the radiochronology of marine and ocean sediments. Although the monograph discusses practically all known methods of nuclear chronology, pride of place is given to four so-called "nonequilibrium" methods of determining the age and rate of formation of sediments in the seas and oceans (ionium, ionium—thorium, protactinium—ionium, and radium—ionium methods) since these are the methods that the author has studied over a period of many years.

The monograph consists of three parts encompassing 12 chapters. The first part contains general information about seawater as a physicochemical system; experimental data about the spatial distribution of the isotopes of thorium, uranium, radium, and protactinium in the surface layer of the ocean sediments, their vertical distribution in marine and ocean sediments of various types, their distribution in ocean waters and suspended solid matter, and, finally, the results of experimental studies on the mechanism by which ^{230}Th, ^{232}Th, ^{238}U, and ^{226}Pa enter sediments. In these chapters of the monograph, the author sums up the information he has acquired about the mechanisms by which the isotopes mentioned get into ocean and marine sediments and formulates the radiochemical foundations of the nuclear geochronology of the ocean by nonequilibrium methods. The author makes extremely interesting conclusions which are well-based and are accompanied by extensive experimental material, about the various forms ^{230}Th and ^{232}Th found in the ocean and the mechanisms of their entry into the sediments, about the similarity of the geochemical behavior of ^{230}Th and ^{231}Pa in the marine environment, about the fact that marine and ocean sediments contain ^{226}Ra deposited right out of the water. Theoretical and experimental substantiation has been given for the conclusion as to the similarity of the mechanisms by which isotopes of uranium, radium, thorium, and protactinium entered the sediments in the modern age and in ages past.

The second part of the monograph consists of six chapters in which, from the position of his radiochemical research done in the ocean and information known from the literature, the author considers the reality of the basic theoretical premises of the nonequilibrium methods of dating sedimentary formations, discusses the possibilities and the limitations of each of the methods, and compares the data from dating by these methods with those obtained by other methods. Particular attention should be paid to a method presented by Kuznetsov for normalizing experimental ionium curves which makes it possible not only to determine the mean rate of sedimentation but in a number of cases also to find the relative age of each layer. Of particular interest as well is the improvement presented by the author for the Kosti method, an improvement based on the simultaneous use of data about the ^{230}Th and ^{231}Pa contents in samples from the surface of ocean sediments to determine the present rate of sedimentation.

The third and final part of the monograph is devoted to the radiochronology of sediments on the basis of nuclides which are not part of radioactive series. Here in brief form Kuznetsov presents the essence of the radiocarbon method of dating and such uncommon methods as the radioberyllium, radiosilicon, and radioaluminum methods as well as those based on the the use of isotopes of a technical origin (^{55}Fe and ^{137}Cs).

*Atomizdat, Moscow (1976), 278 pp., 2 rubles, 10 kopecks.

Translated from Atomnaya Énergiya, Vol. 42, No. 5, pp. 436-437, May, 1977.

The monograph of Yu. V. Kuznetsov is written in a clear, lucid language, is well illustrated (47 tables and 62 drawings), and contains an extensive list of references (487 entries). Although original experimental material forms its basis, this is at the same time the most up-to-date generalization of the ideas in the literature about the behavior of natural radioactive isotopes in a marine environment and methods of nuclear geochronology of the ocean.

This book will certainly be useful to a wide range of researchers engaged in "dating" various sedimentary deposits by nuclear-physical methods. It is also a major contribution to the geochemistry of natural radioactive elements.

engineering science

continued
from back cover

Title	# of Issues	Subscription Price
Metallurgist *Metallurg*	12	$225.00
Metal Science and Heat Treatment *Metallovedenie i termicheskaya obrabotka metallov*	12	$215.00
Polymer Mechanics *Mekhanika polimerov*	6	$195.00
Problems of Information Transmission *Problemy peredachi informatsii*	4	$175.00
Programming and Computer Software *Programmirovanie*	6	$95.00
Protection of Metals *Zashchita metallov*	6	$195.00
Radiophysics and Quantum Electronics (Formerly Soviet Radiophysics) *Izvestiya VUZ. radiofizika*	12	$225.00
Refractories *Ogneupory*	12	$195.00
Soil Mechanics and Foundation Engineering *Osnovaniya, fundamenty i mekhanika gruntov*	6	$195.00
Soviet Applied Mechanics *Prikladnaya mekhanika*	12	$225.00
Soviet Atomic Energy *Atomnaya energiya*	12 (2 vols./yr. 6 issues ea.)	$235.00
Soviet Journal of Glass Physics and Chemistry *Fizika i khimiya stekla*	6	$ 95.00
Soviet Journal of Nondestructive Testing (Formerly Defectoscopy) *Defektoskopiya*	6	$225.00
Soviet Materials Science *Fiziko-khimicheskaya mekhanika materialov*	6	$195.00
Soviet Microelectronics *Mikroélektronika*	6	$135.00
Soviet Mining Science *Fiziko-tekhnicheskie problemy razrabotki poleznykh iskopaemykh*	6	$225.00
Soviet Powder Metallurgy and Metal Ceramics *Poroshkovaya metallurgiya*	12	$245.00
Strength of Materials *Problemy prochnosti*	12	$295.00
Theoretical Foundations of Chemical Engineering *Teoreticheskie osnovy khimicheskoi tekhnologii*	6	$195.00
Water Resources *Vodnye Resursy*	6	$190.00

Back volumes are available. For further information, please contact the Publishers.

SEND FOR YOUR
FREE EXAMINATION COPIES

Plenum Publishing Corporation

Plenum Press • Consultants Bureau
• IFI/Plenum Data Corporation
227 WEST 17th STREET
NEW YORK, N.Y. 10011

United Kingdom: Black Arrow House
2 Chandos Road, London NW10 6NR England

breaking the language barrier

WITH COVER-TO-COVER
ENGLISH TRANSLATIONS
OF SOVIET JOURNALS

in engineering science

Title	# of Issues	Subscription Price
Automation and Remote Control *Avtomatika i telemekhanika*	24	$260.00
Biomedical Engineering *Meditsinskaya tekhnika*	6	$195.00
Chemical and Petroleum Engineering *Khimicheskoe i neftyanoe mashinostroenie*	12	$275.00
Chemistry and Technology of Fuels and Oils *Khimiya i tekhnologiya topliv i masel*	12	$275.00
Combustion, Explosion, and Shock Waves *Fizika goreniya i vzryva*	6	$195.00
Cosmic Research (Formerly Artificial Earth Satellites) *Kosmicheskie issledovaniya*	6	$215.00
Cybernetics *Kibernetika*	6	$195.00
Doklady Chemical Technology *Doklady Akademii Nauk SSSR*	2	$65.00
Fibre Chemistry *Khimicheskie volokna*	6	$175.00
Fluid Dynamics *Izvestiya Akademii Nauk SSSR mekhanika zhidkosti i gaza*	6	$225.00
Functional Analysis and Its Applications *Funktsional'nyi analiz i ego prilozheniya*	4	$150.00
Glass and Ceramics *Steklo i keramika*	12	$245.00
High Temperature *Teplofizika vysokikh temperatur*	6	$195.00
Industrial Laboratory *Zavodskaya laboratoriya*	12	$215.00
Inorganic Materials *Izvestiya Akademii Nauk SSSR, Seriya neorganicheskie materialy*	12	$275.00
Instruments and Experimental Techniques *Pribory i tekhnika eksperimenta*	12	$265.00
Journal of Applied Mechanics and Technical Physics *Zhurnal prikladnoi mekhaniki i tekhnicheskoi fiziki*	6	$225.00
Journal of Engineering Physics *Inzhenerno-fizicheskii zhurnal*	12 (2 vols./yr. 6 issues ea.)	$225.00
Magnetohydrodynamics *Magnitnaya gidrodinamika*	4	$175.00
Measurement Techniques *Izmeritel'naya tekhnika*	12	$195.00

SEND FOR YOUR FREE EXAMINATION COPIES

Back volumes are available.
For further information,
please contact the Publishers.

continued on inside back cover

Declassified and Approved For Release 2013/04/01 : CIA-RDP10-02196R000700090005-4